SEPTEMBER 2021 M.Sc. in Mechanical Engineering YAHYA KHALEEL KAREEM KAREEM

REPUBLIC OF TURKEY

GAZİANTEP UNIVERSITY

GRADUATE SCHOOL OF NATURAL & APPLIED SCIENCES

TWO-PHASE FLOW AND DRIFT-FLUX MODELS FOR RAINY WEATHER CONDITIONS

M.Sc. THESIS

IN

MECHANICAL ENGINEERING

BY

YAHYA KHALEEL KAREEM KAREEM

SEPTEMBER 2021

TWO-PHASE FLOW AND DRIFT-FLUX MODELS FOR RAINY WEATHER CONDITIONS

M.Sc. Thesis
in
Mechanical Engineering
Gaziantep University

Supervisor
Prof. Dr. Mehmet Yaşar GÜNDOĞDU

By
Yahya Khaleel Kareem KAREEM

September 2021

TWO-PHASE FLOW AND DRIFT-FLUX MODELS FOR RAINY WEATHER CONDITIONS

submitted by **YAHYA KHALEEL KAREEM KAREEM** in partial fulfillment of the requirements for the Master of Science in **Mechanical Engineering, Gaziantep University** is approved by,

Assoc. Prof. Dr. Mehmet İshak YÜCE
Director of the Graduate School of Natural and Applied Sciences …………..............

Prof. Dr. Sait SÖYLENMEZ
Head of the Department of …..........................

Prof. Dr. Mehmet Y. GÜNDOĞDU
Thesis Supervisor, Mechanical Engineering
Gaziantep University …..........................

Exam Date: 6 September 2021

Examining Committee Members:

Prof. Dr. Mehmet Y. GÜNDOĞDU
Thesis Supervisor, Mechanical Engineering
Gaziantep University …..........................

Asst. Prof. Dr. Fuat YILMAZ
Mechanical Engineering
Gaziantep University …..........................

Asst.Prof. Dr. M. Veysel ÇAKIR
Mechanical Engineering
Kilis University …..........................

I hereby declare that all information in this document has been obtained and presented in accordance with academic rules and ethical conduct. I also declare that, as required by these rules and conduct, I have fully cited and referenced all material and results that are not original to this work.

Yahya Khaleel Kareem KAREEM

ABSTRACT

TWO-PHASE FLOW AND DRIFT-FLUX MODELS FOR RAINY WEATHER CONDITIONS

Yahya Khaleel Kareem KAREEM
M.Sc. in Mechanical Engineering
Supervisor: Prof. Dr. Mehmet Y. GÜNDOĞDU
September 2020
95 pages

The energy from wind turbines is an essential source of clean energy, and depending on clean energy has increased recently due to climate changes. Therefore, it's necessary to study the factors that affect wind turbines' efficiency while focusing on weathers changes. In this study, the effect of parameters on the efficiency of wind turbines such as (humidity, volumetric flux, drift-flux, void fraction, relative velocity, or drift velocity) has been investigated by utilizing a drift-flux model in a two-phase flow (water and air) and considering that there is a relative velocity between air and water which are known as drift velocity, also, taking into account volumetric fraction. Besides, the hourly weather data has been obtained from the Directorate General of Meteorology in Turkey for Mersin province for the year 2017

Key Words: Drift-flux, Two-phase flow, Wind turbine, Available power in the wind, Rainy weather.

ÖZET

YAĞMURLU HAVA ŞARTLARI İÇİN İKİ FAZLI AKIŞ VE DRIFT-FLUX MODELLERİ

Yahya Khaleel Kareem KAREEM
Yüksek Lisans Tezi, Makine Mühendisliği
Danışman: Prof. Dr. Mehmet Y. GÜNDOĞDU
Eylül 2021
95 sayfa

Rüzgar türbinlerinden elde edilen enerji, temel bir temiz enerji kaynağıdır ve son zamanlarda iklim değişiklikleri nedeniyle temiz enerjiye bağlı olarak artmıştır. Bu nedenle rüzgar türbinlerinin verimini etkileyen faktörlerin hava koşullarındaki değişimlere odaklanırken araştırılması gerekmektedir. Bu çalışmada, rüzgar türbinlerinin verimliliği üzerine nem, hacimsel akı, sürüklenme-akı, boşluk oranı, bağıl hız veya sürüklenme hızı gibi parametrelerin etkisi, iki yönlü bir sürüklenme-akı modeli kullanılarak araştırılmıştır. Faz akışı (su ve hava) ve hava ile su arasında sürüklenme hızı olarak bilinen nispi bir hız olduğu göz önüne alındığında, hacimsel fraksiyon da dikkate alınarak. Ayrıca Mersin ili için 2017 yılı için Türkiye Meteoroloji Genel Müdürlüğünden saatlik hava durumu verileri alınmıştır.

Anahtar Kelimeler: Sürüklenme Akısı, İki Fazlı Akış, Rüzgar Türbini, Rüzgarda Mevcut Güç, Yağmurlu Hava.

ACKNOWLEDGMENTS

I want to express my special appreciation and gratitude to my supervisors Prof. Dr. Mehmet Y. GÜNDOĞDU and Dr. Fuat YILMAZ, for all their help, patience, valuable advice, always providing and guiding me in the right direction. I'm very grateful and proud to work under their academic guidance; special thanks to my friend Ziad ALWINDAWI for supporting me. I want to express heartfelt appreciation to the Republic of Turkey and their people for hospitality and generosity throughout my study, which cannot be denied; special thanks to my family.

TABLE OF CONTENTS

Pages

ABSTRACT……………………………………..……………………………vi
ÖZET……………………………………………………………………………vii
ACKNOWLEDGMENTS .... **viii**
TABLE OF CONTENTS... **ix**
LIST OF TABLES .... **xi**
LIST OF FIGURES .... **xii**
LIST OF SYMBOLS .... **xii**
CHAPTER 1 : **INTRODUCTION** **1**
1.1 Introduction 1
1.2 The Main Types Of Wind Turbines Being Used Today 2
1.3 Factors affecting the wind power 5
1.3.1 Wind speed 5
1.3.2 Air density 5
1.3.3 The swept area of the turbine.. 6
1.4 The effect of rain on wind power 6
1.5 The objective of this study 6
CHAPTER 2 : LITERATURE REVIEW.. **8**
2.1 Introduction... 8
2.2 Literature survey 8
CHAPTER 3 : THEORY.. **13**
3.1 Introduction 13
3.2 Application of the Drift-flux Model Two-Phase Flow on Standard Wind power.. 15
CHAPTER 4 : WIND POWER ANALYSIS ACCORDING TO DRIFT-FLUX MODEL **19**

4.1 Introduction 19
4.2 Seasonally Wind Power Analysis According to Two-phase flow Drift-flux Model 19
4.3 Wind Power Analysis According to Two-phase flow Drift-flux Model Throughout 2017.. 23
CHAPTER 5 : WIND TURBINE POWER ANALYSIS ACCORDING TO TWO-PHASE FLOW DRIFT-FLUX MODEL 31
5.1 Introduction 31
5.2 General Specification for Vestas 126-3.3MW 31
5.3 Application Two-phase Flow Drift-flux Model on Vestas 126-3.3MW Wind Turbine 33
5.4 Wind Turbine Power Analysis According to Meteorology Data................. 34
5.5 Wind Turbine Power Curve Analysis According to Two-Phase Flow. 37
CHAPTER 6 : CONCLUSION AND RECOMMENDATION 41
6.1 Conclusion.. 41
6.2 Recommendation.. 43
REFERENCES 44
APPENDIX A 48
APPENDIX B 60

LIST OF TABLES

Page

Table 4.1 Wind power analysis and power deviation for four seasons in 2017........ 23

Table 4.2 Wind power analysis and power deviation throughout 2017……………......23

Table 4.3 Wind Power Analysis According to Two-phase flow Drift-flux Model in January 22

Table 5. 1 Mechanical specification for Vestas 126-3300 KW …………………... 32

Table 5. 2 Vestas 126-3300KW turbine generation information 32

Table 5. 3 Vestas126-3300 Kw power analysis according to meteorology changes 34

Table 5. 4 Power loss 38

LIST OF FIGURES

Page

Figure 4.1 Wind power deviation with seasons in 2017 20

Figure 4.2 Wind power deviation with relative humidity along the seasons in 201720

Figure 4.3 Wind power deviation with temperature along the seasons in 2017 21

Figure 4.4 Wind power deviation with the atmospheric pressure along the seasons in 2017.. 22

Figure 4.5 Drift-flux density changes with the humidity along the seasons in 2017.22

Figure 4.6 Drift-flux density changes with the temperature along the seasons in 2017.. 22

Figure 4.7 Wind power deviation with months throughout 2017 24

Figure 4.8 Wind power deviation with relative humidity throughout 2017.............. 24

Figure 4.9 Wind power deviation with temperature throughout 2017...................... 25

Figure 4.10 Wind power deviation with atmospheric pressure throughout 2017 25

Figure 4.11 Drift-flux density changes with the humidity throughout 2017 26

Figure 4.12 Drift-flux density changes with the temperature throughout 2017........ 26

Figure 4.13 Wind power deviation with days in January…………………………..27

Figure 4.14 Wind power deviation with humidity in January……………………...27

Figure 4.15 Wind power deviation with temperature in January…………………..28

Figure 4.16 Wind power deviation with atmospheric pressure in January………..28

Figure 4.17 Drift-flux density changes with the humidity in January……………..29

Figure 4.18 Drift-flux density changes with the temperature in January…………29

Figure 5.1 Illustration of outer dimensions – structure (1 is hub Hight 117m and 2) the diameter of turbine 126 40

Figure 5.2 Effect of temperature change on wind turbine power…………………. 35

Figure 5.3 Effect of relative humidity on wind power turbine................................ 36

Figure 5.4 Effect of atmospheric pressure on wind turbine power. 36

Figure 5.5 The deviation in wind turbine power. 37

Figure 5.6 Vestas 126-3300 power curve changes.. 39

Figure 5.7 Vestas 126-3300 power curve changes in moisture by Two-phase flow Homogeneous method 40

LIST OF SYMBOLS

A	Swept area of wind turbine (m^2)
C_p	Wind turbine power coefficient
C_t	Thrust coefficient
P_{out}	Power output from turbine (K.W.)
$P_{out\ D}$	Power output from turbine according to Drift-flux model theor (K.W.)
P_{in}	Available power in wind (K.W.)
$P_{in\ dry}$	Available power in wind when density is dry (K.W.)
Pin atm	Available power in wind when density is moisture (K.W.)
Patm	Atmospheric pressure (Pa)
Pdry	Atmospheric pressure for dry air (Pa)
Pv	Pressure for vapor (Pa)
Pg	Saturation pressure (Pa)
Qv	Volumetric flow rate of vapor phase (m^3/s)
Qdry	Volumetric flow rate of dry air (m^3/s)
Ra	Gas constant of dry air (J·K−1·mol−1)
R_v	Gas constant of vapor ($J \cdot K^{-1} \cdot mol^{-1}$)
T	Atmospheric temperature (°C)
V	Wind velocity (m/s)
v_m	Mixture center of mass velocity (m/s)
V_m	Fixed mass volume
V_{km}	Diffusion velocity (m/s)
J	Volumetric flux
J_{21}	Drift Flux

t	Time(s)
$\overline{\mathbf{q}}$	Mixture conduction heat flux
$\mathbf{q}^{\mathbf{T}}$	Turbulent conduction heat flux
Ꞷ	Humidity ratio
λ	Available wind power deviation
λ_t	Wind turbine power deviation
ρ_D	Atmospheric density according to Drift-flux model theory (g/m³)
ρ_v	Water vapor density (g/m³)
ρ_{dry}	Dry air density (g/m³)
ρ_m	Mixture density (g/m³)
$\overline{\overline{\rho}}_k$	Mean density (g/m³)
α	Volumetric void fraction
α_H	Two-phase flow Homogenous model volumetric void fraction
α_D	Two-phase flow Drift-flux model volumetric void fraction
Ø	Relative humidity (%)
$\overline{\mathfrak{G}}$	Mixture viscous tensor ($kg\cdot m^{-1}\cdot s^{-1}$)
$\mathfrak{G}^{T}$	Turbulent stress tensor (N/m^2)
Γ	Constant
Φ_m^{μ}	Mixture viscous dissipation ($kg\cdot m^{-1}\cdot s^{-1}$)
Φ_m^{σ}	surface tension effect in the mixture thermal energy equation (N/m)
Φ_m^{i}	Interfacial mechanical energy exchange effect in the mixture thermal energy equation (J)

CHAPTER 1

INTRODUCTION

1.1 Introduction

Renewable energy is essential because, in contrast to fossil fuels "dirty" energy—its sources are consistently replenished, even as their availability is often affected by factors like weather and time. Today, an overdue energy revolution is finally underway, with renewables increasingly ousting fossil fuels, particularly in the power sector. But not all forms of renewable energy are created equal. Broadly, there are six main types of renewable and clean energy sources: solar, wind, geothermal, hydro, tidal, and biomass. This research highlights wind energy, wind energy, and tidal energy that can be harnessed through turbines; technically, the wind is a subtype of solar power created when three events converge. Understanding how to harness wind energy is relatively simple if one considers it a "fan in reverse" - meaning, instead of using electricity to produce wind, the way a fan works, wind turbines rely on this naturally renewable resource to produce electricity. The renewable energy law was revised in Turkey thanks to the growing share of clean energy since 2010. Serious problems are sure to occur if the meteorological characteristics of those renewable energy sources aren't documented and understood. Wind patterns and speeds vary significantly across the terrain and seasonally, but some of those patterns are predictable enough to plan around. The best locations to place a wind turbine are the tops of rounded hills, open plains (or open water for offshore wind), and mountain passes where the wind is naturally funneled through (producing average high wind speeds). Generally, the higher the elevation, the better, since higher elevations usually have more wind. During this research different, approaches supported meteorological parameters like wind speed, temperature, ratio, and atmospheric pressure are analyzed.

Wind flow patterns and speeds vary greatly across the United States and are modified by bodies of water, vegetation, and differences in terrain. Humans use this wind flow, or motion energy, for many purposes: sailing, flying a kite, and even generating electricity.

The terms "wind energy" and "wind power" both describe the process by which the wind is used to generate mechanical power or electricity. This mechanical power can be used for specific tasks (such as grinding grain or pumping water) or a generator can convert this mechanical power into electricity.

A wind turbine turns wind energy into electricity using the aerodynamic force from the rotor blades, which work like an airplane wing or helicopter rotor blade. When wind flows across the blade, the air pressure on one side of the blade decreases. The difference in air pressure across the two sides of the blade creates both lift and drag. The force of the lift is stronger than the drag and this causes the rotor to spin. The rotor connects to the generator, either directly (if it's a direct drive turbine) or through a shaft and a series of gears (a gearbox) that speed up the rotation and allow for a physically smaller generator. This translation of aerodynamic force to the rotation of a generator creates electricity [1].

1.2 The Main Types Of Wind Turbines Being Used Today

Capturing the earth's natural energy through wind was once an abstract idea. Eventually, however, engineers were able to focus the idea and put it into action through innovative technology. Throughout the development of wind turbines, many prototypes were created, and many of the first ones designed are still used today, just with more modern engineering. Here are a few of the different wind turbines we are used to seeing today, and some we definitely are not [2].

1.2.1 HAWT Wind Turbines

A "HAWT" is a Horizontal Access Wind Turbine. These are the types of wind turbines that are most widely used, and are usually the first to come to mind when we think of wind energy. These turbines can have two, but more often three, blades on top of a tower reaching up to 120m tall. The blades can be upwards of 60m long and can produce up to 20 MW of energy.

Up wind Turbines

These are turbines that face the wind. This means that the wind blows directly into the turbine, rather than coming from behind it. These are the HAWT wind turbines most often used.

Pro: This is the more efficient way to get energy from wind, given that it helps prevent wind shade from behind the tower.

Con: Wind shade occurs in front of the tower as wind comes toward it. To avoid this, the rotor must be further from the tower, which is an expensive shift.

Down wind Turbines

These turbines do not face the wind, so the wind actually hits the back of the turbine to make it move.

Pro: The rotor can be made much more flexible. This means the wind shade can be more easily reduced, and a lighter model can be designed to take the stress off the tower in high winds.

Con: The wind power is variable because the wind blows directly through the wind shade. Although its design can more easily reduce wind shade, there is still significantly more in down-wind turbines.

Shrouded Turbines

Shrouded turbines, also known as Diffuser-Augmented Wind Turbines, have blades situated in a ring-shaped airfoil, which increases the airflow in the system.

Pro: As explained by Open-Source Ecology, this design can increase the power of a HAWT by up to 5 times due to the increased air flow created from the airfoil. Turbulence and noise are also reduced because blade tips are covered by the airfoil.

Con: These are very expensive turbines and cannot compete with the modern, high-speed turbines.

1.2.2 VAWT Wind Turbines

A "VAWT" is a Vertical Access Wind Turbine. These types of wind turbines harness power from the wind in the opposite direction than the HAWT. VAWT are used less frequently because their vertical design is not as effective or as efficient as the horizontal design.

Savonius Turbines

This wind turbine is shaped like an "S" and works the same way as a cup anemometer. Wind is captured in its curves, which moves the contraption in a circle.
Pro: It is a much smaller design, which means it can be used as a "small scale" renewable.
Con: The blades have an extremely slow rotation speed, and therefore cannot produce as much electricity as other turbines can.

Flapping Panel Turbines

With this turbine, wind can come from any direction. It is designed with moving panels that are each attached to the base with two poles.
Pro: Wind can hit the turbine from any direction to produce power.
Con: This turbine lacks speed and durability in higher winds.

Darrieus Turbines

This is the most well-known of the VAWTs. It has two to three "C" shaped blades that capture the wind.
Pro: This design is much smaller, so it produces less noise and requires much less space.
Con: They are not self-starting, so they require extra energy to start, and its energy production does not compare to that of a HAWT.

Giromill Turbines

This is powered by three vertical airfoils with horizontal supports.
Pro: This design is extremely inexpensive to make, and it is good in turbulent wind conditions.
Con: Besides the low cost, in comparison, it does not stand up to the energy production of HAWTs.

Overall, the HAWT designs come up on top for their high energy production at the lowest cost. Although VAWT are still useful on a smaller scale, the horizontal design is the best option for large scale wind energy production.

New turbine designs are coming out every day. There are even bladeless turbines now, that only require wind to move through the design, rather than needing the wind to circulate the design. They are even beginning to design turbines based off of how birds fly by using the nature of birds' wings to learn how to better harness energy from wind using less material.

The fact that engineers have found a way to use wind to our human advantage is already impressive. The fact that more and more designs are coming out daily is just a bonus. Soon enough, the most efficient designs will be considered the norm for wind energy production [2].

1.3 Factors affecting the wind power

Many aerodynamic factors affect the wind turbine power generation, such as wind speed, air density and the swept area of the turbine.

1.3.1 wind speed

The wind speed is divided into four categories based on the operation of a wind turbine, Start-up Speed, Cut-in Speed, Rated Speed, and Cut-out Speed; most manufacturers provide graphs, called "power curves," showing how them wind turbine output varies with the wind speed.[3]

1.3.2 Air density

Three factors of effective on-air density are temperature, pressure, and humidity. Air density varies with elevation and temperature; the denser the air, the more energy the turbine receives. The atmosphere is warm air is less thick than cold air and less dense at higher elevations than sea level. Turbines will produce more power at lower elevations and in locations with cooler average temperatures when all else is equal.[3] Any increasing pressure means more air molecules in the given volume. Humidity also plays a critical factor.[4]

1.3.3 The swept area of the turbine

The power that the turbine can capture from the wind increases the more significant the swept area (the size of the area through which the rotor spins), the more power the turbine can capture from the wind.[3]

1.4 The effect of rain on wind power

Zhenlong Wu et al. (2010) [5] studied the effects of rain on vertical axis wind turbine performance by simulating a NACA 0015 vertical axis wind turbine airfoil in rainy conditions using Eulerian-Lagrangian CFD. They found that the rain causes a premature boundary layer separation and causes a significantly lower pressure difference between the lower and upper surfaces than in the dry condition, which is an important cause for the decreases in the lift and tangential force coefficients in the rain. Also, the air velocity in the innermost boundary layer goes through extreme fluctuations.[5]

1.5 The objective of this study

We did not observe designs for turbine types intended for areas with a wet or dry environment where there are only specific indicators of energy production compared to the wind speed in that area. Nor were we able to find data for companies on the effect of weather conditions on turbine performance or losses in energy production and not include these effects in the calculations needed to select the area of spread of wind farms. When selecting sites by companies, only the energy data is measured. It is estimated only by changing the speed, where the only wind is neglected for other changes that have an apparent effect on the energy production of any turbine due to the change in air density, where there is either an increase or decrease in density. It negatively and positively affects the efficiency, life, and capacity of the turbine. Thus, all required analyses must be made when selecting any wind farm area, including the metrological effect. Therefore, we want to study the changes in wind energy if dry air mixes with water molecules. Consequently, we used a two-phase flow Drift-flux model in the atmospheric rainy weather based on the General Directorate of Meteorology data for the year 2017 in Turkey for Mersin Province.

CHAPTER 2

LITERATURE REVIEW

2.1 Introduction

Some researches and studies were made about the assessment of wind power potential and wind turbine performance in rainy weather; all previous research that we found was conducted in laboratories or theoretically, as we will see in this section. This Chapter will be devoted to the summary of previous works done to measure or to estimate two-phase flow rate. Since the motivation of this research focuses on flow rate measurements with differential pressure methods, these methods will be covered extensively.

2.2 Literature survey

Many laboratory studies and research in the analysis of the Drift-flux model have been conducted recently. Hibiki, T., & Ishii, M. (2003) have studied and reviewed the drift-flux in a large diameter pipe [6].

Goda et al. (2003) investigated the drift-flux model for downward two-phase flow for 25.4 mm and 50.8 mm diameter tubes. [7].

Osiptsov et al. (2014) researched the drift-flux model for two-phase flow in a circular pipe [8]. Hibiki (2009) studied the drift-flux in channels with inner diameter ranges between 25.4 mm -60.0 mm [9].

Hibiki, T. et al. looked at the drift-flux model and constitutive equations for relative motion at microgravity conditions. They found that the effect of gravity on the void fraction in a two-phase flow system is more recognizable for low liquid flow conditions. In contrast, the gravity effect may be neglected for high fluid velocity conditions [10].

There is also a study for two-phase flow in small diameter channels ranging from 0.5 to 13.84 mm, in horizontal and vertical directions, for both diabatic and adiabatic conditions, and fluids such as air-water, R410a, R404a, R134a, R290, R12, and R22 obtained by Gardenghi, Á. R et al. (2020) numerically adjusted a new drift flux void fraction correlation with microchannel database include 731 data points ($0.5 < D < 3.0$ mm), then the performance of the new correlation can be complete that the optimization of void fraction correlations for small scale diameters channels has not yet reached the limit. There is still space for advancement for new correlations [11]. Another numerical study obtained by Zou, L. et al. (2016) presents a numerical review on using the Jacobian-free Newton-Krylov (JFNK) method to solve the two-phase flow four-equation drift flux model for vertical channel flow, such as two-phase flow pressure drop, flow regime map, wall boiling, and interfacial heat transfer models, were taken from the RELAP5-3D Code Manual and included to fill up the model [12].

Sahin AZ. Besides that, there are many types of research on wind energy according to two-phase flow such as Öztopal, A. et.al. (2000), they presented wind speed energy maps of Turkey, and the potential areas are indicated that along the Aegean and the Black Sea, coastal areas wind energy generation amounts are higher in Winter than in summer [13].

Abdul-Kareem (2015) demonstrated that the influence of moisture is still limited on the wind energy at average annual extracted the minimum altitude that was used in the power plant of Nasiriyah (44m for α=0.3 and 32m for α=0.4) [14].

The analysis of the different nature conservation criteria effect on the wind energy potential in quantitative terms has been developed by W. Krewitt and J. Nitsch [15].

Aksakal A. (1998) have investigated the wind energy potential for the northeastern and eastern regions of Saudi Arabia based on a whole year's data at coastal locations [16].

Danook, S. et.al. studied the extracted power loss outside the wind turbine as an electricity production of renewable energy due to the humidity at Kirkuk city north of Iraq during winter and summer seasons and noted that the frequency spread across the ranges. Still, a higher percentage appears in 46% and 80% [17].

The Wind Power Density for all meteorological stations in Ninawa Governorate has been expressed Air Temperature, Relative Humidity, Sunshine, Air pressure, Height, Cloudiness, Solar Radiation applying a variety of Regressions Models by Hamam, F. et.al [18]. Thompson, B. E. et.al; studied the impact of rain on the wing, noted the spray of the tiny and fine droplets that are splashed back would slow down the boundary layer, and this can change the flow stream of air over the wing, increasing drag and decreasing the Lift [19]. The effect of temperature on the energy extracted from wind power as electric energy was studied during the three years 2011-2013 for the city of Nasiriyah in southern Iraq, the study shows that the air temperature in this region affects the energy extracted from the wind, and this effect depends on the height and value of the temperature, the average annual percentage of energy loss decreases as the height increases. Average yearly values for power loss range from 6.1% watts at 40 meters height to 2.6% watts at 300 meters height studied by Abdul Kareem, M.S. (2015) [20].

Lorenzi and Muzzio's, study was to develop a rational relationship on basis of the total energy equation for the total mass flow rate of the mixture. For a given pressure drop and gas-mixture mass ratio, they introduced a correction factor which permitted the prediction of the two-phase flow rate. In the experimental part of the study, air-water mixture was tested in a 36 mm pipe while fre quality was between 0.00065% and 0.102%. Water flow rate was varied between 0.18 and 1.48 kg's. Diameter ratio ofthe orifices were 0.29, 0.45 and 0.56. The experiments were restricted to bubbly flow regime in order to cancel out the effect of flow regime on the correction factor [21].

Also, Lorenzi and Muzzio, examined air-water mixtures through venturi meters in 1979. The theoretical interpretation of the experimental results based on the physical description of the flow, in terms of one-dimensional total mass balance and energy equations, showed that the data can be satisfactorily predicted by means of a simple correlation for void fraction at the throat. The water flow rates were ranging between 0.69 and 1.67 kg's and tested quality values were smaller than 0.467%. At the end of the study, the authors stated that obtaining the data at fixed geometry and practically constant physical properties of the fluids lacks the allowance for die effect of these parameters and more data are required for generalization [22]. In 1982 Reimann, John, and Müller, presented a study for comparing different flow rate measuring systems in two-phase flow. The particular systems investigated include the true mass flow meter (TMFM); the radionuclide technique, the combination of a free field drag disk-turbine meter-transducer (DTD and a gamma densitometer; and the combination of a venturi nozzle and a full flow turbine meter. The experiments were performed under similar conditions in steady-state steam-water flow and test matrix included wave, slug and annular flow regimes. The conclusion of this study reflected that the accuracy of last two methods is distinctively dependant on phase distribution and calibration is required for every geometry. Also, TN'IFM was the only device which measures directly the two-phase mass flow rate [23].

Salcudean, Groeneveld, and Leung, reported an interesting study in 1983 on the effect of flow obstruction geometry on pressure drops in horizontal air-water flow. Measurements have been carried Out for two different flow blockages and Six obstruction shapes. Among many conclusions, the most important one was the pressure drop the obstructions in two-phase flow was found to depend strongly on the kinetic energy and momentum of the liquid intercepted by the flow obstruction, i.e. the contribution Of liquid phase on pressure drop was greater. In addition, it was also seen that buoyancy induced flow stratification caused a strongly non-symmetrical effect, and resulted in large pressure drops for flow obstructions located in the bottom part of the channel [24].

The studies on globe and gate valves were extended to two-phase flows in 1998. Banerjee and S. K. Das, performed experiments to evaluate the two-phase pressure drop across half-inch valves. Mixture of air and different concentrations of dilute solutions were utilized. Experimental data were correlated in an acceptable accuracy. Resulting generalized equations showed that two-phase pressure drop across the valves depends on Reynolds numbers of both phases, valve opening and fluid properties [25].

One of recent studies of Samanta, Baneöee and Das, reported gas and non-Newtonian flow across orifices. Orifices of diameter ratios 0.465, 0.598, and 0.709 were tested in a pipe of 12.7 mm internal diameter. Experimental investigations were followed with a dimensional analysis and data were correlated. Two-phase flow loss multiplier was found in terms of Reynolds numbers of each phase, diameter ratio and dimensionless liquid property group. The generalized equation is valid for Reynolds numbers of 45 to 2200 for liquid phase and 230 to 2200 for gas phase [26].

So, we used a two-phase flow Drift-flux model in the atmospheric rainy weather based on the General Directorate of Meteorology data for the year 2017 in Turkey for Mersin Province, as will show in next chapters.

CHAPTER 3

THEORY

3.1 Introduction

A mathematical explanation of the winds is almost quickly done by considering the momentum balance of the atmosphere. So, this chapter explains the idea for using drift-flux two-phase flow to find the kinetic energy and air density and then find the available power in the wind. Also, the laws of thermodynamics, the ideal gas laws, are used to find the density of dry air and find the available energy hypothesis when it is only dry air to see the difference between them. Below is a guiding explanation of the mechanism of work in this research to find the available energy to set the laws and find the drift-flux density and dry air and then apply them to turbines and find the resulting difference in energy extraction in terms of two conditions. Based on this theory, this theory obtained accurate data on the impact of atmospheric changes on the turbine's performance and the extent of the variation of kinetic energy in the wind.

3.2 Two-Phase Drift-flux Model

The basic idea of the drift-flux model is to consider the mixture as a whole rather than two phases separately, and it takes into account the presence of a relative velocity. The drift-flux model formulation will be more straightforward than the two-fluid model. However, it requires some constitutive severe assumptions that lead to the loss of some of the dominant characteristics of two-phase flow. It is totally this simplicity of the drift-flux model that makes it very practical in many engineering applications. As is the case with the analyses of two-phase flow system dynamics, information required in engineering problems is often the response of the total mixture and not of each essential phase. The most important aspect of the drift-flux model is reducing the number of field and constitutive equations required in the formulation compared to the two-fluid model [20]. Consider a class of models of multiphase flows in which the relative motion between the phases is governed by a particular subset of the flow parameters. The members of this subset are called drift flux models. To define the subset, consider the one-dimensional flow of a mixture of the two components, 1 and 2. The volumetric fluxes of the two components, j_1 and j_2, are related to the total volumetric flux,j , the drift flux, j_{12}, and the volume fraction $\alpha = \alpha_1 = 1 - \alpha_2$, by [27]

$$j_1 = \alpha j + j_{12} \;;\; j_2 = (1 - \alpha) j - j_{12} \tag{3.1}$$

The drift-flux model is expressed in four field equations: the mixture continuity, momentum; energy equations; and the gas continuity equation [28].

The mixture continuity equation:

$$\frac{\partial \rho_m}{\partial t} + \nabla(\rho_m v_m) = 0 \tag{3.2}$$

The continuity equation for phase 2:

$$\frac{\partial\, \alpha_2 \bar{\bar{\rho}}_2}{\partial t} + \nabla(\alpha_2 \bar{\bar{\rho}}_2 v_m) = \Gamma_2 - \nabla(\alpha_2 \bar{\bar{\rho}}_2 V_{2m}) \tag{3.3}$$

The mixture momentum equation:

$$\frac{\partial \rho_m v_m}{\partial t} + \nabla(\rho_m v_m^2) =$$

$$-\nabla \rho_m + \nabla \left| \bar{\mathfrak{G}} + \mathfrak{G}^T - \sum_{k=1}^{2} \alpha_k \bar{\bar{\rho}}_k V_{km}^2 \right|$$

$$+ \rho_m g_m + M_m \tag{3.4}$$

And the thermal energy equation:

$$\frac{\partial \rho_m v_m}{\partial t} + \nabla(\rho_m i_m v_m) = -\nabla(\bar{q} q^T)$$

$$-\nabla\left(\sum_{k=1}^{2} \alpha_k \,\bar{\bar{\rho}}_k \hat{\imath}_k V_{km}\right) + \frac{Dp_m}{Dt}$$

$$+\Phi_m^{\mu}\Phi_m^{\sigma}\Phi_m^{i} \tag{3.5}$$

3.2 Application of the Drift-flux Model Two-Phase Flow on Standard Wind power

A wind First, we will explain the difference between the Homogeneous model two-phase and Drift-flux model yow-phase. The basis of the Homogeneous model is that the velocities of both fluids (1,2) are homogeneous and, therefore, equal, which means in rainy weather, consider that both air dry and rain velocities are equal [29]. In the case of the Drift-flux model, the basis is to consider a relative velocity between the velocity of the first fluid and the velocity of the second fluid, in addition, the void fraction on drift-flux will be [29]:

$$\alpha_D = \frac{1}{C_o}\alpha_H \tag{3.6}$$

Where α_H Is a Homogeneous model void fraction.

Based on what was mentioned above, in the beginning, we will explain the method of calculating the α_H for each hour of each day of the year 2017, obtained from the Directorate General of Meteorology in Turkey for Mersin province obtained by Alwindawi, Z. [4].

When air is wet, it means that it contains a quantity of water vapor, so the atmospheric air in this condition is the two-phase case and considers there is a relative velocity between two phases, a single-phase equation for continuity, momentum, and energy can apply by replacing the fluid propriety with mixture property as following [28]:

$$\rho = \alpha\rho_{dry} + (1-\alpha)\rho_v \tag{3.7}$$

According to the ideal gas law, the density of dry air is:

$$\rho_{dry} = \frac{P_{dry}}{R_a\ T_{Atm}} \tag{3.8}$$

From T_{Atm} finding the saturation pressure of the vapor P_g from thermodynamics table and then from relative humidity and saturation pressure of vapor, find the pressure of vapor:

$$P_v = \emptyset P_g \tag{3.9}$$

Then from the pressure of vapor and atmospheric pressure obtained from metrology data, find the pressure of dry air:

$$P_{dry} = P_{Atm} - P_v \tag{3.10}$$

After calculating the density of dry air (equation 3.8), it's necessary to calculate the vapor density in the atmosphere to obtain the density of mixture air (atmosphere) thus from the pressure of vapor, the temperature of the atmosphere, and constant of vapor R_V calculate the density of vapor:

$$\rho_v = \frac{P_v}{R_v\ T_{Atm}} \tag{3.11}$$

Using Colebrode-white Equation to find the humidity ratio (ω):

$$\omega = \frac{mas\ of\ vapor}{mass\ of\ dry\ air} \tag{3.12}$$

$$M_v = \frac{P_v\, V}{R_v\ T} \tag{3.13}$$

$$M_{dry} = \frac{P_{dry}\, V}{R_a\ T} \tag{3.14}$$

$$\frac{R_a}{R_v} = 0.622 \tag{3.15}$$

$$w = 0.622 \frac{P_v}{P_{dry}} \tag{3.16}$$

The volumetric concentration is defined as the ratio between volumetric vapor flow and total volumetric flow in a given cross-section.

$$\alpha_H = \frac{Q_v}{Q_v + Q_{dry}} \tag{3.17}$$

From humidity ratio, ω find the balance between the volume flow rate of vapor and dry and substituted it in the volume concentration equation.

$$\omega = \frac{\rho_v \, Q_v}{\rho_{dry} \, Q_{dry}} \tag{3.18}$$

$$\frac{Q_v}{Q_{dry}} = \frac{\rho_{dry} \, \omega}{\rho_v} \text{ substitute in Equation (3.17)}$$

So, now the Homogeneous model void fraction calculations are done.

Here comes the role of the Equation as mentioned above (3.6), which states that $\alpha_D = (1/C_o)\alpha_H$ to find the value of the void fraction of the drift-flux model as following [29]:

$$\alpha_D = (1/C_o)\alpha_H \tag{3.18}$$

Note: when $C_o = 1$ means that there is no relative velocity between the phases, so the drift-flux model does not exist so that a homogeneous model will apply.

Now, according to Serio et.al (2019) [30], the terminal velocity of rainfall

$$V_D = \alpha' \quad D \exp(-\beta' \quad D) \tag{3.19}$$

The constants α'and β' are equal to 48.74 and 1.95 (Uplinger,1981) [31]. Leone and Pica (1993) [32], using raindrop terminal velocity measurements carried out in the laboratory by Beard (1976) [33], Laws (1941) [34], and Gunn and Kinzer (1949) [35], estimated α'=49 and β' = 2. Taking into account that for D < 0.10 cm, the drop has a slow terminal velocity and small mass-producing a negligible kinetic power, and for D > 0.55 cm, the raindrops are unstable and tend to break up before reaching their terminal velocity (Pruppacher and Pitter, 1971) [36], Leone and Pica (1993) [32] considered only raindrops having a diameter varying in the range 0.10–0.55 cm.

Now, to calculate drift-flux density, it's necessary find values of volumetric flux of each phase, using the formulas that taken from Wallis, G. B. (2020). [29]:

$$j_{21} = V_D \, \alpha_D \, (1 - \alpha_D)^n \tag{3.20}$$

Where n is a function of Reynolds number.

$$j_1 = V_W \, \alpha_D \tag{3.21}$$

$$j_2 = V_D\ \alpha_D \tag{3.22}$$

$$j = j_1 + j_2 \tag{3.23}$$

Now it's easy to calculate the drift-flux density (mean density) [29]:

$$\rho_D = \frac{j_1\,\rho_1 + j_2\,\rho_2}{j} + (\rho_1 - \rho_2)\frac{j_{21}}{j} \tag{3.24}$$

found from the following Equation, the power available in the wind (kinetic energy) can be found:

$$P_{in} = \frac{1}{2} A\rho V^3 \tag{3.25}$$

Where ρ is the air density, A is the swept area, and V is the wind speed. So, through this Equation, extract the power available in the wind in the first use the density of dry air and in the second use the density of the mixture, drift-flux density and through them have extracted the power deviation as the rate of change in the kinetic energy from dry air density to the mix (atmosphere) density according to metrology condition.

$$P_{in\ dry} = \frac{1}{2} A\rho_{dry} V^3 \tag{3.26}$$

$$P_{in\ atm} = \frac{1}{2} A\rho_D V^3 \tag{3.27}$$

$$\lambda = \frac{P_{in\ dry} - P_{in\ atm}}{P_{in\ dry}} \tag{3.28}$$

Or

$$\lambda = \frac{\rho_{dry} - \rho_D}{\rho_{dry}} \tag{3.29}$$

The variability of wind power will be an increasing challenge for the power system as wind penetration grows and thus needs to study. Therefore, from Equation (28) find the deviation of kinetic power of wind when supposition the wind is dry and when the wind is atmospheric according to the drift-flux flow.

CHAPTER 4

WIND POWER ANALYSIS ACCORDING TO DRIFT-FLUX MODEL

4.1 Introduction

To decide the best suitable site for installing a wind farm and select the turbine model suited for any location. It is necessary to perform an accurate wind energy resource estimate. The statistical characteristics of wind power have been analysed using meteorology data recorded by the General Directorate of Meteorology in Ankara for Mersin city in Turkey for the 2017 year. Assuming the weather is rainy, with raindrop $D = 0.1$ (cm), throughout the year to show analysis output clearly. In this chapter, the rate of wind power will be analysed for each season and one year. The meteorology data in the Excel program was analysed using the equations that were complete in chapter three, as it resulted in 12 monthly tables. An annual schedule explains the change in the rate of wind power and then compares it with wind power when hypothesis the density of air is dry.

4.2 Seasonally Wind Power Analysis According to Two-phase flow Drift-flux Model

The analysis for four seasons in 2017 is as follows:

Table 4.1 Wind power analysis and power deviation for four seasons in 2017

Season	Temp(°c)	Ø %	V (m/s)	Patm(pa)	Pg (pa)	P dry (pa)	Pv (pa)	ω	ρ (dry)	ρ (v)	α(D)	Vd	Vr	ρ(D)	λ
Winter	11.95119	47.57292	1.106399	102108.1	1447.843	101427.1	680.9842	0.004179	1280.712	5.164082	2.59E-05	4.011781	2.905382	1009.44	26.87355
Spring	18.67581	60.25682	1.465282	101282.6	2211.742	99971.9	2376.355	0.008248	1233.191	9.71601	9.44E-05	4.011781	2.546498	914.5097	34.86044
Summer	28.67912	64.52612	1.478538	100573.4	3974.871	98032.9	2557.062	0.016236	1169.542	18.23123	0.000416	4.011781	2.526549	859.4914	36.08928
Autumn	22.62071	52.32554	1.05667	101341.1	2876.304	99815.39	1504.924	0.009415	1215.389	10.82483	0.000142	4.011781	2.960566	967.9923	25.83705
Average	20.50751	57.44594	1.266561	101293.9	2633.276	99759.25	1797.666	0.009648	1223.921	11.13697	0.000169	4.011781	2.734749	937.8583	30.91508

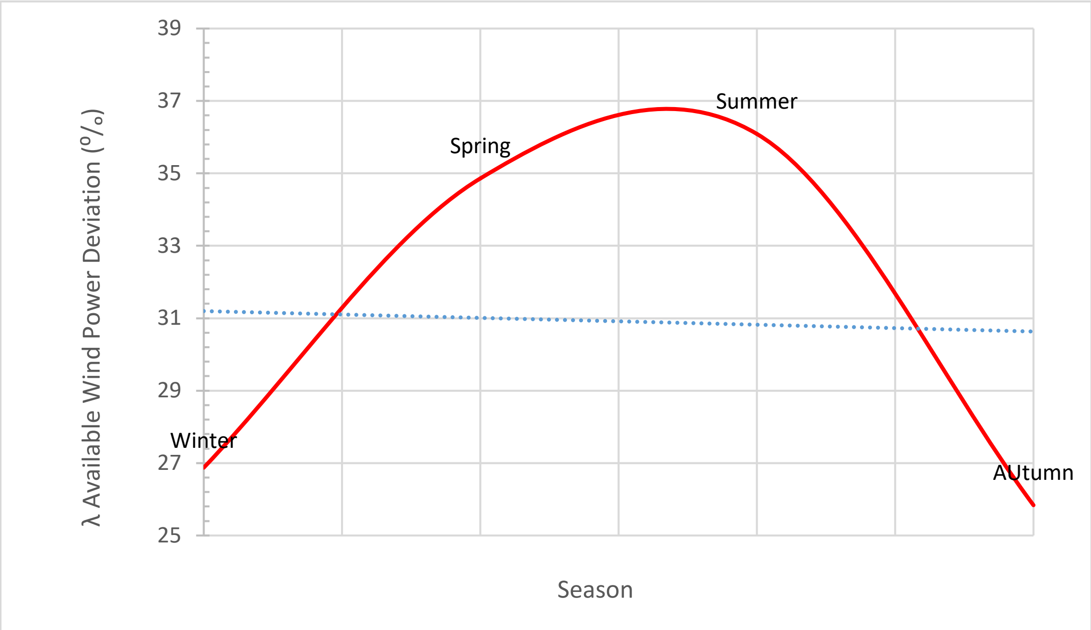

Figure 4.1 Wind power deviation with seasons in 2017

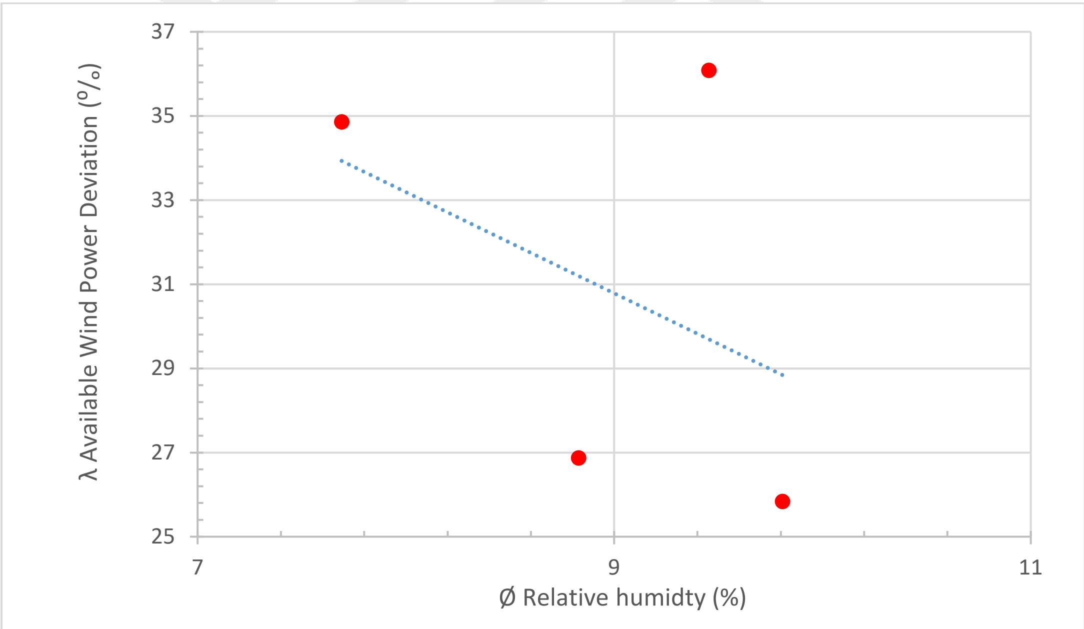

Figure 4.2 Wind power deviation with relative humidity along the seasons in 2017

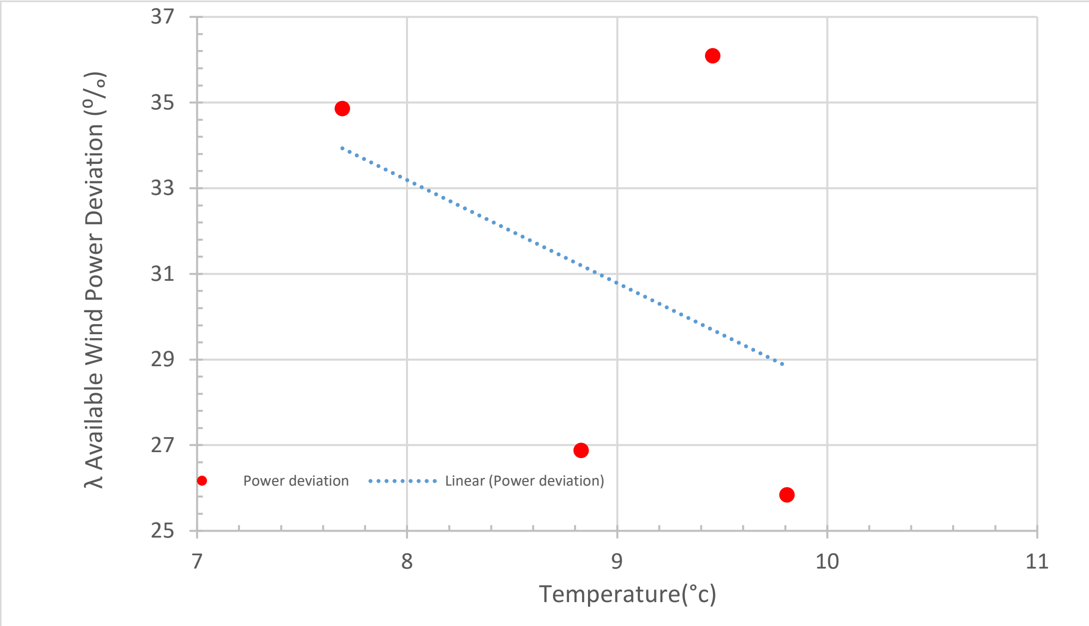

Figure 4.3 Wind power deviation with temperature along the seasons in 2017

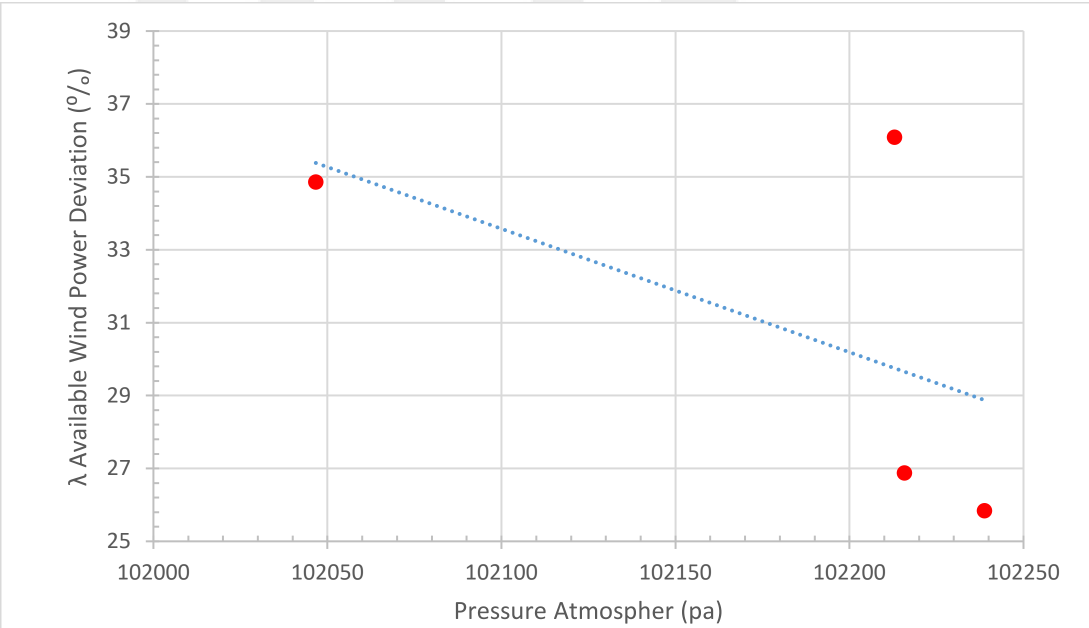

Figure 4.4 Wind power deviation with the atmospheric pressure along the seasons in 2017

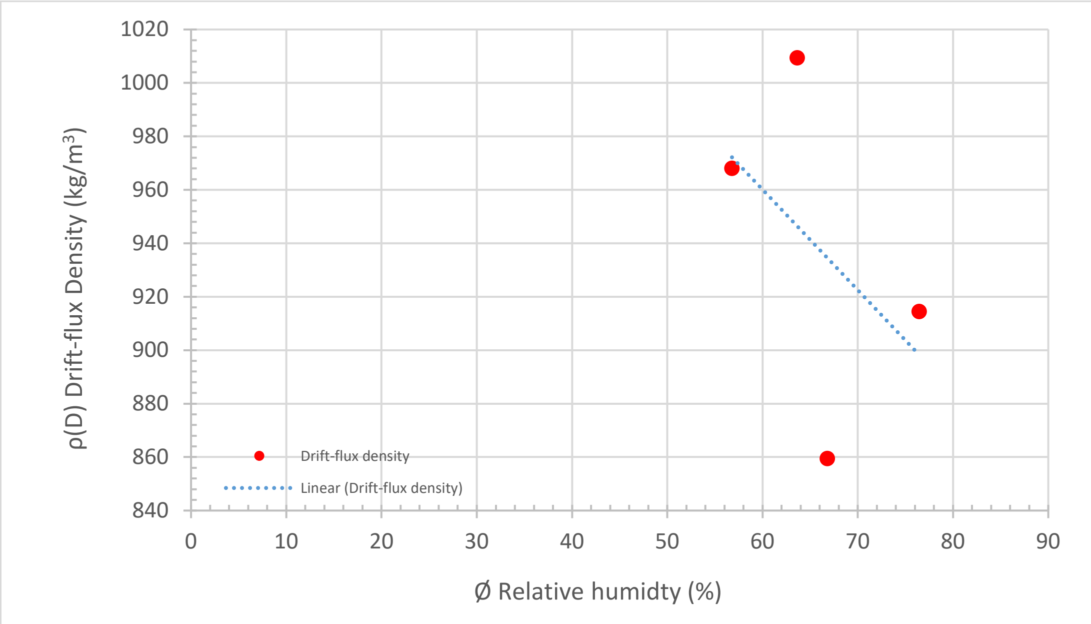

Figure 4.5 Drift-flux density changes with the humidity along the seasons in 2017

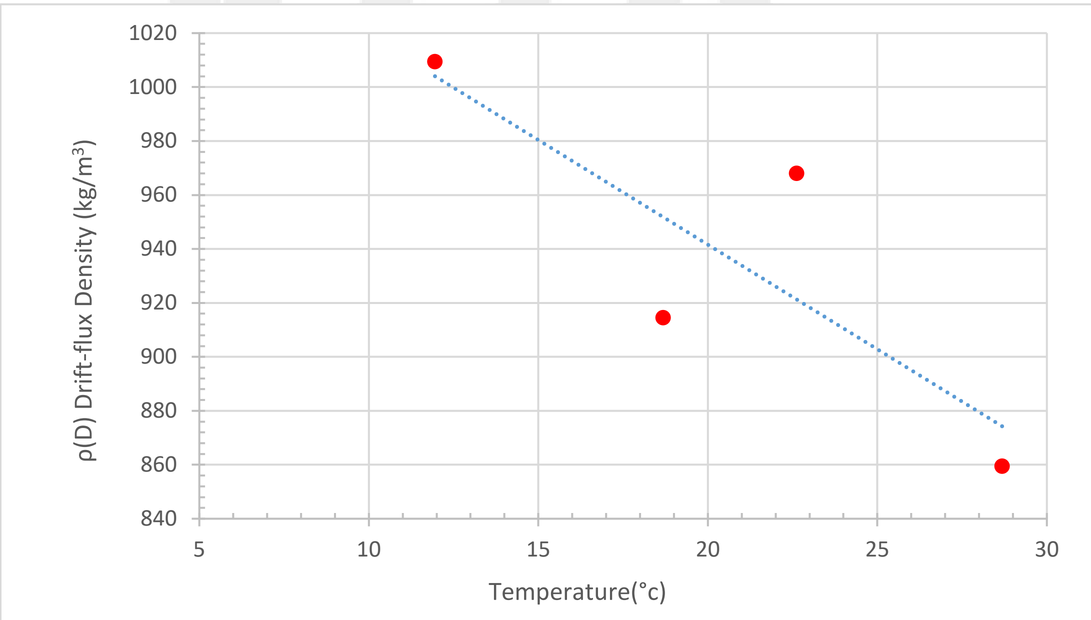

Figure 4.6 Drift-flux density changes with the temperature along the seasons in 2017.

Any rising in deviation means reducing available wind power in the atmosphere. This increasing and decreasing deviation are due to increasing or dropping in temperature, relative humidity, and atmospheric pressure. As can be seen from Figure 4.1 that the maximum power deviation appears in Summer while the minimum deviation occurs in Winter. The deviation of the wind power increases gradually from the winter season through the spring to reach its highest value in the summer. It then begins to decrease significantly in the autumn season. During the summer, the average temperature is 28.67°C, and relative humidity at 64.52% makes an increase in water vapor content to 18.23 g/m³ while Winter, the temperature is at a low value of 11.95 °C and relative humidity at 47.57 %, making the moisture content low at 5.16 g/m³. In comparison, which makes the air more moisture content with the rain existence, known as water vapor, has less weight from other content.

4.3 Wind Power Analysis According to Two-phase flow Drift-flux Model Throughout 2017

Table 4.2 Wind power analysis and power deviation throughout 2017

Month	Temp(°c)	Ø %	V (m/s)	Patm(pa)	Pg (pa)	P dry (pa)	Pv (pa)	ω	ρ (dry)	ρ (v)	α(D)	Vd	Vr	ρ(D)	λ
January	9.656048	55.61022	1.119489	101891.8	1224.84	101223.3	668.6253	0.004113	1288.361	5.123324	2.37E-05	4.011781	2.892291	1012.907	27.1944
February	11.95119	47.57292	1.106399	102108.1	1447.843	101427.1	680.9842	0.004179	1280.712	5.164082	2.59E-05	4.011781	2.905382	1009.44	26.87355
March	15.50484	58.18145	1.390726	101316.2	1793.95	100302.9	1026.312	0.006367	1250.743	7.607542	5.43E-05	4.011781	2.621055	935.999	33.62656
April	18.65458	58.05139	1.550417	101414.8	2191.832	100185.2	1244.543	0.007733	1235.808	9.133142	8.16E-05	4.011781	2.461364	910.4897	35.72999
May	21.86801	64.53763	1.454704	101116.9	2649.445	99427.68	4858.21	0.010644	1213.021	12.40735	0.000147	4.011781	2.557076	897.0405	35.22478
June	25.97028	67.09583	1.529028	100875.2	3385.644	98614.93	2273.898	0.01435	1186.609	16.36944	0.000268	4.011781	2.482753	865.8335	37.04822
July	30.05726	63.70699	1.528763	100238.3	4278.33	97538.3	2722.937	0.01737	1159.22	19.30052	0.000568	4.011781	2.468586	843.1796	37.48198
August	30.00981	62.77554	1.377823	100606.7	4260.639	97945.48	2674.35	0.016988	1162.796	19.02375	0.000411	4.011781	2.628308	869.4609	33.73763
September	28.01528	59.1625	1.090972	101021.1	3819.095	98761.56	2259.522	0.014249	1180.316	15.81894	0.000274	4.011781	2.920808	932.9657	26.51226
October	22.79005	44.74328	1.003898	101328.8	2818.052	100024.7	1241.587	0.007727	1217.316	9.085802	9.79E-05	4.011781	3.025114	980.565	24.39417
November	17.05681	53.07083	1.075139	101673.6	1991.765	100659.9	1013.663	0.006269	1248.535	7.569748	5.43E-05	4.011781	2.935775	990.4462	26.6047
December	14.55591	54.84274	0.971371	101935.4	1737.877	101000	907.3648	0.005787	1263.612	7.040051	6.37E-05	4.011781	3.038864	1022.998	24.05819
Average	**20.50751**	**57.44594**	**1.266561**	**101293.9**	**1737.877**	**99759.25**	**1797.666**	**0.009648**	**1223.921**	**11.13697**	**0.000172**	**4.011781**	**2.744781**	**939.2771**	**30.7072**

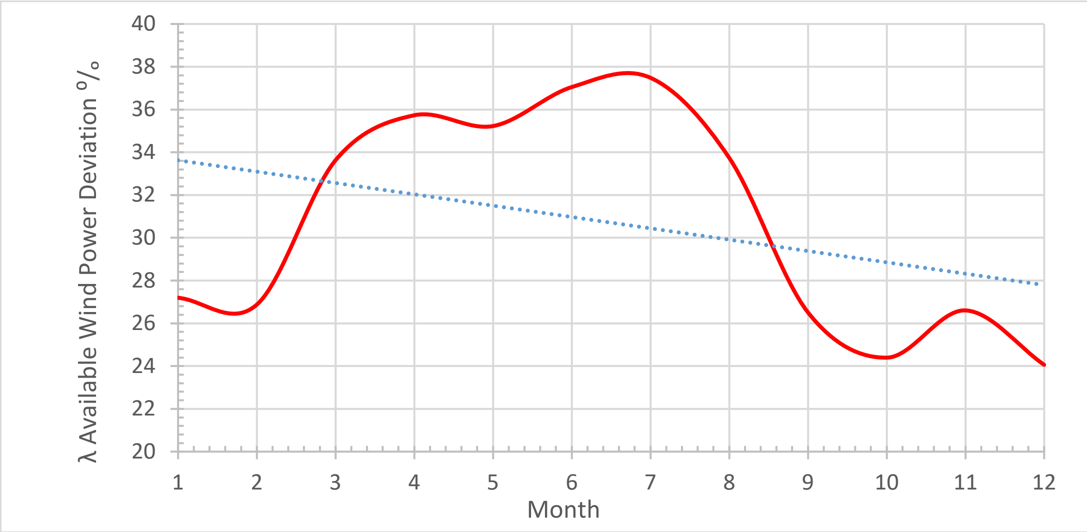

Figure 4. 7 Wind power deviation with months throughout 2017

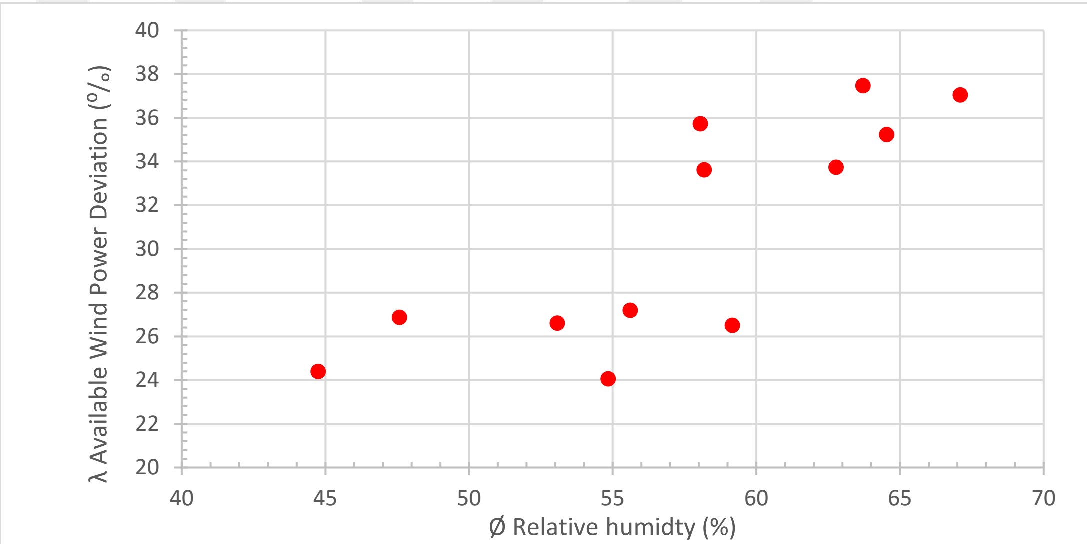

Figure 4.8 Wind power deviation with relative humidity throughout 2017

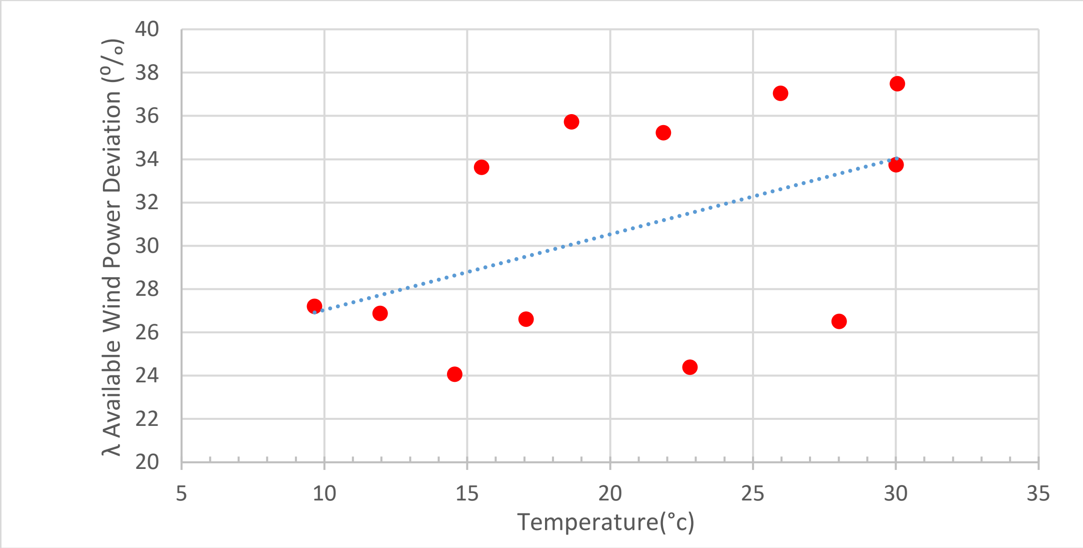

Figure 4.9 Wind power deviation with temperature throughout 2017

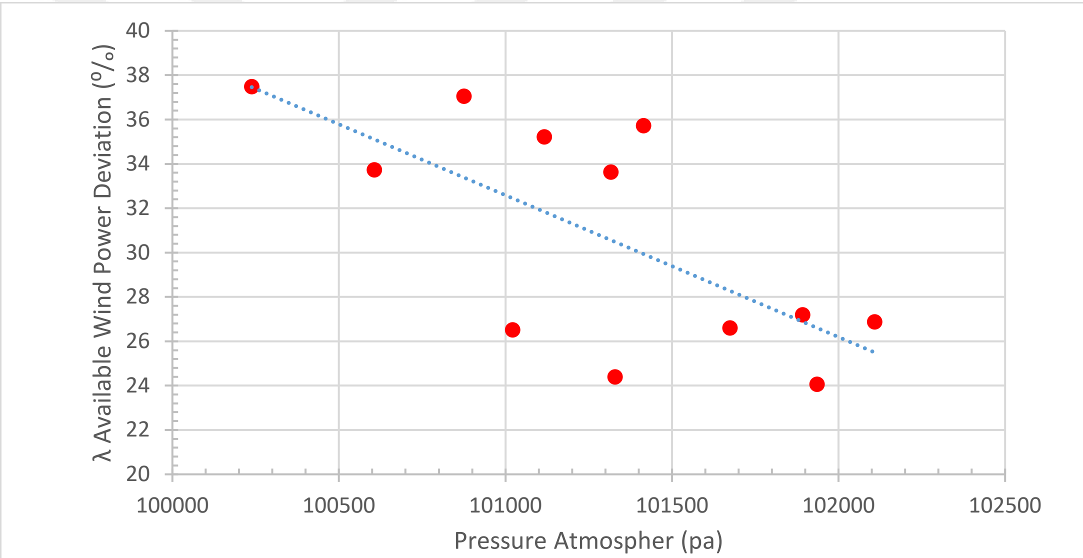

Figure 4.10 Wind power deviation with atmospheric pressure throughout 2017

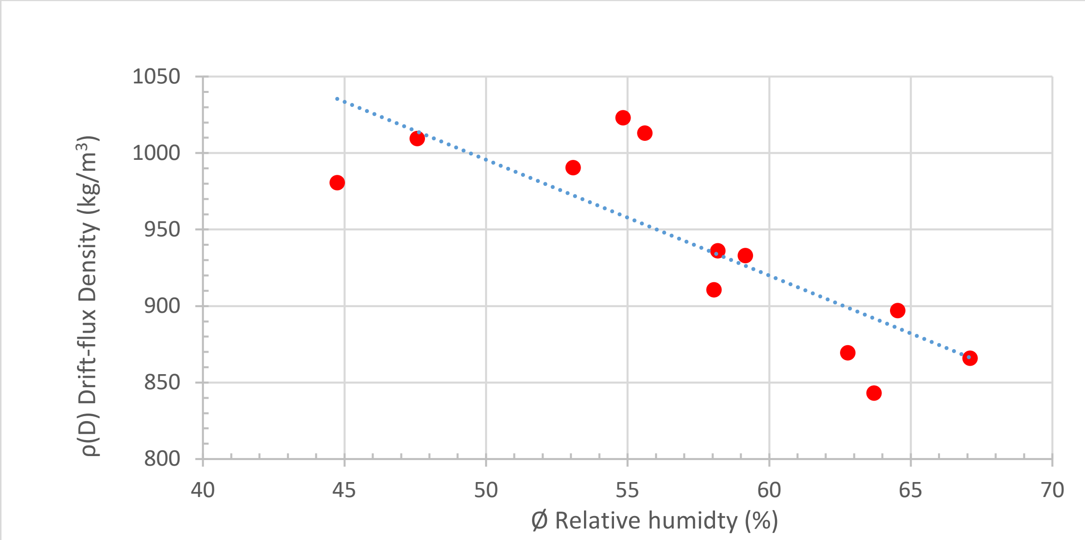

Figure 4.11 Drift-flux density changes with the humidity throughout 2017

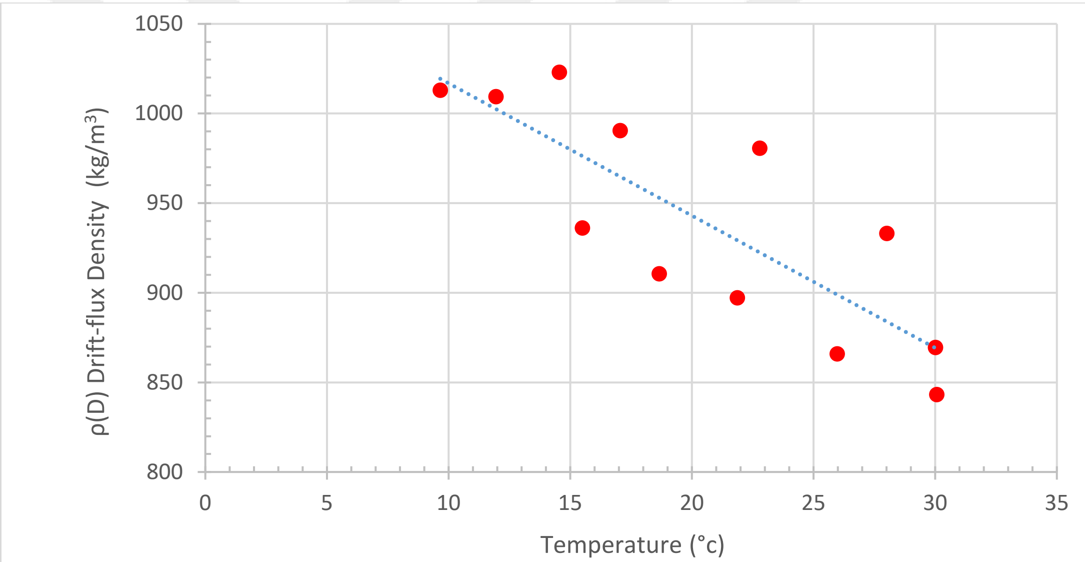

Figure 4.12 Drift-flux density changes with the temperature throughout 2017

We can notice through Figure 4.7 minimum deviation of 24.05 is in December, while the maximum wind power deviation occurs in July at approximately 37.48. Generally, a higher monthly deviation means more moisture content, guiding a decrease in available wind power in these months. The power deviation increases gradually from January until reaching the max deviation in July and always decreases to December. The reason for rising in deviation in July is growing seriously in temperature. Relative humidity, which reaches 30.5°C, 63.7%, respectively due to the increase in the amount of water vapor in the air to 19.3 g/m, as shown in Figure 4.8. Figure 4.78 indicates that when the temperature rose to 30.5°C, the atmospheric density decreased to a minimum value along the 2017 year. Because of rising in temperature from 25°C to 30°C in Jun and July, the amount of water vapor increases from 25°C to 30°C, eve the relative humidity is almost the same average for both months. Any increase in the amount of water vapor makes the density of the airless dense from dry air due to replacing nitrogen and oxygen with water vapor decreases the weight of the air in the cubic foot; that is, its density decreases.

We notice the deviation more precisely when we calculate the data for each month over the days for that month, for example January due to fluctuation in humidity and relative speed despite the low temperatures and as follows:

Table 4.3 Wind Power Analysis According to Two-phase flow Drift-flux Model in January

Day	Temp(°c)	Ø %	V (m/s)	Patm(pa)	Pg (pa)	P dry (pa)	Pv (pa)	Ѡ	ρ (dry)	ρ (v)	α(D)	Vd	Vr	ρ(D)	λ
1	8.829167	63.625	1.420833	102215.8	1151.72	101495	723.78	0.004491	1295.559	5.535062	2.55E-05	4.011781	2.590947	958.1217	35.21859
2	7.691667	76.45833	1.741667	102046.7	1051.679	101244.3	804.0959	0.00494	1297.47	6.194382	3.14E-05	4.011781	2.270114	906.5311	43.12475
3	9.454167	66.79167	0.766667	102212.9	1196.045	101430.9	782.0139	0.004796	1291.822	5.999379	2.97E-05	4.011781	3.245114	1085.443	19.0133
4	9.808333	56.79167	0.9	102238.8	1230.017	101544.6	694.114	0.004252	1291.679	5.31332	2.37E-05	4.011781	3.111781	1055.916	22.32777
5	9.408333	79.08333	1.6875	102256.3	1181.977	101323.1	933.1898	0.005729	1290.584	7.160295	4.27E-05	4.011781	2.324281	910.5083	41.74328
6	12.57083	62	1.895833	101876.3	1466.671	100983.2	893.0386	0.005501	1272.072	6.777156	3.97E-05	4.011781	2.115947	865.9678	46.896
7	11.2125	71.08333	1.25	101103.8	1333.931	100161.7	942.0965	0.00585	1267.698	7.183652	4.61E-05	4.011781	2.761781	968.1564	30.93943
8	9.595833	79.66667	1.320833	100617.5	1197.942	99666.93	950.5721	0.005932	1268.665	7.288363	4.57E-05	4.011781	2.690947	956.1477	32.68502
9	8.0125	72.54167	1.516667	101255	1081.121	100474.7	780.3043	0.004831	1286.208	6.014056	3.04E-05	4.011781	2.495114	934.9486	37.56991
10	6.845833	69.66667	1.6125	102028.8	995.7071	101333.7	695.0329	0.004266	1302.569	5.378925	2.43E-05	4.011781	2.399281	930.6196	39.96789
11	10.2	65.33333	1.191667	102512.9	1261.923	101709.2	803.7332	0.004915	1291.981	6.148264	3.13E-05	4.011781	2.820114	997.441	29.5296
12	10.85833	53.25	0.975	102154.2	1317.054	101461	693.1294	0.004249	1285.869	5.286947	2.38E-05	4.011781	3.036781	1035.438	24.18602
13	10.04167	59.66667	1.025	101727.9	1246.258	101004.6	723.3168	0.004454	1283.734	5.538397	2.56E-05	4.011781	2.986781	1023.559	25.41865
14	9.104167	47.45833	0.895833	101707.9	1165.243	101173.1	534.7679	0.003288	1290.121	4.111365	1.42E-05	4.011781	3.115947	1055.338	22.24712
15	10.63333	44.125	1.029167	101849.2	1301.844	101291.9	557.3031	0.003422	1284.738	4.256972	1.53E-05	4.011781	2.982614	1023.279	25.55117
16	10.19167	52.95833	0.45	102200.8	1254.461	101544	656.8784	0.004024	1289.889	5.024393	2.09E-05	4.011781	3.561781	1160.238	11.17457
17	12.09167	46.875	0.916667	102002.9	1428.649	101351	651.9255	0.004001	1278.892	4.955231	2.07E-05	4.011781	3.095114	1041.896	22.74655
18	12.85833	49.625	0.745833	101897.1	1507.324	101162.3	734.7685	0.004518	1273.117	5.565229	2.7E-05	4.011781	3.265947	1074.338	18.50255
19	11.69167	54.08333	0.625	102213.8	1400.34	101475.5	738.2587	0.004525	1282.314	5.762855	2.66E-05	4.011781	3.386781	1110.171	15.506
20	11.44167	55.45833	0.808333	102062.9	1373.638	101315.1	747.7822	0.004591	1281.396	5.692042	2.81E-05	4.011781	3.203447	1067.389	20.04959
21	10.1125	53.25	0.933333	102003.8	1255.751	101344.9	658.8779	0.004044	1287.78	5.038319	2.16E-05	4.011781	3.078447	1045.625	23.1588
22	9.183333	52.25	0.775	102362.9	1185.549	101756.2	606.6956	0.003709	1297.299	4.653566	1.82E-05	4.011781	3.236781	1087.966	19.24071
23	9.170833	48.20833	0.670833	102495.8	1187.447	101946.7	549.1655	0.003351	1299.794	4.215888	1.46E-05	4.011781	3.340947	1114.148	16.66256
24	11.675	31.66667	1.05	102142.5	1398.499	101712.2	430.2707	0.002631	1285.396	3.27315	9.1E-06	4.011781	2.961781	1019.416	26.09142
25	14.01667	37.20833	1.508333	101315	1617.104	100716.6	598.3701	0.003695	1262.362	4.513045	2.03E-05	4.011781	2.503447	918.6289	37.41809
26	11.17083	58.66667	1.0375	101191.3	1334.534	100404.6	786.6987	0.004874	1271.003	5.993757	3.15E-05	4.011781	2.974281	1011.005	25.71677
27	7.129167	61.95833	1.0125	100925	1017.956	100296.8	628.21	0.003896	1287.96	4.856715	1.99E-05	4.011781	2.999281	1029.341	25.12466
28	5.7625	34.83333	1.083333	101540.8	933.739	101228.6	312.2529	0.001919	1306.351	2.428418	4.95E-06	4.011781	2.928447	1029.098	26.94145
29	5.916667	46.83333	1.216667	102437.5	945.0705	102002.2	435.2777	0.002654	1315.636	3.378104	9.44E-06	4.011781	2.795114	1010.252	30.2285
30	7.283333	39.79167	1.166667	102062.9	1041.251	101674.2	388.6858	0.002378	1305.036	3.008738	7.41E-06	4.011781	2.845114	1011.683	28.99656
31	5.375	32.70833	1.475	101986.7	909.5999	101693.9	292.7786	0.001791	1314.208	2.277069	4.69E-06	4.011781	2.536781	961.5159	36.68086
Average	9.656048	55.61022	1.119489	101891.8	1224.84	101223.3	668.6253	0.004113	1288.361	5.123324	2.37E-05	4.011781	2.892291	1012.907	27.1944

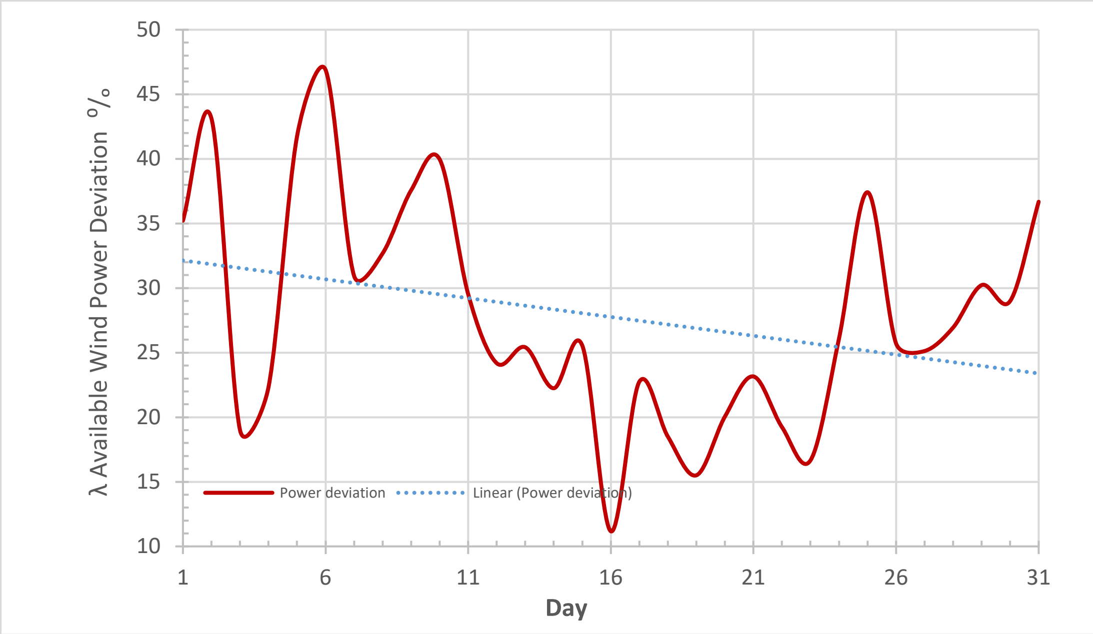

Figure 4.13 Wind power deviation with days in January

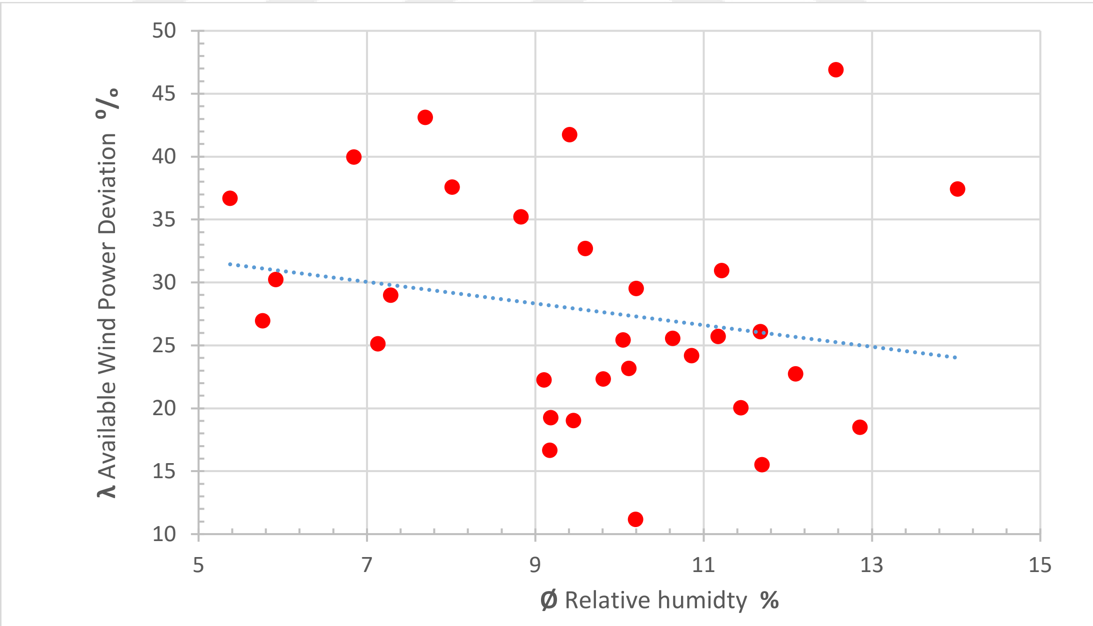

Figure 4.14 Wind power deviation with humidity in January

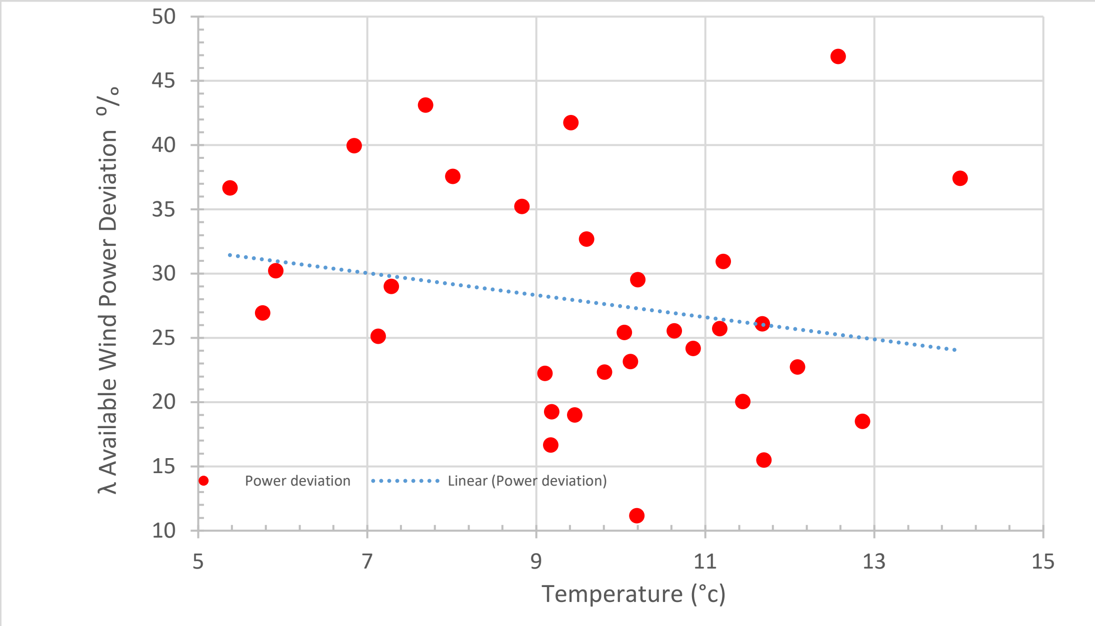

Figure 4.15 Wind power deviation with temperature in January

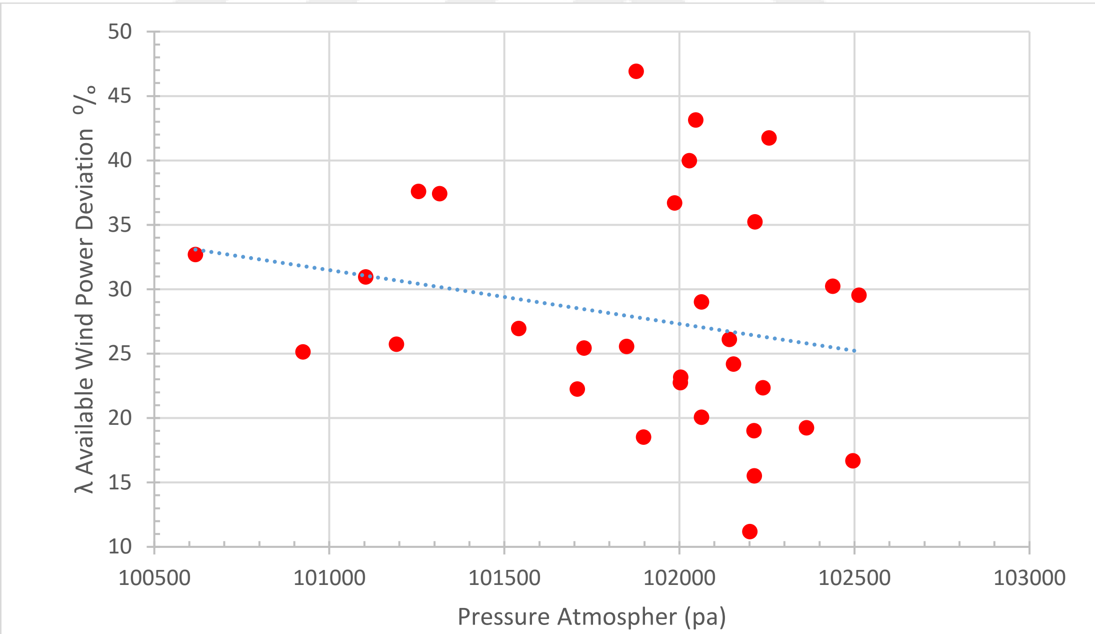

Figure 4.16 Wind power deviation with atmospheric pressure in January

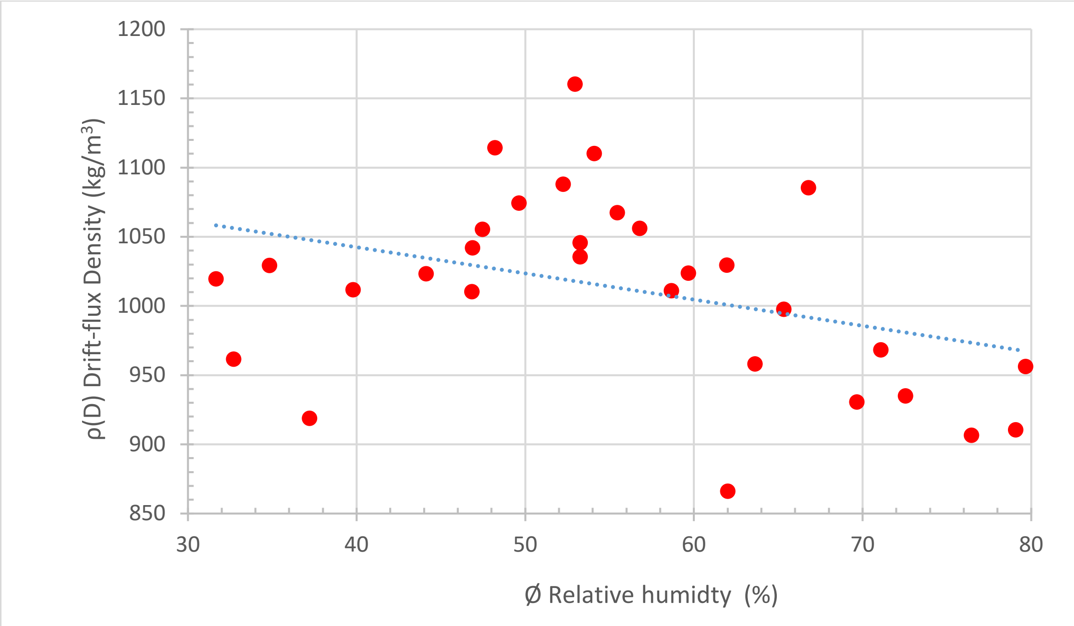

Figure 4.17 Drift-flux density changes with the humidity in January

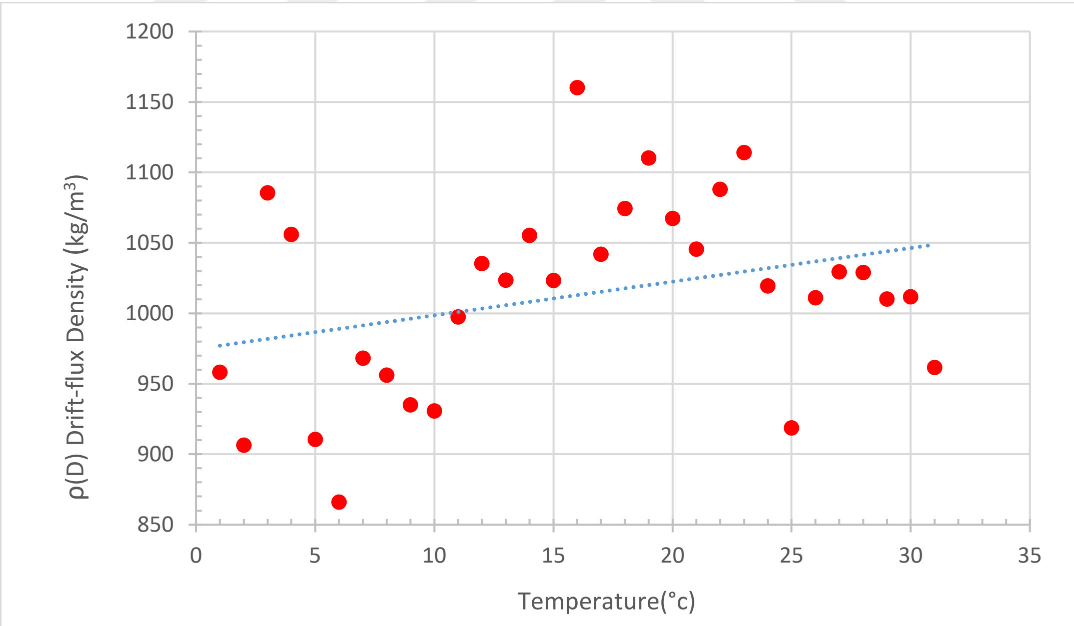

Figure 4.18 Drift-flux density changes with the temperature in January

The tables extracted from our calculations for each month over the course of 2017, were attached as appendix A and B at the end of the research.

CHAPTER 5

WIND TURBINE POWER ANALYSIS ACCORDING TO TWO-PHASE FLOW DRIFT-FLUX MODEL

5.1 Introduction

In this section, a careful analysis was performed to find the effect of meteorologies such as temperature, relative humidity, and atmospheric pressure on the power extracted from the turbines, according to the data obtained from the General Directorate of meteorology Ankara for Mersin city in Turkey for the 2017-year. The Mersin province is considered a high-moisture region in Turkey, located on the Mediterranean Sea. The wind turbine was selected for the current Study is V126-3.3 MW 50/60 Hz.

5.2 General Specification for Vestas 126-3.3MW

The Vestas V126-3.3 M.W. turbine is a throw-organized upwind turbine with a yaw and a three-blade rotor. The Vestas V126-3.3 M.W. turbine characteristics a rotor diameter of 126 m and an output power ratio is 3300 KW. The turbine utilizes the Opti Tip® concept and an influence system supported by an induction generator and a full-scale converter. The turbine can work the rotor at variable speed with these characteristics, thereby maintaining the facility output at or near rated power even in wind speed. At low wind speed, the Opti Tip® concept and the power grid work together to maximize the ability output by operating at the optimal rotor speed and throw angle. Table 5.1 shows the turbine's mechanical specifications, like rotor, blades, and hub information [37].

Table 5.1 Mechanical specification for Vestas 126-3300 KW [27].

Rotor characteristic	
Diameter	126 m
Swept area	12496 m^2
Cut-in Wmd speed	3 m/s
Cut-out Wmd speed	22.5 m/s
Orientation	Upwind
Number of Blades	3
Tilt	6°
Blade Coning	4°
Blade characteristic	
Blade Length	61.66 m
Airfoils	High lift profile
Blade Connection	Steel roots inserted
Maximum Chord	4 m
Hub	
Types	Cast ball shell hub
Material	Cast iron

Table 5. 2 Vestas 126-3300KW turbine generation information

And, Table 5.2 describes the generation information.

Table 5. 2 Vestas 126-3300KW turbine generation information

Type	**Asynchronous with cage rotor**
Rated Power [PN]	3500 kW
Frequency [fN]	0-100 Hz
Voltage, Stator [UNS]	3 x 750 V (at rated speed)
Rated rpm	1450-1550
Rated Generator Voltage	750 V
Rated generator Current	3286 A
Generator Bearing	Hybrid/ceramic

Figure 5.1 indicates the wind turbine drawing and Structural Design – Illustration of Outer Dimensions.

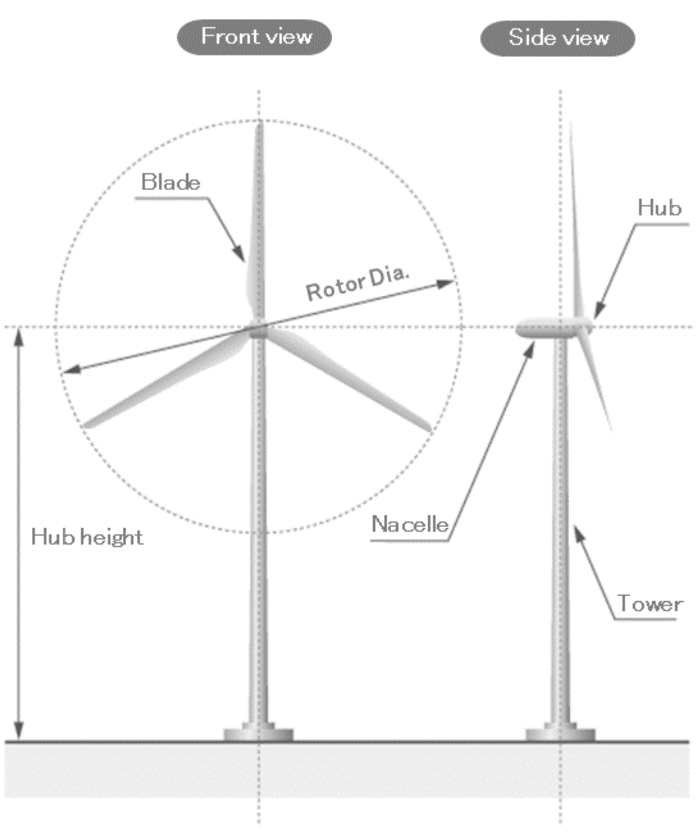

Figure 5. 1 Illustration of outer dimensions – structure (1 is hub Hight 117m and 2 is the diameter of turbine 126 m) [37].

5.3 Application Two-phase Flow Drift-flux Model on Vestas 126-3.3MW Wind Turbine

Most manufacturers rate their turbines by the amount of power they can safely produce at a particular wind speed, usually, the following formula using to find the extracted power from the turbine:

$$P_{out} = \frac{1}{2} A\rho V^3 \tag{3.30}$$

Thus, to application, the two-phase flow homogeneous model on power extracted from the wind turbine must change the property of air to mixture property; therefore, the above Equation of power can be replaced by:

$$P_{out\ D} = \frac{1}{2} A\rho_D V^3 \tag{3.31}$$

The following formula shows factors that are leading to the performance of a wind turbine. Notice that the wind speed, V, has an exponent of 3 applied to it. That means that even a slight increase in wind speed results in a significant increase in power.

Also, the density of air affected on power extracted due to its varied temperature and humidity.

5.4 Wind Turbine Power Analysis According to Meteorology Data

After getting the meteorology data for Mersin city from the General Directorate of Meteorology in Ankara Mersin city in Turkey for the 2017 year, the data of the Vestas 126-3300 KW turbine was used for our study, according to the methodology of a two-phase flow Drift-flux model, the wind power deviation profiles analyzed. The deviation is computed according to for statistical method by entering the Drift-flux model formula in the Excel program. The data required for analysis are density, wind speed, and power coefficient of Vistas 126 turbine. The power coefficient of Vestas 126 finds from the thrust coefficient that was obtained from the company site [37]. According to the relation, $C_p = (1 - a)$, C_t where C_t is the thrust coefficient, and C_p Is power coefficient from the thrust formula find the C_t= 4 (1- a) a , therefore, in the analysis in the wind turbine, it is ordinary to define an indication ratio an as independent parameter such that $a = v_i/V$, in which the V is wind speed and v_i Is the turbine speed.

Table 5. 3 Vestas126-3300 Kw power analysis according to meteorology changes

Month	Temp(°c)	Ø %	ω	Patm(pa)	ρ (dry)	ρ(D)	V wind (m/s)	V relative (m/s)	α(D)	Pout(dry)	Pout(d)	λt %
1	9.6560484	55.610215	0.0041134	101891.79	1288.3613	1012.9073	3	2.892291443	2.37E-05	75.905127	53.476813	0.4194026
2	11.95119	47.572917	0.0041794	102108.11	1280.7123	1009.44	3	2.905381881	2.587E-05	75.454478	54.020655	0.3967709
3	15.504839	58.181452	0.0063665	101316.22	1250.7432	935.99896	3	2.621054884	5.426E-05	73.68882	36.776753	1.0036793
4	18.654583	58.051389	0.0077335	101414.78	1235.8076	910.48973	3	2.461364023	8.158E-05	72.808871	29.625949	1.4576047
5	21.868011	64.537634	0.0106443	101116.95	1213.021	897.04047	3	2.557076389	0.0001472	71.466377	32.727499	1.1836798
6	25.970278	67.095833	0.0143499	100875.22	1186.6095	865.83355	3	2.482752912	0.0002684	69.910313	28.913761	1.4178907
7	30.057258	63.706989	0.0173696	100238.27	1159.2201	843.17964	3	2.468586246	0.0005681	68.29664	27.678	1.4675425
8	30.009812	62.775538	0.0169883	100606.67	1162.7964	869.46089	3	2.628308468	0.0004108	68.507343	34.446788	0.9887876
9	28.015278	59.1625	0.0142491	101021.08	1180.316	932.96569	3	2.920808468	0.0002736	69.539528	50.727632	0.3708412
10	22.790054	44.74328	0.0077267	101328.76	1217.3162	980.56496	3	3.025114023	9.793E-05	71.719434	59.234031	0.2107809
11	17.056806	53.070833	0.0062688	101673.57	1248.5354	990.44618	3	2.935774943	5.427E-05	73.558742	54.685078	0.3451337
12	14.555914	54.842742	0.0057865	101935.43	1263.6122	1022.9976	3	3.038864023	6.366E-05	74.447008	62.643803	0.1884178
AVERAGE	**20.507506**	**57.445943**	**0.009648**	**101293.9**	**1223.9209**	**939.27708**	**3**	**2.744781475**	**0.0001725**	**72.108557**	**43.746397**	**0.7875443**

First, the dry air density is calculated according to an ideal gas. Then, the output power from a turbine is calculated using the general formula extracted. The extracted power from the turbine was analyzed by taking each month status throughout 2017 of meteorology changes in Mersin city and by applied the two-phase flow and drift-flux model to find the extracted power of the turbine by substituting the dry density with Drift-flux density with rain in the air then compared it with power that was computed by substitute dry density in power output equation. By taking the wind speed at 3 m/s at all status to find the impact of temperature, relative humidity, and atmospheric pressure on power. The deviation in power extracted from the turbine when temperatures, relative humidity, and atmospheric pressure change, indicates in Table 5.3.

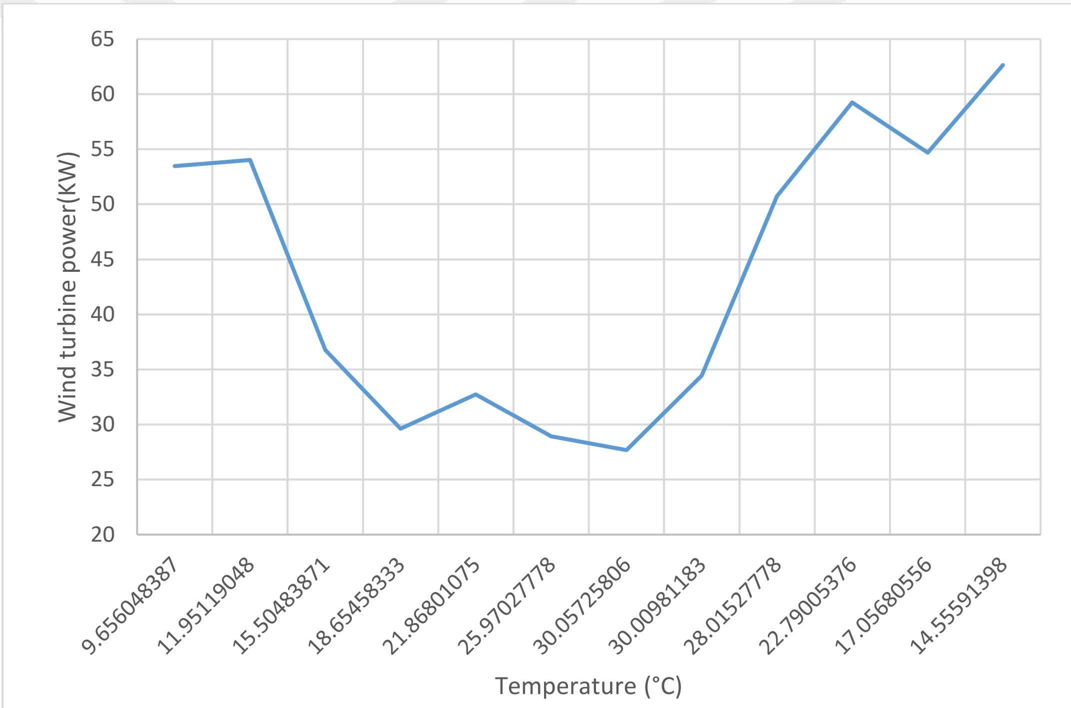

Figure 5. 2 Effect of temperature change on wind turbine power.

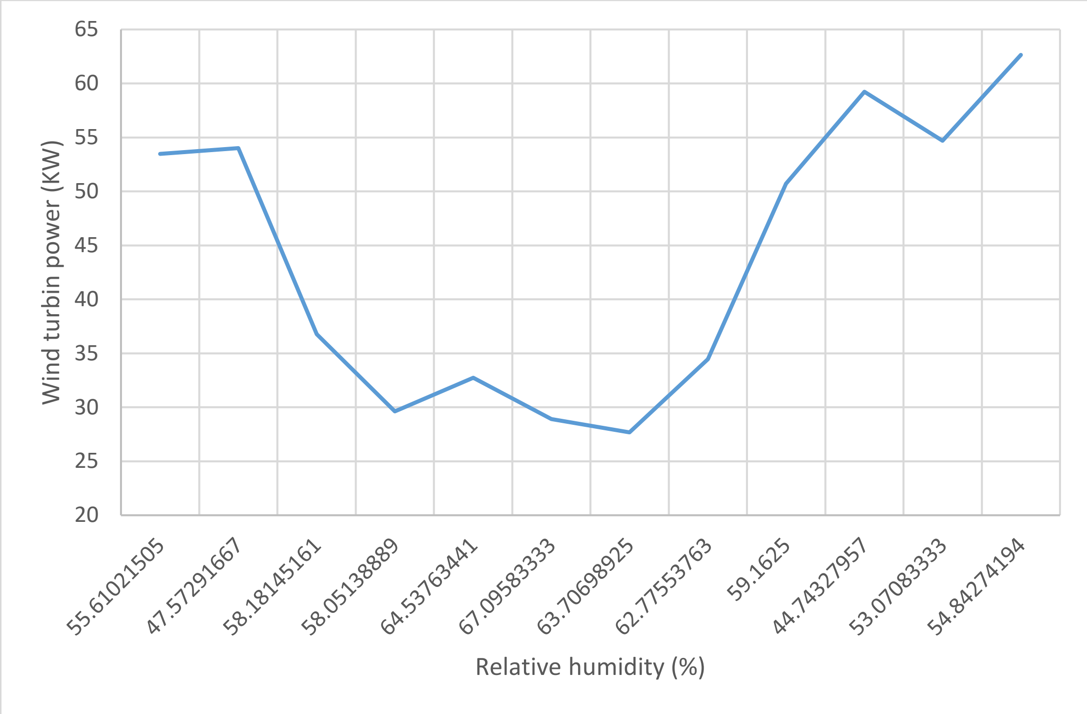

Figure 5. 3 Effect of relative humidity on wind power turbine

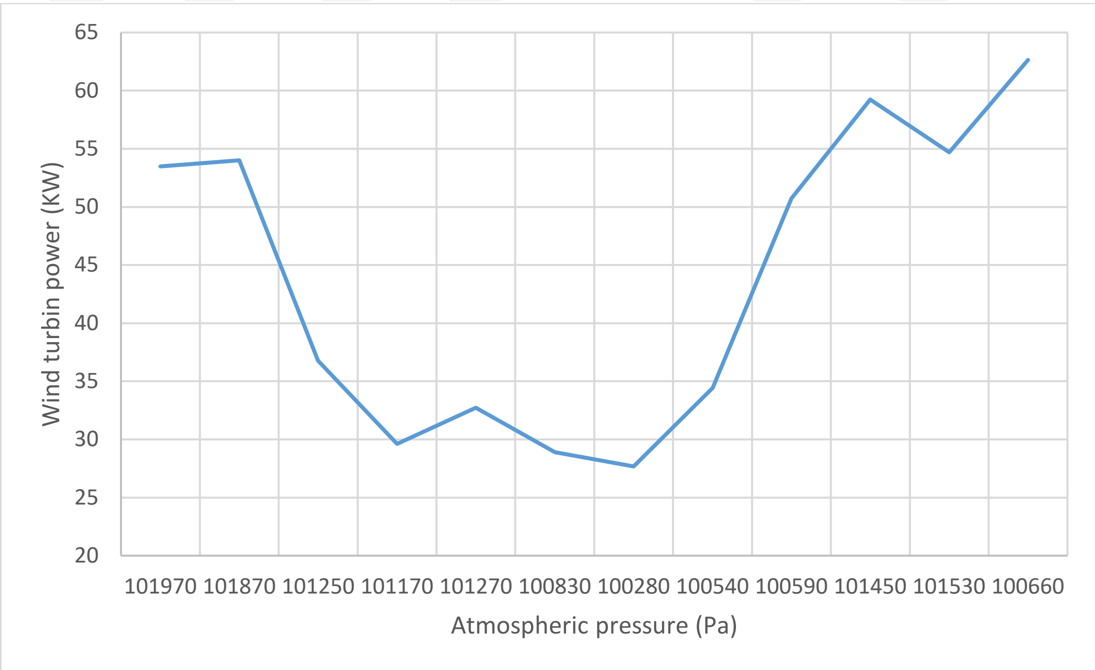

Figure 5. 4 Effect of atmospheric pressure on wind turbine power.

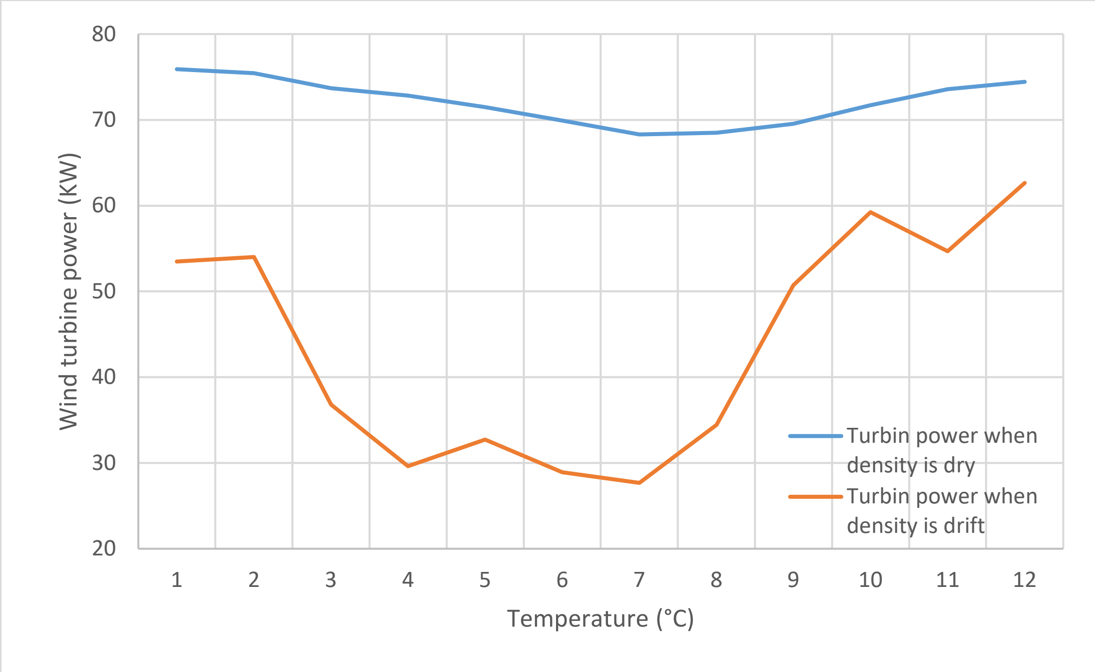

Figure 5. 5 The deviation in wind turbine power.

When the temperature increases above 25°C and the relative humidity at approximately 60 %, Figure (5.2,5.3), the wind turbine power decrease. While the atmospheric pressure decreases, the turbines will obtain low power, as shown in Figure 5.4. From the previous, we conclude that the energy obtained from the turbine is significantly reduced due to the low density in the atmosphere. This is the effect of rain and moisture, as the water molecules mix with the dry air and rising the amount of water vapor in dry air resulting in a lower density needed.

5.5 Wind Turbine Power Curve Analysis According to Two-Phase Flow.

This section analyzes the power curve of Vestas126-3300 kW, by calculating the power curve at the dry density, then comparing it with to the power curve when the air is rain to show the power loss due to that change. So, by using a 12 status for each month with deferential in temperature and relative humidity and atmospheric pressure, apply the Two-phase flow Drift-flux model to find the atmospheric density and then find the loss in wind turbine power a result.

Table 5. 4 Power loss

MONTH	T(°c)	Ø %	V (m/s)	patm(pa)	ρ (D)	ρ (Dry)	Ct	Cp	Pout (KW)	Pout (D) KW	Loss (Kw)
1	9.656048	55.6102	3	101891.788	1012.907	1288.361316	0.92	0.14	30.42779607	23.92227646	6.5055196
2	11.95119	47.5729	4	102108.11	1009.44	1280.712306	0.84	0.37	189.4847668	149.3493091	40.135458
3	15.50484	58.1815	5	101316.216	935.999	1250.74324	0.8	0.42	410.2687976	307.0263796	103.24242
4	18.65458	58.0514	6	101414.778	910.4897	1235.807593	0.79	0.43	717.1567441	528.3701582	188.78659
5	21.86801	64.5376	7	101116.949	897.0405	1213.021025	0.77	0.44	1143.815944	845.8626594	297.95328
6	25.97028	67.0958	8	100875.222	865.8335	1186.609462	0.75	0.44	1670.211483	1218.703523	451.50796
7	30.05726	63.707	9	100238.266	843.1796	1159.220096	0.73	0.44	2323.202825	1689.823466	633.37936
8	30.00981	62.7755	10	100606.667	869.4609	1162.796427	0.65	0.38	2760.757789	2064.308819	696.44897
9	28.01528	59.1625	11	101021.083	932.9657	1180.316012	0.47	0.3	2944.683547	2327.587446	617.0961
10	22.79005	44.7433	12	101328.763	980.565	1217.316234	0.34	0.235	3088.559947	2487.877484	600.68246
11	17.05681	53.0708	13	101673.569	990.4462	1248.535394	0.26	0.185	3170.616128	2515.206734	655.40939
12	14.55591	54.8427	14	101935.43	1022.998	1263.612208	0.21	0.15	3249.6022	2630.819323	618.78288
AVERAGE	**20.50751**	**57.4459**	**8.5**	**101293.904**	**939.2771**	**1223.920943**	**0.6275**	**0.3275**	**1808.232331**	**1399.071465**	**409.16087**

Table 5.4 shows the loss that happened in turbine power due to decreasing atmospheric density with rising temperature and relative humidity in conjunction with dropping in atmospheric pressure.

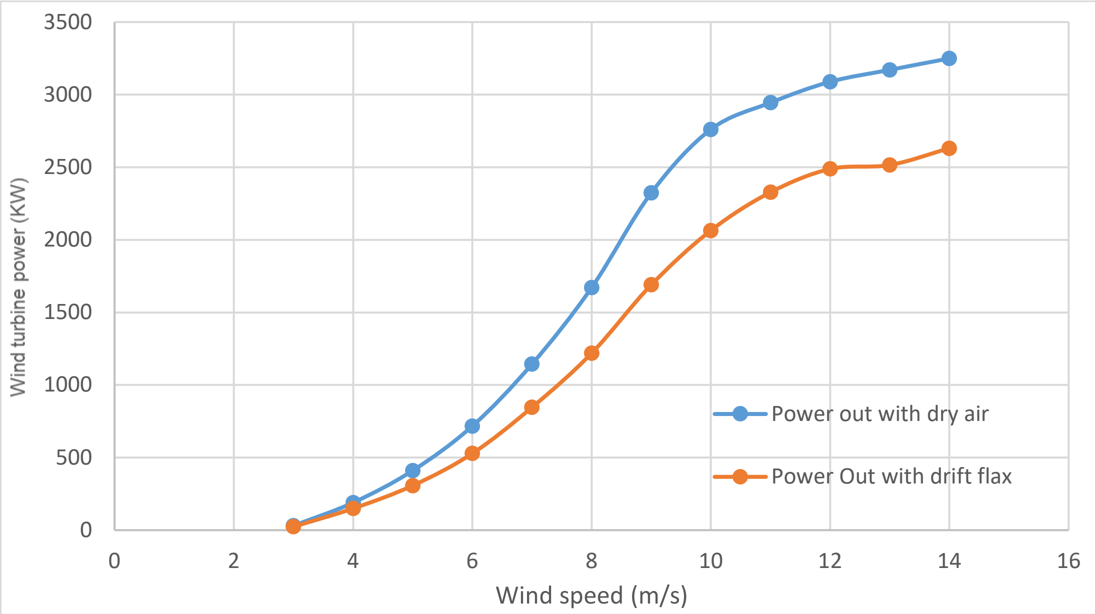

Figure 5. 6 Vestas 126-3300 power curve changes.

Figure 5.6 shows a difference between the power curve when the density is imposed as dry and when the density is assessed as a drift-flux density in rainy weather. The difference occurs due to the effects of density decreasing due to rising relative humidity and the temperature, which reduces the turbine power output. Notice that both types of nonideal losses tend to fall power output which means decrease turbine efficiency. In addition, by comparing Figure (5.6) with Figure (5.7) [4], for which the Two-phase flow Homogeneous method was used in moisture, we notice the effect of the rain, which leads to dissipated in power, more than moisture.

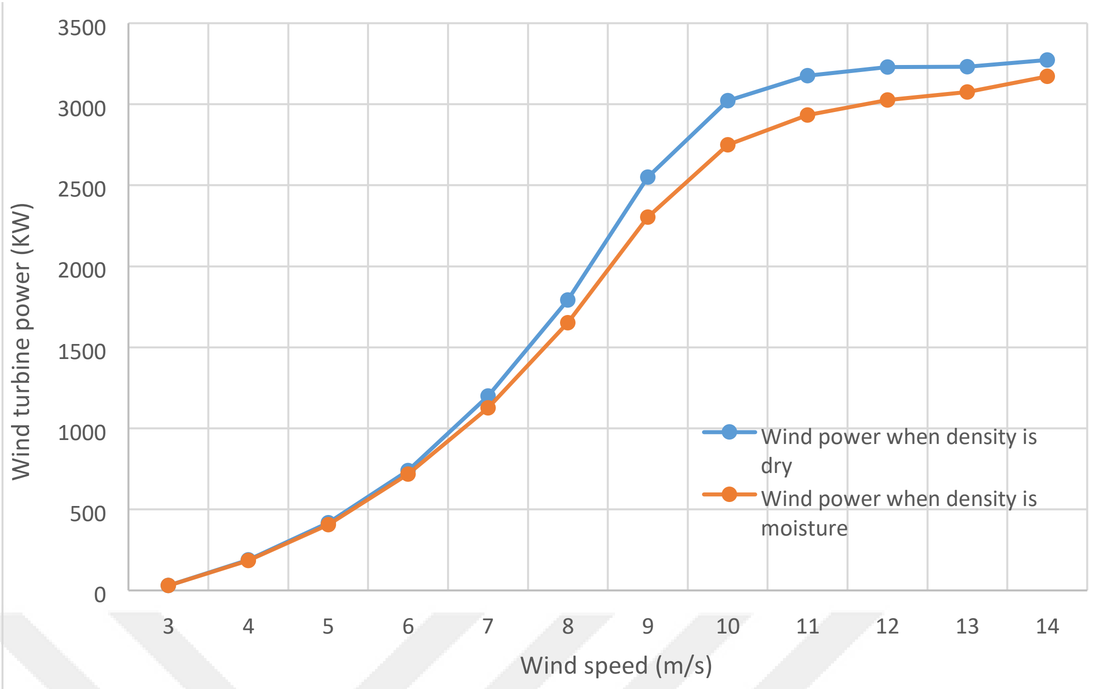

Figure 5. 7 Vestas 126-3300 power curve changes in moisture by Two-phase flow Homogeneous method

CHAPTER 6

CONCLUSION AND RECOMMENDATION

6.1 Conclusion

This paper presents a meteorology effect on wind power for the wind farm based on a statistical and physical model. The two-phase flow Drift-flux model is used as the statistical model to analyse the losses inlet of the wind farm due to wind density changes. The Excel program is used in the physical model to find this variation in wind power by entering the meteorology data and analysing it according to the Drift-flux model formula. The current model based on the turbine properties is applied to calculate the wind turbine power losses due to wind density power change. So, we note that:

1. The power curve calculates the output power of the turbine, the first when density is dry and then calculated when density in rainy weather with raindrop $D = 0.1$ (cm) and then find the differential between them.
2. After analysis for each month throughout the year 2017 of Mersin, there was an energy fluctuation of winds around the clock and today.
3. This fluctuation is due to the increase or decrease in temperature and relative humidity for each hour, which leads to changes in air density and, consequently, to wind power deviation.
4. During the Winter, the deviation is less due to the lower temperatures and relative humidity than other seasons, which records deviation increases in the
5. Over the months of 2017, July records the highest values of energy deviation in Mersin, as a result of high temperatures to 30°C and relative humidity of nearly 65%.
6. Any rising in moisture due to rain content leads to decreasing in atmospheric density.
7. Two main factors affecting density are temperature and humidity

8. A decrease in atmospheric density causes a difference in the turbine power curve.
9. Any dropping in atmospheric density leads to a decrease in the efficiency of turbines.

Therefore, when selecting the wind farm's location, a careful analysis of the weather characteristics is necessary to avoid losses resulting from density loss. It is essential to review the turbine designs, especially for high humidity areas, and create a unique model for places with high humidity.

6.2 Recommendation

Wind energy is renewable energy, and it has been continuously developing, especially in the past few years; there have been significant developments in design and raising the output of extracted energy. But it is not without problems, including wind fluctuation and air density, due to climatic changes in the world. One of the most important ways to further develop this field is scientific research through careful analysis and finding the reasons for those problems to reach appropriate solutions. The current study used the two-flow phase flow Drift-flux model to analyze wind power and turbine power. It is possible to repeat the recent analysis, but using another model, the drift flux flow model, and enter the relative velocity between air content to find the power deviation that occurs due to change in meteorology condition and replace the dry air with drift flux model atmospheric density. Then compute the effect on turbine efficiency. Also, can use the CFD to simulate the power of wind turbines according to Drift-flux flow by entering the moisture percent to program and then find the effect of increasing and decreasing the density on the power curve. An analysis can also be done using a laboratory model turbine, placing it inside the air channel, adding some water vapor to the air, and finding energy losses as a result. Then compared it with the power that was computed when density was imposed as dry. Finally, simulate the more suitable design of wind turbines for high humidity regions.

REFERENCES

[1] How Do Wind Turbines Work? https://www.energy.gov/eere/wind/how-do-wind-turbines-work 06.07.2021

[2] The Main Types of Wind Turbines Being Used Today https://blog.arcadia.com/types-of-wind-turbines-being-used-today/ 06.07.2021

[3] Marimuthu, C., Kirubakaran, V. (2014). A critical review of factors affecting wind turbine and solar cell system power production. *Int J Adv Engg Res Stud.-March*, **143**, 147.

[4] Alwindawi, Z. (2020). *Homogeneous Two-Phase Flow Model Applications on a Standard Wind Rose Designed for the Case of Single-Phase Air Flow*. M.sc thesis, Gaziantep University.

[5] Wu, Z., Cao, Y., Nie, S., Yang, Y. (2017). Effects of rain on vertical axis wind turbine performance. *Journal of Wind Engineering and Industrial Aerodynamics*, **170**, 128-140.

[6] Hibiki, T., Ishii, M. (2003). *One-dimensional drift–flux model for two-phase flow in a large diameter pipe. International Journal of Heat and Mass Transfer*, **46(10)**, 1773-1790.

[7] Goda, H., Hibiki, T., Kim, S., Ishii, M., Uhle, J. (2003). *Drift-flux model for downward two-phase flow. International journal of heat and mass transfer*, **46(25)**, 4835-4844.

[8] Osiptsov, A. A., Sin'kov, K. F., Spesivtsev, P. E. (2014). *Justification of the drift-flux model for two-phase flow in a circular pipe. Fluid Dynamics*, **49(5)**, 614-626.

[9] Hibiki, T. (2019). *One-dimensional drift-flux correlations for two-phase flow in medium-size channels. Experimental and Computational Multiphase Flow*, **1(2)**, 85-100.

[10] Hibiki, T., Takamasa, T., Ishii, M. (2004, January). *One-dimensional drift-flux model and constitutive equations for relative motion between phases in various two-phase flow regimes at microgravity conditions. In International Conference on Nuclear Engineering* (Vol. **4689**, pp. 377-386).

[11] Gardenghi, Á. R., Chagas, D. G., Scagnolatto, G., Oliveira, R. M., Tibiriçá, C. B. (2020). *Overview of Void Fraction Measurement Techniques, Databases and Correlations for Two-Phase Flow in Small Diameter Channels. Fluids*, **5(4)**, 216.

[12] Zou, L., Zhao, H., Zhang, H. (2016). *Numerical implementation, verification and validation of two-phase flow four-equation drift flux model with Jacobian-free Newton–Krylov method. Annals of Nuclear Energy*, **87**, 707-719.

[13] Öztopal, A., Şahin, A. D., Akgün, N., Şen, Z. (2000). *On the regional wind energy potential of Turkey. Energy*, **25(2)**, 189-200.

[14] Salih, A. M., Majli, A. S. (2015). *Relative humidity effect on the extracted wind power for electricity production in Nassiriyah City*. J Fundam Renew Energy Appl, **6(1)**, 1-6.

[15] Krewitt, W., Nitsch, J. (2003). *The potential for electricity generation from on-shore wind energy under the constraints of nature conservation: a case study for two regions in Germany. Renewable energy*, **28(10)**, 1645-1655.

[16] Şahin, A. Z., Aksakal, A. (1998). *Wind power energy potential at the northeastern region of Saudi Arabia. Renewable Energy*, **14(1-4)**, 435-440.

[17] Danook, S. H., Jassim, K. J., Hussein, A. M. (2019). *The impact of humidity on performance of wind turbine. Case Studies in Thermal Engineering*, **14**, 100456.

[18] Hamam, F. M., AL-Rijabo, W. I. (2019). *Correlations between Wind Power Density and Different Meteorological Parameters in Nineveh Governorate*.**-98** , 111.

[19] Thompson, B. E., Jang, J., Dion, J. L. (1995). *Wing performance in moderate rain. Journal of Aircraft*, **32(5)**, 1034-1039.

[20] Abdul Kareem, M.S. (2015). *Theoretical Study of Temperature Effect on The Wind Power Extracted as A Renewable Energy for Electricity Production in Nassiriyah District*. JCBPS, section **D. 5(2)**,1958-1966.

[21] Lorenzi, A., Muzzio, A., *"Two-Phase Flow Measurement with Sharp-Edged Orifices", Two-Phase Transport and Reactor Safety'* (Edited by T. N. Veziroglu, S. Kakaq), **vol. 4**, pp. 1269-1280, 1976.

[22] Lorenzi, A. Muzzio, A., *'Total Mass Flow-Rate and Quality Measurement in Air-Water Mixtures with Venturimeters", Multiphase Transport (Edited by T. N. veziroglu*), **vol. 5**, pp. 2681-2694, 1979.

[23] Reimann, J., John, H. and Müller, U., *'Measurements of Two-Phase Mass Flow Rate: A Comparison of Different Techniques", International Journal of Multiphase Flow*, **vol. 8**, No. 1, pp. 33-46, 1982.

[24] Salcudean, M. E., Groeneveld, D. C. and Leung, L. K. El., "*Effect of Flow-Obstruction Geometry on Pressure Drops in Horizontal Air-Water Flow", International Journal of Multiphase Flow*, **Vol. 9**, NO. 1, pp. 73-85, 1983.

[25] Banerjee, T. K. Das, S. K., *'"Gas-Non-Newtonian Liquid Flow Through Globe and Gate Valves*", Chemical Engineering Communications, **Vol. 167**, pp. 133-146, 1998.

[26] Samanta, A. K., Banerjee, T. K. Das S. K., "*Pressure Losses in Orifices for The Flow of Gas-Non-Newtonian Liquids*", The Canadian Journal of Chemical Engineering, **Vol. 77**, pp. 579-583, 1999.

[27] Brennen, E. (2005), *Fundamentals of Multiphase Flows*.

[28] Ishii, M., Hibiki, T. (2006). *Thermo-fluid dynamics of two-phase flow*.

[29] Graham B.Wallis, (1969*). One Dimensional Two-Phase Flow*.

[30] Serio, M. A., Carollo, F. G., & Ferro, V. (2019). *Raindrop size distribution and terminal velocity for rainfall erosivity studies. A review*. Journal of Hydrology, **576**, 210-228.

[31] Uplinger, W.G., 1981. *A new formula for raindrop terminal velocity. In: Proceedings of the 20th Conference on Radar Meteorology*, 30 Nov–3 Dec 1981. Amer. Meteorol. Soc. Boston, Mass, USA, pp. 389–391.

[32] Leone, A., Pica, M., 1993. *Caratteristiche dinamiche e simulazione delle piogge. Parte prima, Fondamenti teorici. Rivista di Ingegneria Agraria* **3**, 167–175

[33] Beard, K.V., 1976. *Terminal velocity of cloud and precipitation drops aloft. J. Atmos*. **Sci. 33**, 851–864.

[34] Laws, J.O., 1941. *Measurements of the fall-velocity of water-drops and raindrops. Am. Geophys. Union Trans*. **22**, 709–721.

[35] Gunn, R., Kinzer, G.D., 1949. *The terminal velocity of fall for water droplets in stagnant air. J. Meteorol*. **6**, 243–248.

[36] Pruppacher, H.R., Pitter, R.L., 1971. *A semi-empirical determination of the shape of cloud and rain drops*. J. Atmos. Sci. **28**, 86–94.

[37] Vestas. *V126-3.3MW Onshore Brochure*. Vestas, 2012.

APPENDIX A

Tables of Wind Power Analysis According to Two-phase flow Drift-flux Model Throughout 2017 For Each Month

Table A.1 Wind Power Analysis According to Two-phase flow Drift-flux Model in January

Day	Temp(°c)	Ø %	V (m/s)	Patm(pa)	Pg (pa)	P dry (pa)	Pv (pa)	Ꞷ	ρ (dry)	ρ (v)	α(D)	Vd	Vr	ρ(D)	λ
1	8.829167	63.625	1.420833	102215.8	1151.72	101495	723.78	0.004491	1295.559	5.535062	2.55E-05	4.011781	2.590947	958.1217	35.21859
2	7.691667	76.45833	1.741667	102046.7	1051.679	101244.3	804.0959	0.00494	1297.47	6.194382	3.14E-05	4.011781	2.270114	906.5311	43.12475
3	9.454167	66.79167	0.766667	102212.9	1196.045	101430.9	782.0139	0.004796	1291.822	5.999379	2.97E-05	4.011781	3.245114	1085.443	19.0133
4	9.808333	56.79167	0.9	102238.8	1230.017	101544.6	694.114	0.004252	1291.679	5.31332	2.37E-05	4.011781	3.111781	1055.916	22.32777
5	9.408333	79.08333	1.6875	102256.3	1181.977	101323.1	933.1898	0.005729	1290.584	7.160295	4.27E-05	4.011781	2.324281	910.5083	41.74328
6	12.57083	62	1.895833	101876.3	1466.671	100983.2	893.0386	0.005501	1272.072	6.777156	3.97E-05	4.011781	2.115947	865.9678	46.896
7	11.2125	71.08333	1.25	101103.8	1333.931	100161.7	942.0965	0.00585	1267.698	7.183652	4.61E-05	4.011781	2.761781	968.1564	30.93943
8	9.595833	79.66667	1.320833	100617.5	1197.942	99666.93	950.5721	0.005932	1268.665	7.288363	4.57E-05	4.011781	2.690947	956.1477	32.68502
9	8.0125	72.54167	1.516667	101255	1081.121	100474.7	780.3043	0.004831	1286.208	6.014056	3.04E-05	4.011781	2.495114	934.9486	37.56991
10	6.845833	69.66667	1.6125	102028.8	995.7071	101333.7	695.0329	0.004266	1302.569	5.378925	2.43E-05	4.011781	2.399281	930.6196	39.96789
11	10.2	65.33333	1.191667	102512.9	1261.923	101709.2	803.7332	0.004915	1291.981	6.148264	3.13E-05	4.011781	2.820114	997.441	29.5296
12	10.85833	53.25	0.975	102154.2	1317.054	101461	693.1294	0.004249	1285.869	5.286947	2.38E-05	4.011781	3.036781	1035.438	24.18602
13	10.04167	59.66667	1.025	101727.9	1246.258	101004.6	723.3168	0.004454	1283.734	5.538397	2.56E-05	4.011781	2.986781	1023.559	25.41865
14	9.104167	47.45833	0.895833	101707.9	1165.243	101173.1	534.7679	0.003288	1290.121	4.111365	1.42E-05	4.011781	3.115947	1055.338	22.24712
15	10.63333	44.125	1.029167	101849.2	1301.844	101291.9	557.3031	0.003422	1284.738	4.256972	1.53E-05	4.011781	2.982614	1023.279	25.55117
16	10.19167	52.95833	0.45	102200.8	1254.461	101544	656.8784	0.004024	1289.889	5.024393	2.09E-05	4.011781	3.561781	1160.238	11.17457
17	12.09167	46.875	0.916667	102002.9	1428.649	101351	651.9255	0.004001	1278.892	4.955231	2.07E-05	4.011781	3.095114	1041.896	22.74655
18	12.85833	49.625	0.745833	101897.1	1507.324	101162.3	734.7685	0.004518	1273.117	5.565229	2.7E-05	4.011781	3.265947	1074.338	18.50255
19	11.69167	54.08333	0.625	102213.8	1400.34	101475.5	738.2587	0.004525	1282.314	5.762855	2.66E-05	4.011781	3.386781	1110.171	15.506
20	11.44167	55.45833	0.808333	102062.9	1373.638	101315.1	747.7822	0.004591	1281.396	5.692042	2.81E-05	4.011781	3.203447	1067.389	20.04959
21	10.1125	53.25	0.933333	102003.8	1255.751	101344.9	658.8779	0.004044	1287.78	5.038319	2.16E-05	4.011781	3.078447	1045.625	23.1588
22	9.183333	52.25	0.775	102362.9	1185.549	101756.2	606.6956	0.003709	1297.299	4.653566	1.82E-05	4.011781	3.236781	1087.966	19.24071
23	9.170833	48.20833	0.670833	102495.8	1187.447	101946.7	549.1655	0.003351	1299.794	4.215888	1.46E-05	4.011781	3.340947	1114.148	16.66256
24	11.675	31.66667	1.05	102142.5	1398.499	101712.2	430.2707	0.002631	1285.396	3.27315	9.1E-06	4.011781	2.961781	1019.416	26.09142
25	14.01667	37.20833	1.508333	101315	1617.104	100716.6	598.3701	0.003695	1262.362	4.513045	2.03E-05	4.011781	2.503447	918.6289	37.41809
26	11.17083	58.66667	1.0375	101191.3	1334.534	100404.6	786.6987	0.004874	1271.003	5.993757	3.15E-05	4.011781	2.974281	1011.005	25.71677
27	7.129167	61.95833	1.0125	100925	1017.956	100296.8	628.21	0.003896	1287.96	4.856715	1.99E-05	4.011781	2.999281	1029.341	25.12466
28	5.7625	34.83333	1.083333	101540.8	933.739	101228.6	312.2529	0.001919	1306.351	2.428418	4.95E-06	4.011781	2.928447	1029.098	26.94145
29	5.916667	46.83333	1.216667	102437.5	945.0705	102002.2	435.2777	0.002654	1315.636	3.378104	9.44E-06	4.011781	2.795114	1010.252	30.2285
30	7.283333	39.79167	1.166667	102062.9	1041.251	101674.2	388.6858	0.002378	1305.036	3.008738	7.41E-06	4.011781	2.845114	1011.683	28.99656
31	5.375	32.70833	1.475	101986.7	909.5999	101693.9	292.7786	0.001791	1314.208	2.277069	4.69E-06	4.011781	2.536781	961.5159	36.68086
Average	9.656048	55.61022	1.119489	101891.8	1224.84	101223.3	668.6253	0.004113	1288.361	5.123324	2.37E-05	4.011781	2.892291	1012.907	27.1944

Table A.2 Wind Power Analysis According to Two-phase flow Drift-flux Model in February

Day	Temp(°c)	Ø %	V (m/s)	Patm(pa)	Pg (pa)	P dry (pa)	Pv (pa)	ω	ρ (dry)	ρ (v)	α(D)	Vd	Vr	ρ(D)	λ
1	5.2625	39.45833	1.229167	102516.7	909.3231	102165.3	351.3917	0.002139	1320.884	2.732723	6.14E-06	4.011781	2.782614	1011.723	30.55784
2	7.1	46.75	1.216667	102924.2	1032.829	102450.1	474.0778	0.002878	1315.886	3.661488	1.15E-05	4.011781	2.795114	1010.505	30.22059
3	8.7875	49.20833	0.941667	102832.5	1159.827	102276.1	556.3825	0.003384	1305.791	4.273938	1.54E-05	4.011781	3.070114	1058.331	23.3821
4	9.979167	51	0.6125	102498.3	1245.85	101880.8	617.5103	0.00377	1295.209	4.72698	1.85E-05	4.011781	3.399281	1124.228	15.20873
5	11.65833	54.79167	0.904167	102197.5	1392.831	101449.6	747.8921	0.004585	1282.119	5.689431	2.8E-05	4.011781	3.107614	1047.284	22.42328
6	11.26667	69.54167	1.05	102387.1	1337.455	101457.9	929.2284	0.005697	1283.856	7.08269	4.18E-05	4.011781	2.961781	1018.913	26.00259
7	14.7375	55.45833	1.095833	102167.5	1696.083	101239	928.5188	0.005705	1265.746	6.987467	4.26E-05	4.011781	2.915947	995.5886	27.13542
8	16.12917	32.83333	2.4125	101514.6	1847.82	100921.8	592.7948	0.003654	1255.662	4.444109	1.73E-05	4.011781	1.599281	785.7778	59.79858
9	14.13333	52.16667	1.3	101892.1	1630.774	101046.9	845.1438	0.005202	1265.987	6.371933	3.78E-05	4.011781	2.711781	957.6372	32.19903
10	12.89583	58.54167	0.716667	101882.5	1630.774	100933.7	948.7526	0.005847	1270.071	7.183917	4.49E-05	4.011781	3.295114	1078.543	17.75803
11	14.14167	45.04167	0.8125	101465.8	1640.205	100741.2	724.6144	0.004474	1262.183	5.462583	2.66E-05	4.011781	3.199281	1050.461	20.15514
12	14.40417	37.33333	1.204167	101501.3	1657.318	100896.5	604.7272	0.003728	1262.891	4.559612	1.82E-05	4.011781	2.807614	972.3524	29.87996
13	10.81667	39.20833	1.391667	101564.6	1307.659	101052.1	512.4506	0.003154	1280.819	3.908957	1.33E-05	4.011781	2.620114	951.9242	34.55055
14	8.820833	34.16667	1.0375	101852.1	1145.269	101467.1	385.0276	0.00236	1295.186	2.959684	7.3E-06	4.011781	2.974281	1029.649	25.78903
15	8.325	36.16667	1.270833	101787.9	1112.595	101384.7	403.1793	0.002474	1296.468	3.100277	8.27E-06	4.011781	2.740947	985.3073	31.58009
16	9.295833	27.16667	1.5875	102027.5	1188.566	101718.8	308.6702	0.001887	1296.256	2.371157	4.73E-06	4.011781	2.424281	929.4076	39.47119
17	8.441667	41.83333	1.504167	102434.2	1125.951	101963.7	470.4255	0.00287	1303.365	3.614686	1.13E-05	4.011781	2.507614	948.9108	37.35381
18	10.175	47.08333	1.0375	102848.8	1266.325	102263.4	585.3804	0.00356	1299.195	4.474056	1.71E-05	4.011781	2.974281	1033.124	25.7541
19	11.02917	46.20833	0.833333	102808.8	1339.173	102211.5	597.2999	0.003635	1294.617	4.556053	1.71E-05	4.011781	3.178447	1072.69	20.68882
20	11.30833	42.58333	0.966667	102245.4	1369.991	101677.3	568.0794	0.003475	1286.649	4.324256	1.6E-05	4.011781	3.045114	1037.622	23.9998
21	11.72083	47.91667	0.891667	101891.7	1405.721	101220.5	671.1865	0.004124	1279.005	5.097022	2.35E-05	4.011781	3.120114	1047.294	22.12471
22	12.86667	58.54167	1.125	101739.6	1502.722	100856.7	882.9046	0.005445	1269.223	6.682061	4.03E-05	4.011781	2.886781	992.6296	27.86469
23	13.69583	58.66667	1.204167	102037.5	1588.417	101095.4	942.0633	0.005796	1268.578	7.103477	4.69E-05	4.011781	2.807614	977.2555	29.8103
24	14.15833	61.79167	1.233333	102387.5	1635.626	101376.2	1011.262	0.006205	1270.023	7.619361	5.18E-05	4.011781	2.778447	973.078	30.51604
25	14.22083	66.29167	0.945833	102419.2	1643.251	101334.3	1084.916	0.006659	1269.228	8.174273	5.86E-05	4.011781	3.065947	1028.502	23.40548
26	14.2375	62.29167	0.845833	102076.3	1640.935	101061.2	1015.067	0.006247	1265.709	7.65087	5.12E-05	4.011781	3.165947	1046.523	20.94417
27	15.05417	48.79167	0.404167	101666.3	1729.254	100835.6	830.6218	0.005124	1259.313	6.244562	3.66E-05	4.011781	3.607614	1144.515	10.03034
28	19.97083	21.20833	1.204167	101460	2357.052	100982	477.9899	0.002944	1240.025	3.536677	1.15E-05	4.011781	2.807614	954.5432	29.90768
Average	11.95119	47.57292	1.106399	102108.1	1447.843	101427.1	680.9842	0.004179	1280.712	5.164082	2.59E-05	4.011781	2.905382	1009.44	26.87355

Table A.3 Wind Power Analysis According to Two-phase flow Drift-flux Model in March

Day	Temp(°c)	Ø %	V (m/s)	Patm(pa)	Pg (pa)	P dry (pa)	Pv (pa)	ω	ρ (dry)	ρ (v)	α(D)	Vd	Vr	ρ(D)	λ
1	20.13333	25.875	1.958333	101336.3	2374.767	100736.4	614.4709	0.003794	1236.224	4.43551	1.89E-05	4.011781	2.053447	832.1454	48.55868
2	16.31667	57.54167	1.370833	101193.3	1870.358	100155.8	1076.235	0.006684	1245.308	7.777902	5.78E-05	4.011781	2.640947	930.0309	33.89961
3	12.39583	80.83333	1.708333	101322.1	1448.494	100165.7	1170.866	0.007271	1262.53	8.779515	6.67E-05	4.011781	2.303447	887.9914	42.17812
4	13.30833	66.375	1.183333	101674.6	1547.041	100652.3	1026.848	0.006346	1264.701	7.726623	5.31E-05	4.011781	2.828447	978.2807	29.27793
5	13.9125	55.625	1.2	101995	1614.941	101099.1	898.3108	0.005527	1267.67	6.754659	4.13E-05	4.011781	2.811781	977.2626	29.71637
6	15.32917	53.66667	0.695833	101660.4	1775.769	100724	952.9962	0.005885	1256.792	7.028345	4.41E-05	4.011781	3.315947	1071.948	17.24379
7	16.32917	52.54167	0.879167	101269.2	1886.597	100278.9	991.2497	0.006148	1246.891	7.4026	5.2E-05	4.011781	3.132614	1023.964	21.77094
8	15.38333	61.04167	0.816667	101496.3	1765.917	100414.6	1077.945	0.006677	1252.611	8.116232	6.04E-05	4.011781	3.195114	1041.972	20.21539
9	20.31667	33.75	1.6375	101293.3	2440.726	100529.3	823.7451	0.005097	1233.071	5.649906	2.9E-05	4.011781	2.374281	877.2456	40.56162
10	17.34167	47.16667	1.754167	100766.3	2021.261	99894.59	953.3615	0.005936	1237.761	6.521978	4E-05	4.011781	2.257614	863.1246	43.40463
11	13.32917	75.16667	1.183333	100598.8	1538.31	99459.34	1156.297	0.007231	1249.55	8.6239	6.6E-05	4.011781	2.828447	966.7607	29.25124
12	13.15833	79.91667	2.525	100833.8	1519.665	99625.13	1214.466	0.007582	1252.374	9.14928	7.4E-05	4.011781	1.486781	772.0834	62.20703
13	14.35417	70.91667	1.4	101146.3	1647.377	99985.67	1168.265	0.007268	1251.681	8.747305	6.75E-05	4.011781	2.611781	930.0189	34.58662
14	14.19167	61.875	2.491667	101269.2	1636.983	100262.8	1012.883	0.006284	1255.922	7.585269	5.16E-05	4.011781	1.520114	777.6015	61.51231
15	13.77917	46.66667	1.304167	101366.3	1595.543	100638.8	744.5869	0.004602	1262.435	5.495395	2.63E-05	4.011781	2.707614	954.0183	32.32819
16	13.55417	49.25	1.325	101241.5	1560.249	100478.9	768.4225	0.004757	1261.351	5.76553	2.89E-05	4.011781	2.686781	949.5632	32.83487
17	12.325	63.66667	1.166667	101170.8	1437.255	100257.6	915.0524	0.005677	1263.992	6.933042	4.19E-05	4.011781	2.845114	980.6987	28.88687
18	13.03333	51.66667	1.295833	101052.5	1523.247	100298.2	787.0109	0.004881	1261.445	5.717778	2.94E-05	4.011781	2.715947	954.8075	32.11514
19	13.575	48.41667	1.691667	101125.4	1582.781	100359.6	766.3296	0.004749	1259.892	5.779476	3.09E-05	4.011781	2.320114	887.8694	41.90058
20	14.7125	62.875	1.070833	101057.5	1683.706	99999.57	1058.63	0.006585	1250.299	7.962237	5.7E-05	4.011781	2.940947	988.4335	26.49297
21	16.40417	60.75	1.041667	101253.8	1895.358	100120.9	1151.43	0.007153	1244.582	8.473933	6.5E-05	4.011781	2.970114	989.6416	25.76089
22	16.175	62.79167	1.345833	101131.3	1849.805	99962.68	1161.523	0.007227	1243.534	8.746921	7.06E-05	4.011781	2.665947	933.2254	33.25123
23	16.5625	47.79167	1.616667	101202.9	1899.554	100304.1	907.8285	0.00563	1246.113	6.7232	4.06E-05	4.011781	2.395114	890.0572	40.00371
24	16.09583	47.20833	1.383333	101516.7	1851.421	100656	874.0251	0.005401	1252.558	6.445097	3.82E-05	4.011781	2.628447	932.9791	34.2536
25	16.10833	63.95833	1.3375	101532.1	1849.839	100335.5	1183.126	0.007334	1248.504	8.952263	7.54E-05	4.011781	2.674281	938.4344	33.04119
26	16.99583	69.5	1.408333	101552.1	1947.865	100202.7	1353.766	0.008403	1242.968	10.07811	9.11E-05	4.011781	2.603447	922.4585	34.74511
27	16.57917	73.16667	1.266667	101486.7	1897.575	100104.5	1388.392	0.008627	1243.54	10.33781	9.55E-05	4.011781	2.745114	947.4255	31.25467
28	16.62917	69.875	1.316667	101518.3	1908.59	100193.4	1333.627	0.008279	1244.456	9.906058	8.79E-05	4.011781	2.695114	939.2324	32.49714
29	17.59583	54	1.1625	101776.7	2040.457	100690.2	1101.847	0.006807	1246.516	8.093833	6.07E-05	4.011781	2.849281	968.1571	28.75144
30	18.07917	47.45833	0.720833	101520.8	2090.788	100523.8	992.2532	0.00614	1242.342	7.413478	5.13E-05	4.011781	3.290947	1054.115	17.85634
31	16.64583	62.29167	1.854167	101442.9	1910.204	100278.8	1189.898	0.007381	1245.429	8.710607	6.86E-05	4.011781	2.157614	854.4212	45.76287
Average	15.50484	58.18145	1.390726	101316.2	1793.95	100302.9	1026.312	0.006367	1250.743	7.607542	5.43E-05	4.011781	2.621055	935.999	33.62656

Table A.4 Wind Power Analysis According to Two-phase flow Drift-flux Model in April

Day	Temp(°c)	Ø %	V (m/s)	Patm(pa)	Pg (pa)	P dry (pa)	Pv (pa)	ω	ρ (dry)	ρ (v)	α(D)	Vd	Vr	ρ(D)	λ
1	16.47083	62.5	1.329167	101457.9	1886.117	100288.1	1178.823	0.007311	1246.297	8.75314	6.81E-05	4.011781	2.682614	938.1908	32.84051
2	16.15833	69.33333	1.525	101616.3	1852.506	100337.6	1284.404	0.007962	1248.277	9.574377	8.21E-05	4.011781	2.486781	906.9631	37.63261
3	17.58333	70.20833	1.6625	101844.2	2026.013	100426.9	1422.43	0.00881	1243.255	10.561	0.000101	4.011781	2.349281	881.935	40.96902
4	17.8	65.20833	1.0375	102141.3	2053.056	100807.9	1338.764	0.00826	1247.043	9.928654	8.93E-05	4.011781	2.974281	992.6518	25.62741
5	22.03333	31.08333	1.691667	101548.3	2684.953	100730.3	834.5729	0.005153	1228.264	6.004543	3.42E-05	4.011781	2.320114	865.6853	41.88338
6	20.57083	54.83333	1.766667	100881.3	2435.131	99584.99	1335.264	0.00834	1220.234	9.577565	9.48E-05	4.011781	2.245114	849.9619	43.56343
7	18.69583	76.125	2.1125	101092.1	2164.459	99452.48	1647.695	0.010305	1226.457	12.17734	0.000136	4.011781	1.899281	807.4517	51.89229
8	16.9125	69.70833	3.508333	101136.3	1931.165	99788.5	1346.183	0.008391	1238.16	10.06982	9.18E-05	4.011781	0.503447	665.2008	86.13332
9	15.0375	57.16667	1.6875	101590.4	1718.446	100618.8	982.3784	0.006073	1256.6	7.309211	4.66E-05	4.011781	2.324281	886.6264	41.72826
10	15.825	38.5	1.25	101756.3	1816.737	101070.5	699.4436	0.004304	1258.851	5.143918	2.31E-05	4.011781	2.761781	960.9719	30.99766
11	18.35	30.04167	1.4	101498.8	2161.013	100893.1	649.2044	0.004002	1245.886	4.507253	1.84E-05	4.011781	2.611781	924.7143	34.73195
12	19.53333	32.625	2.179167	101330	2283.871	100611.9	745.1129	0.004606	1237.199	5.326198	2.89E-05	4.011781	1.832614	803.5574	53.96521
13	16.86667	73.16667	1.4125	100741.7	1927.293	99341.9	1410.136	0.008829	1232.819	10.46382	9.95E-05	4.011781	2.599281	914.339	34.83173
14	16.37083	80.20833	1.2875	100931.3	1873.087	99445.65	1502.372	0.009397	1236.239	11.12239	0.000111	4.011781	2.724281	938.3778	31.74216
15	16.25	83.70833	0.845833	101479.6	1854.178	99933.47	1552.102	0.00966	1242.809	11.57944	0.000119	4.011781	3.165947	1028.133	20.88015
16	17.20417	75.25	1.25	101668.8	1980.704	100189.2	1490.48	0.009253	1241.953	11.03902	0.00011	4.011781	2.761781	949.3219	30.82529
17	18.025	72.83333	1.291667	101479.6	2081.942	99970.64	1516.348	0.009434	1235.724	11.2288	0.000115	4.011781	2.720114	937.2797	31.84156
18	18.05	69.41667	1.995833	101407.1	2082.262	99965.12	1445.437	0.008994	1235.539	10.72933	0.000105	4.011781	2.015947	828.5072	49.12837
19	18.33333	70.04167	1.245833	101815.4	2117.965	100336.5	1483.458	0.009196	1238.909	10.99504	0.000109	4.011781	2.765947	947.7338	30.7233
20	18.12917	68.5	1.591667	101887.1	2094.748	100458	1434.902	0.008884	1241.297	10.63099	0.000102	4.011781	2.420114	891.5626	39.22713
21	19.02083	67.33333	1.0375	101634.2	2215.708	100154.1	1491.91	0.009265	1233.772	10.9779	0.000109	4.011781	2.974281	982.2827	25.60257
22	22.8375	46.91667	0.679167	100874.6	2834.804	99586.77	1329.995	0.008307	1211.087	9.427174	8.61E-05	4.011781	3.332614	1036.887	16.80026
23	18.25	56.625	5.266667	100715.8	2104.873	99520.49	1191.884	0.007449	1229.203	8.887735	7.42E-05	4.011781	-1.25489	536.56	129.0896
24	16.82917	46.5	1.933333	101686.3	1934.89	100793.9	899.7238	0.005552	1251.054	6.667083	4.01E-05	4.011781	2.078447	846.331	47.82092
25	18.00417	45.41667	1.245833	101853.3	2094.871	100922.4	951.4207	0.005864	1247.639	6.927776	4.33E-05	4.011781	2.765947	953.5576	30.8404
26	20.15833	39.20833	0.866667	101607.5	2403.065	100679.5	942.2016	0.005821	1235.535	6.849478	4.53E-05	4.011781	3.145114	1017.149	21.47042
27	23.11667	30.41667	0.708333	101339.6	2892.015	100464.8	879.6544	0.005446	1220.637	6.386921	4.29E-05	4.011781	3.303447	1038.309	17.56013
28	22.4125	50.20833	0.7125	101292.1	2753.844	99931.51	1382.659	0.008606	1216.972	9.97041	0.000101	4.011781	3.299281	1034.682	17.61801
29	21.62917	59.04167	1.166667	101192.1	2615.843	99676.2	1544.437	0.009638	1217.054	11.14415	0.000118	4.011781	2.845114	945.1376	28.77002
30	23.17917	49.41667	0.825	100944.6	2879.391	99573.54	1422.899	0.008888	1209.462	10.03378	0.000104	4.011781	3.186781	1004.631	20.38864
Average	18.65458	58.05139	1.550417	101414.8	2191.832	100185.2	1244.543	0.007733	1235.808	9.133142	8.16E-05	4.011781	2.461364	910.4897	35.72999

Table A.5 Wind Power Analysis According to Two-phase flow Drift-flux Model in May

Day	Temp(°c)	Ø %	V (m/s)	Patm(pa)	Pg (pa)	P dry (pa)	Pv (pa)	ω	ρ (dry)	ρ (v)	α(D)	Vd	Vr	ρ(D)	λ
1	22.725	53.08333	1.191667	100892.5	2773.038	99444.99	1472.021	0.009207	1209.644	10.61216	0.000116	4.011781	2.820114	934.8219	29.39833
2	20.92083	63.83333	1.295833	101106.3	2485.844	99512.43	1586.797	0.009918	1217.918	11.74131	0.000131	4.011781	2.715947	923.192	31.92471
3	20.48333	69.33333	1.633333	101221.7	2422.928	99543.4	99543.4	0.010497	1220.123	12.38349	0.000144	4.011781	2.378447	870.4614	40.16974
4	20.89583	73.25	1.241667	101285.4	2479.771	99478.45	1816.432	0.011357	1217.589	13.32092	0.000164	4.011781	2.770114	932.6436	30.5524
5	20.87917	72.58333	1.458333	101367.9	2475.49	99573.6	1796.793	0.011224	1218.819	13.2268	0.000162	4.011781	2.553447	897.1342	35.85697
6	21.56667	72.66667	1.475	101237.1	2584.658	99369.03	1878.185	0.011756	1213.483	13.73923	0.000176	4.011781	2.536781	890.6657	36.24453
7	20.95417	72.45833	2.016667	100956.3	2488.448	99160.15	1803.088	0.01131	1213.456	13.23733	0.000164	4.011781	1.995114	811.7574	49.485
8	21.32083	71.29167	1.295833	101283.8	2545.385	99478.95	1814.648	0.011346	1215.833	13.28613	0.000164	4.011781	2.715947	921.9324	31.8787
9	22.46667	66.25	0.783333	101175.4	2738.844	99381.52	1814.484	0.011356	1209.974	13.15319	0.000163	4.011781	3.228447	1014.067	19.31894
10	23.84167	56.58333	1.466667	100641.3	2999.867	98994.77	1697.425	0.010665	1199.743	12.01804	0.000143	4.011781	2.545114	881.5347	36.09712
11	21.91667	68.70833	1.608333	101045.4	2644.058	99244.09	1816.688	0.011386	1210.525	13.23308	0.000164	4.011781	2.403447	867.6385	39.51955
12	22.9125	65.54167	1.6125	101419.6	2818.575	99607.59	1847.341	0.011536	1210.907	13.26917	0.000167	4.011781	2.399281	867.2843	39.62052
13	22.76667	68.25	1.195833	101365	2791.444	99475.44	1905.16	0.011913	1209.897	13.83719	0.000182	4.011781	2.815947	934.8918	29.41578
14	22.73333	72.45833	1.0625	101042.1	2777.748	99037.65	2012.71	0.012641	1204.678	14.68165	0.000205	4.011781	2.949281	955.08	26.13374
15	23.74167	69.95833	1.079167	100930.4	2957.465	98877.6	2068.993	0.013015	1198.661	14.98489	0.000216	4.011781	2.932614	947.3068	26.53356
16	24.02083	51.58333	1.283333	101182.1	3013.319	99643.68	1554.37	0.009703	1206.83	11.21798	0.000123	4.011781	2.728447	916.8325	31.63036
17	23.92917	45.54167	1.05	101029.6	3004.156	99664.88	1368.143	0.008538	1207.495	9.947185	9.65E-05	4.011781	2.961781	958.8764	25.9281
18	22.91667	55.875	1.016667	100892.9	2809.158	99315.45	1569.617	0.00983	1207.312	11.54141	0.000131	4.011781	2.995114	965.2674	25.07542
19	22.06667	59.875	2.254167	100551.7	2674.085	98960.9	1601.109	0.010063	1206.489	11.67615	0.000131	4.011781	1.757614	776.5254	55.37022
20	19.3125	71.08333	1.325	100683.8	2264.156	99101.61	1609.438	0.010101	1219.615	11.72476	0.000127	4.011781	2.686781	919.4915	32.64021
21	19.84167	67.79167	1.5125	100995.8	2341.574	99427.57	1587.392	0.00993	1221.423	11.59631	0.000125	4.011781	2.499281	889.9774	37.24199
22	18.66667	70.375	1.15	100990	2159.66	99474.26	1519.861	0.009503	1226.845	11.25749	0.000117	4.011781	2.861781	955.7867	28.35973
23	20.0375	61	1.416667	100970.8	2372.323	99551.49	1447.117	0.009042	1222.131	10.49179	0.000102	4.011781	2.595114	905.7515	34.93009
24	20.82917	62.29167	1.275	101440.4	2491.7	99896.64	1552.121	0.009664	1223.083	11.37111	0.000122	4.011781	2.736781	930.6288	31.42545
25	21.87917	65.45833	1.295833	101439.6	2640.352	99718.44	1728.33	0.010781	1216.489	12.64129	0.00015	4.011781	2.715947	922.2976	31.89765
26	22.13333	64.70833	1.875	101149.6	2687.548	99422.22	1739.067	0.01088	1211.853	12.6746	0.000152	4.011781	2.136781	829.7039	46.05853
27	21.8125	64.875	1.65	101080	2630.973	99385.76	1706.844	0.010682	1212.703	12.44829	0.000145	4.011781	2.361781	862.6974	40.57111
28	22.96667	62.75	1.4125	101085.4	2833.194	99323.56	1777.829	0.011133	1207.26	12.88948	0.000159	4.011781	2.599281	895.9699	34.74341
29	22.55833	60.29167	1.595833	101233.8	2757.929	99563.97	1662.801	0.010388	1211.846	12.2271	0.000145	4.011781	2.415947	870.23	39.25583
30	22.2375	60.875	2.25	101500.4	2707.298	99851.09	1648.068	0.010266	1216.66	12.09178	0.00014	4.011781	1.761781	783.6895	55.24772
31	22.575	60.04167	2.316667	101429.6	2761.817	99776.78	1658.241	0.010337	1214.364	12.10643	0.00014	4.011781	1.695114	774.1166	56.87096
Average	21.86801	64.53763	1.454704	101116.9	2649.445	99427.68	4858.21	0.010644	1213.021	12.40735	0.000147	4.011781	2.557076	897.0405	35.22478

Table A.6 Wind Power Analysis According to Two-phase flow Drift-flux Model in June

Day	Temp(°c)	Ø %	V (m/s)	Patm(pa)	Pg (pa)	P dry (pa)	Pv (pa)	ω	ρ (dry)	ρ (v)	α(D)	Vd	Vr	ρ(D)	λ
1	22.575	62.79167	1.591667	101299.2	2782.833	99557.46	1747.387	0.010917	1211.701	12.75787	0.000155	4.011781	2.420114	870.8993	39.13218
2	23.4375	67.125	1.625	101293.8	2901.379	99347.43	1947.551	0.012193	1205.594	14.21792	0.000194	4.011781	2.386781	861.8435	39.88545
3	24.1	71.95833	1.216667	101258.3	3016.913	99100.47	2170.92	0.013626	1199.9	15.73406	0.000238	4.011781	2.795114	923.8916	29.87451
4	24.57083	72.625	1.079167	101006.3	3107.679	98766.11	2256.952	0.014214	1193.977	16.30701	0.000257	4.011781	2.932614	943.8142	26.50547
5	24.57083	73.29167	1.3375	100960.8	3104.038	98704.39	2275.001	0.014336	1193.212	16.4285	0.00026	4.011781	2.674281	898.5173	32.79791
6	24.70417	71.75	1.5	101046.7	3125.742	98819.42	2242.72	0.014116	1194.057	16.20932	0.000253	4.011781	2.511781	873.105	36.75985
7	25.45417	70.125	1.420833	101120.8	3272.202	98846.75	2294.632	0.014439	1191.4	16.50817	0.000264	4.011781	2.590947	883.6768	34.823
8	26.64583	67.45833	1.15	100883.8	3522.198	98539.64	2376.016	0.014998	1183.016	16.94628	0.000283	4.011781	2.861781	922.6763	28.21571
9	26.34167	69.70833	1.254167	100689.6	3442.713	98314.37	2399.858	0.015183	1181.471	17.19175	0.000292	4.011781	2.757614	903.6455	30.74494
10	25.525	72.25	1.666667	100855.4	3275.871	98498.74	2366.817	0.014946	1186.889	17.10558	0.000285	4.011781	2.345114	843.1355	40.77082
11	25.45	73.91667	1.7625	100841.7	3269.515	98446.26	2416.716	0.015269	1186.583	17.38994	0.000295	4.011781	2.249281	829.3043	43.08178
12	26.325	69.95833	1.858333	100796.3	3434.717	98409.66	2402.871	0.015187	1182.671	17.27427	0.000294	4.011781	2.153447	813.3587	45.40584
13	25.95	70.33333	1.841667	100824.6	3364.498	98474.51	2366.364	0.014947	1184.926	17.03249	0.000284	4.011781	2.170114	817.1038	45.01542
14	24.67083	64.20833	1.4375	100681.7	3117.175	98697.24	2001.486	0.012614	1192.707	14.44628	0.000202	4.011781	2.574281	881.5492	35.29676
15	25.41667	65.20833	1.645833	101051.7	3268.556	98926.95	2131.371	0.013401	1192.535	15.41849	0.000233	4.011781	2.365947	849.7606	40.33774
16	26.01667	66.83333	1.366667	100985.8	3389.2	98728.61	2265.115	0.01427	1187.766	16.34672	0.000263	4.011781	2.645114	889.6532	33.5089
17	26.175	64.08333	1.1625	100782.9	3414.427	98586.85	2188.079	0.013805	1185.407	15.89486	0.000253	4.011781	2.849281	922.1657	28.54602
18	26.4625	63.5	2.345833	100643.3	3473.085	98436.87	2205.409	0.013935	1182.474	15.9554	0.000257	4.011781	1.665947	751.816	57.28235
19	25.99167	68.33333	2.283333	100583.8	3374.369	98291.91	2305.819	0.014591	1182.572	16.60642	0.000271	4.011781	1.728447	759.3982	55.72484
20	26.06667	58.58333	2.066667	100673.8	3396.169	98708.23	1989.589	0.012537	1187.298	14.23973	0.000198	4.011781	1.945114	788.2362	50.62714
21	24.94167	53.125	1.525	100796.3	3169.146	99116.59	1683.609	0.010565	1196.694	12.21182	0.000146	4.011781	2.486781	870.2187	37.51651
22	25.65	50.79167	1.829167	101006.7	3330.802	99318.28	1691.77	0.010595	1196.373	12.23419	0.00015	4.011781	2.182614	825.3452	44.95421
23	26.3875	57.41667	1.670833	101080	3470.619	99083.43	1992.714	0.012509	1190.562	14.43749	0.000207	4.011781	2.340947	844.4503	40.98663
24	27.07083	65.25	1.325	100922.9	3604.9	98581.13	2352.197	0.014841	1181.824	16.90103	0.000286	4.011781	2.686781	892.0983	32.47692
25	27.61667	67.66667	1.2875	100790.8	3722.588	98285.99	2518.951	0.015941	1176.152	18.0452	0.000327	4.011781	2.724281	894.1969	31.53165
26	27.79583	70.25	1.183333	100703.8	3756.048	98080.75	2638.624	0.016733	1172.972	18.8893	0.00036	4.011781	2.828447	909.4192	28.98037
27	27.74583	71.79167	1.333333	100727.5	3744.304	98058.39	2688.098	0.017051	1172.88	19.22885	0.000369	4.011781	2.678447	884.4631	32.60922
28	27.92083	71.5	1.266667	100685.8	3776.677	98002.9	2700.324	0.017138	1171.53	19.31765	0.000373	4.011781	2.745114	894.3633	30.99036
29	28.325	70.54167	1.366667	100750.4	3864.698	98043.05	2726.222	0.017296	1170.43	19.46921	0.00038	4.011781	2.645114	877.3256	33.4088
30	29.20417	70.5	1.470833	100512.5	4076.265	97675.42	2873.767	0.0183	1162.712	20.33741	0.000422	4.011781	2.540947	855.5751	35.89834
Average	25.97028	67.09583	1.529028	100875.2	3385.644	98614.93	2273.898	0.01435	1186.609	16.36944	0.000268	4.011781	2.482753	865.8335	37.04822

Table A.7 Wind Power Analysis According to Two-phase flow Drift-flux Model in July

Day	Temp(°c)	Ø %	V (m/s)	Patm(pa)	Pg (pa)	P dry (pa)	Pv (pa)	ω	ρ (dry)	ρ (v)	α(D)	Vd	Vr	ρ(D)	λ
1	31.62083	49.79167	1.2	100188.3	4742.544	97961.46	2361.392	0.014994	1156.94	15.85389	0.000279	4.011781	2.811781	893.6918	29.45628
2	31.31667	56.83333	0.854167	100142.1	4611.371	97520.95	2620.796	0.016716	1152.828	18.64542	0.000376	4.011781	3.157614	952.904	20.98046
3	29.55	73.75	1.454167	100256.7	4111.394	97248.06	3032.153	0.019394	1156.256	21.54436	0.000478	4.011781	2.557614	853.6145	35.45408
4	29.8125	70.45833	1.575	100367.9	4213.523	97419.5	2968.778	0.018955	1157.279	21.09717	0.000456	4.011781	2.436781	836.2937	38.38188
5	30.025	70.83333	1.745833	100539.2	4223.679	97566.22	2991.773	0.019073	1158.217	21.25477	0.000464	4.011781	2.265947	812.8427	42.48969
6	29.7125	69.58333	1.679167	100547.5	4200.05	97652	2922.535	0.018615	1160.42	20.72804	0.000438	4.011781	2.332614	823.5299	40.90808
7	29.83333	65.04167	1.616667	100398.3	4219.508	97674.92	2744.439	0.017477	1160.242	19.48533	0.000388	4.011781	2.395114	832.016	39.44951
8	29.6875	56	2.0375	100430.4	4174.475	98132.44	2337.706	0.014817	1166.249	16.45471	0.000276	4.011781	1.974281	778.6684	49.77472
9	29.75417	46.20833	1.5875	100630.4	4217.048	98702.53	1948.628	0.01228	1172.796	13.79268	0.000193	4.011781	2.424281	843.9062	38.97236
10	29.55	59.95833	1.608333	97017.5	4159.46	94520.84	2493.943	0.016412	1168.716	17.8673	0.002787	4.011781	2.403447	835.2681	39.92103
11	29.84583	64.70833	1.5125	100822.5	4235.681	98103.47	2740.839	0.017378	1165.32	19.44708	0.000387	4.011781	2.499281	850.9887	36.93717
12	29.7	66.375	1.5875	100442.9	4196.352	97677.21	2785.329	0.017737	1160.809	19.79156	0.000403	4.011781	2.424281	836.7125	38.73449
13	29.7	66.75	1.454167	100106.3	4189.583	97329.02	2796.547	0.017872	1156.656	19.87651	0.000409	4.011781	2.557614	853.5732	35.50755
14	29.88333	66.45833	1.370833	100172.1	4237.625	97372.07	2816.255	0.01799	1156.471	20.0255	0.000418	4.011781	2.640947	866.3439	33.48865
15	29.80417	69.66667	1.525	100351.3	4211.081	97435.28	2933.72	0.018728	1157.5	20.86447	0.000446	4.011781	2.486781	843.7533	37.1847
16	30.05833	68.54167	1.408333	100497.1	4271.398	97587.57	2927.687	0.01866	1158.333	20.80187	0.000442	4.011781	2.603447	862.0384	34.37144
17	30.30417	65.45833	1.5	100652.1	4344.844	97834.23	2844.062	0.018082	1160.351	20.12662	0.000414	4.011781	2.511781	849.4001	36.60833
18	29.65	62.83333	1.408333	100692.1	4191.852	98068.44	2633.88	0.016705	1165.675	18.77046	0.000361	4.011781	2.603447	867.0732	34.43794
19	29.86667	60.16667	1.608333	100567.9	4235.394	98049.87	2548.295	0.016166	1164.588	18.01323	0.000329	4.011781	2.403447	835.9832	39.30757
20	29.40417	64.33333	1.470833	100393.8	4122.369	97761.43	2652.057	0.016874	1162.933	18.85774	0.000363	4.011781	2.540947	855.433	35.94675
21	30.11667	66.66667	1.641667	96695.42	4288.619	93859.66	2859.079	0.018947	1113.5	20.2715	0.003431	4.011781	2.370114	791.3433	40.71008
22	30.19583	66.125	1.408333	100698.3	4306.029	97865.76	2847.362	0.018097	1161.108	20.2414	0.000417	4.011781	2.603447	863.986	34.38967
23	30.54583	67.08333	1.691667	100581.7	4321.706	97704.8	2899.145	0.018456	1157.871	20.53466	0.000436	4.011781	2.320114	819.9279	41.21619
24	30.5	66.16667	1.4875	100283.8	4387.894	97405.18	2903.323	0.01854	1154.507	20.54916	0.000436	4.011781	2.524281	847.1025	36.28889
25	30.54583	61.875	1.4	100281.3	4400.835	97565.57	2723.017	0.01736	1156.245	19.3764	0.000392	4.011781	2.611781	861.4988	34.21321
26	30.88333	62.66667	1.5125	100424.2	4483.871	97625.13	2809.892	0.017903	1155.654	19.95229	0.000415	4.011781	2.499281	844.0689	36.91459
27	30.65417	67.79167	1.508333	100463.3	4423.558	97487.9	2998.804	0.019133	1154.888	21.23129	0.000464	4.011781	2.503447	844.4091	36.76882
28	29.85417	60.375	2.383333	100682.9	4238.858	98155.96	2559.211	0.016217	1165.906	18.07687	0.000332	4.011781	1.628447	737.8423	58.01567
29	29.22083	57.45833	1.545833	100868.3	4080.34	98538.15	2344.495	0.014799	1172.89	16.70081	0.000281	4.011781	2.465947	850.8676	37.84636
30	30.05	59.29167	1.5125	100645.4	4283.66	98125.55	2539.854	0.0161	1164.807	18.0094	0.000331	4.011781	2.499281	850.3081	36.98647
31	30.12917	65.66667	1.095833	100545.4	4303.617	97736.05	2826.042	0.017985	1159.868	20.07351	0.000417	4.011781	2.915947	914.5132	26.82899
Average	30.05726	63.70699	1.528763	100238.3	4278.33	97538.3	2722.937	0.01737	1159.22	19.30052	0.000568	4.011781	2.468586	843.1796	37.48198

Table A.8 Wind Power Analysis According to Two-phase flow Drift-flux Model in August

Day	Temp(°c)	Ø %	V (m/s)	Patm(pa)	Pg (pa)	P dry (pa)	Pv (pa)	ω	ρ (dry)	ρ (v)	α(D)	Vd	Vr	ρ(D)	λ
1	30.35	65.08333	1.145833	100730.4	4353.531	97917.23	2833.423	0.017999	1161.154	20.08938	0.000412	4.011781	2.865947	906.8677	28.04011
2	30.14583	66.70833	1.379167	100807.1	4294.088	97966.18	2864.514	0.018187	1162.493	20.30692	0.000419	4.011781	2.632614	869.5868	33.68341
3	30.24167	65.875	1.6625	100602.9	4317.35	97779.62	2844.054	0.018092	1159.913	20.17414	0.000415	4.011781	2.349281	825.3945	40.52829
4	29.70833	62.58333	1.304167	100505	4202.371	97909.93	2629.984	0.016708	1163.54	18.57379	0.000356	4.011781	2.707614	882.021	31.91749
5	29.79583	56.45833	1.4625	100510.8	4217.815	98122.35	2381.308	0.015095	1165.736	17.07786	0.000305	4.011781	2.549281	858.3733	35.80755
6	29.69583	74.91667	1.183333	100626.7	4192.06	97464.04	3140.552	0.020043	1158.304	22.61723	0.001561	4.011781	2.828447	896.7288	29.16992
7	29.57083	60	1.170833	100695.8	4166.027	98207.33	2499.616	0.015831	1167.612	17.81139	0.000322	4.011781	2.840947	907.2449	28.69868
8	31.09583	51.04167	1.266667	100616.7	4574.719	98276.42	2335.013	0.014778	1162.665	16.64911	0.000308	4.011781	2.745114	887.1063	31.0627
9	30.49167	67.125	1.175	100750	4380.444	97830.13	2940.373	0.018695	1159.559	20.84584	0.000444	4.011781	2.836781	900.7686	28.73
10	30.29583	67.95833	1.583333	100572.1	4336.01	97654.24	2946.68	0.018769	1158.229	20.84606	0.000444	4.011781	2.428447	835.7087	38.59238
11	30.32083	66.125	1.541667	100472.1	4341.644	97620.18	2870.912	0.018292	1157.727	20.37058	0.000425	4.011781	2.470114	841.3463	37.60414
12	30.42083	66	1.541667	100380.4	4363.463	97523.43	2879.885	0.018368	1156.192	20.40273	0.000429	4.011781	2.470114	840.2411	37.60236
13	30.51667	68.54167	1.258333	100446.7	4386.785	97456.7	3006.776	0.01919	1155.034	21.3438	0.000468	4.011781	2.753447	883.5136	30.73192
14	30.64583	65	1.25	100620.4	4425.065	97772.46	2876.292	0.018298	1158.295	20.32271	0.000423	4.011781	2.761781	887.199	30.55641
15	30.6875	65.25	1.45	100482.9	4433.604	97608.49	2892.927	0.018435	1156.197	20.50586	0.000432	4.011781	2.561781	854.0019	35.38577
16	30.20833	63.95833	1.3	100279.2	4299.394	97547.35	2749.821	0.017534	1157.289	19.52171	0.000391	4.011781	2.711781	878.1518	31.78684
17	29.72083	62.70833	1.204167	100454.6	4192.64	97841.72	2629.134	0.016714	1162.652	18.70024	0.000356	4.011781	2.807614	897.899	29.48581
18	29.7625	63.16667	1.808333	100771.7	4204.635	98136.64	2655.928	0.016834	1165.997	18.85696	0.000359	4.011781	2.203447	809.1083	44.10894
19	30.17083	56.58333	1.545833	100910.4	4204.635	98547.01	2379.123	0.015016	1169.296	16.89013	0.000287	4.011781	2.465947	848.3181	37.83697
20	30.04167	55.5	1.391667	100832.5	4231.358	98499.04	2348.404	0.01483	1169.243	16.67992	0.000283	4.011781	2.620114	871.9235	34.09929
21	29.3625	52.08333	1.416667	100737.5	4114.831	98604.04	2143.141	0.013519	1173.126	15.28228	0.000235	4.011781	2.595114	870.5721	34.75343
22	29.36667	60.20833	1.45	100624.2	4113.808	98154.44	2476.855	0.015696	1167.764	17.69016	0.000322	4.011781	2.561781	861.9198	35.48402
23	29.85833	64.79167	1.675	100712.5	4224.86	97988.55	2737.357	0.017376	1163.864	19.48611	0.000385	4.011781	2.336781	826.2526	40.86055
24	29.9	65.04167	1.283333	100777.5	4163.565	98087.3	2708.052	0.017173	1164.89	19.24178	0.000376	4.011781	2.728447	886.5618	31.39406
25	29.9	67.95833	1.420833	100714.2	4245.06	97852.37	2884.872	0.018338	1162.118	20.46679	0.000428	4.011781	2.590947	862.8344	34.68606
26	30.13333	61.41667	1.191667	100523.3	4308.442	97897.27	2646.101	0.016812	1161.777	18.7623	0.000363	4.011781	2.820114	899.3358	29.18167
27	29.85	59.33333	1.466667	100373.3	4226.729	97859.82	2513.513	0.015989	1162.397	17.97136	0.000338	4.011781	2.545114	855.4766	35.87712
28	29.6625	61.54167	1.266667	100363.8	4163.738	97813.12	2550.628	0.016222	1162.55	18.25502	0.00034	4.011781	2.745114	887.3465	31.01421
29	29.6875	62.83333	1.170833	100459.2	4187.506	97838.64	2620.523	0.016662	1162.759	18.75304	0.000359	4.011781	2.840947	903.6352	28.67566
30	29.36667	62.25	1.5375	100660	4107.456	98113.95	2546.051	0.016143	1167.255	18.24144	0.000336	4.011781	2.474281	848.3889	37.58485
31	29.32917	58	1.208333	100792.9	4106.19	98419.87	2373.05	0.015	1171.064	16.99947	0.000292	4.011781	2.803447	903.3826	29.631
Average	30.00981	62.77554	1.377823	100606.7	4260.639	97945.48	2674.35	0.016988	1162.796	19.02375	0.000411	4.011781	2.628308	869.4609	33.73763

Table A.9 Wind Power Analysis According to Two-phase flow Drift-flux Model in September

Day	Temp(°c)	Ø %	V (m/s)	Patm(pa)	Pg (pa)	P dry (pa)	Pv (pa)	ω	ρ (dry)	ρ (v)	α(D)	Vd	Vr	ρ(D)	λ
1	29.36667	55.04167	1.441667	100684.6	4115.085	98398.84	2285.742	0.014466	1170.692	16.36063	0.000282	4.011781	2.570114	865.075	35.32839
2	29.50833	60.20833	1.383333	100727.9	4145.596	98229.76	2498.159	0.01583	1168.113	17.88186	0.000331	4.011781	2.628447	872.6325	33.86086
3	29.1625	60.75	1.095833	100692.5	4070.285	98214.15	2478.353	0.01571	1169.285	17.75629	0.000329	4.011781	2.915947	921.5777	26.87858
4	29.19167	62.25	1.216667	100831.7	4077.985	98289.4	2542.262	0.016102	1170.065	18.21318	0.000345	4.011781	2.795114	901.3912	29.8066
5	29.22917	63.5	1.1125	100912.1	4078.854	98331.54	2580.548	0.016327	1170.39	18.49458	0.000345	4.011781	2.899281	919.6345	27.2669
6	28.7125	66.08333	1.620833	100671.7	3977.796	98081.37	2590.296	0.016434	1169.457	18.59666	0.000354	4.011781	2.390947	837.769	39.59181
7	27.275	48.125	1.116667	101055.8	3657.967	99350.82	1705.015	0.010679	1190.228	12.31168	0.000149	4.011781	2.895114	933.4514	27.50833
8	27.64167	43.33333	0.7375	101148.8	3755.729	99554.36	1594.392	0.009965	1191.286	11.48459	0.000131	4.011781	3.274281	1007.76	18.21127
9	27.47083	44.16667	0.879167	101068.8	3722.067	99410.02	1658.734	0.01039	1190.28	11.93437	0.000147	4.011781	3.132614	978.1346	21.68882
10	27.94583	53.25	0.970833	101011.7	3809.792	98967.92	2043.743	0.012864	1183.075	14.69069	0.000228	4.011781	3.040947	954.9348	23.8907
11	28.35833	63.95833	0.904167	101029.2	3893.142	98537.16	2492.007	0.015746	1176.283	17.89908	0.00033	4.011781	3.107614	962.5016	22.21104
12	28.47917	68	0.675	101160.8	3907.002	98513.32	2647.511	0.01672	1175.474	19.02066	0.000363	4.011781	3.336781	1008.023	16.61181
13	28.72083	67.79167	0.783333	101188.8	3960.835	98518.82	2669.934	0.016862	1174.592	19.16984	0.000369	4.011781	3.228447	984.9815	19.25017
14	28.59167	67.83333	0.8	100900.8	3935.556	98255.63	2645.202	0.016747	1171.959	19.00244	0.000362	4.011781	3.211781	979.4343	19.65671
15	29.14167	58	0.8375	100705	4074.158	98345.69	2359.308	0.014934	1170.915	16.90944	0.000298	4.011781	3.174281	970.9367	20.59643
16	28.8	65.70833	0.908333	100943.3	3980.204	98349.35	2593.985	0.016406	1172.258	18.62165	0.000347	4.011781	3.103447	958.521	22.29863
17	28.79167	65.16667	0.675	100939.6	3976.321	98358.11	2581.469	0.016327	1172.401	18.52852	0.000344	4.011781	3.336781	1005.369	16.6139
18	29.2875	65.58333	0.8875	101229.6	4089.508	98557.81	2671.773	0.016874	1172.874	19.14622	0.000369	4.011781	3.124281	963.0637	21.78573
19	28.9125	66.70833	0.95	100875.4	4007.771	98221.09	2654.33	0.016811	1170.303	19.04577	0.000365	4.011781	3.061781	949.1016	23.30639
20	28.79583	66.58333	1.233333	100924.2	3977.308	98283.54	2640.63	0.016717	1171.499	18.95159	0.000364	4.011781	2.778447	899.824	30.19201
21	29.04583	66	1.054167	100973.8	4031.271	98322.24	2651.513	0.016776	1170.973	19.01736	0.000364	4.011781	2.957614	930.5304	25.83929
22	27.7625	59.375	1.541667	101014.2	3747.551	98801.55	2212.62	0.013938	1181.718	15.93652	0.000256	4.011781	2.470114	857.6932	37.77865
23	26.6125	51.25	1.225	101290	3509.031	99501.93	1788.07	0.01118	1194.676	0.078286	0.000163	4.011781	2.786781	914.9228	30.57673
24	26.09167	54.75	1.1375	101319.2	3409.25	99467.41	1851.754	0.011582	1196.366	13.40741	0.000174	4.011781	2.874281	934.7	27.99469
25	26.87083	51.41667	1.295833	101230.8	3578.923	99402.16	1828.677	0.011449	1192.508	13.20071	0.000173	4.011781	2.715947	904.2714	31.87503
26	26.55417	53.83333	1.466667	101184.2	3497.467	99303.85	1880.312	0.011782	1192.542	13.5908	0.000183	4.011781	2.545114	876.6182	36.03891
27	26.5375	55.54167	1.404167	101352.5	3490.142	99424.49	1928.007	0.012063	1194.037	13.94159	0.000188	4.011781	2.607614	887.7585	34.50019
28	26.74167	57.16667	1.166667	101301.7	3533.073	99294.34	2007.328	0.012576	1191.667	14.50528	0.000205	4.011781	2.845114	926.064	28.68089
29	26.45417	56.91667	1.15	101104.2	3477.85	99130.52	1973.65	0.012389	1190.864	14.27114	0.000201	4.011781	2.861781	928.3366	28.27937
30	24.40417	56.58333	1.058333	101160	3085.323	99429.68	1730.323	0.010828	1202.697	12.59927	0.000153	4.011781	2.953447	953.9577	26.0745
Average	28.01528	59.1625	1.090972	101021.1	3819.095	98761.56	2259.522	0.014249	1180.316	15.81894	0.000274	4.011781	2.920808	932.9657	26.51226

Table A.10 Wind Power Analysis According to Two-phase flow Drift-flux Model in October

Day	Temp(°c)	Ø %	V (m/s)	Patm(pa)	Pg (pa)	P dry (pa)	Pv (pa)	ω	ρ (dry)	ρ (v)	α(D)	Vd	Vr	ρ(D)	λ
1	25.00417	56.75	1.520833	101289.2	3196.038	99488.8	1800.366	0.011259	1200.985	13.08269	0.000166	4.011781	2.490947	874.1823	37.38375
2	24.90417	54.45833	0.8625	101272.1	3177.263	99559.54	1712.54	0.010701	1202.255	12.44829	0.000149	4.011781	3.149281	991.3769	21.27127
3	24.7	40.45833	1.341667	101342.1	3126.663	100095	1247.132	0.007751	1209.56	9.070884	7.86E-05	4.011781	2.670114	908.5552	33.13
4	23.575	38.83333	1.404167	101470.4	2946.917	100330.2	1140.256	0.007072	1217.021	8.319558	6.69E-05	4.011781	2.607614	903.5298	34.69625
5	23.24167	34.41667	1.179167	101271.3	2890.443	100292.9	978.3049	0.006071	1217.966	7.148759	4.97E-05	4.011781	2.832614	942.8201	29.18324
6	23.44583	31	1.016667	101164.6	2932.079	100267.6	896.9937	0.005568	1216.811	6.549421	4.26E-05	4.011781	2.995114	972.0246	25.18315
7	24.04167	35.45833	0.854167	101205.8	3034.485	100116	1089.802	0.006778	1212.544	7.931023	6.39E-05	4.011781	3.157614	1000.937	21.14092
8	24.44167	43.41667	0.908333	101002.5	3087.848	99661.3	1341.2	0.008376	1205.335	9.76147	9.38E-05	4.011781	3.103447	984.4006	22.44358
9	23.40417	53.83333	1.566667	101367.9	2901.915	99819.24	1548.672	0.00965	1211.435	11.31601	0.000122	4.011781	2.445114	874.1974	38.57685
10	23.18333	53	1.0625	101255	2870.347	99752.02	1502.98	0.009373	1211.578	10.98894	0.000114	4.011781	2.949281	959.9486	26.21282
11	23.20833	34.875	1.016667	101454.6	2878.842	98537.16	980.4884	0.00607	1220.248	7.171779	4.77E-05	4.011781	2.995114	974.8815	25.1689
12	22.63333	35.95833	0.958333	101522.5	2796.304	100536.3	986.1979	0.006102	1223.408	7.223373	4.85E-05	4.011781	3.053447	988.7957	23.72709
13	22.8125	33.08333	0.7375	101467.1	2840.382	100548	919.1123	0.005688	1222.89	6.722015	4.33E-05	4.011781	3.274281	1033.926	18.27632
14	23.1625	34.25	1.1375	101297.1	2886.396	100314.7	982.362	0.006095	1218.572	7.175614	5.05E-05	4.011781	2.874281	950.8666	28.15386
15	23.04167	30	1.175	101512.9	2860.525	100658.4	854.4815	0.005282	1223.219	6.244065	3.76E-05	4.011781	2.836781	947.4535	29.10595
16	22.72083	38.25	1.104167	101562.9	2804.802	100479	1083.94	0.006716	1222.378	7.923627	6.22E-05	4.011781	2.907614	960.1353	27.31309
17	22.9625	36.29167	1.104167	101717.1	2846.344	100682.9	1034.148	0.006393	1223.853	7.556685	5.62E-05	4.011781	2.907614	961.2254	27.3222
18	22.74167	37.08333	0.804167	101645	2815.375	100576	1068.958	0.006622	1223.513	7.805252	6.42E-05	4.011781	3.207614	1020.358	19.91015
19	23.05833	28.91667	0.6875	101570.4	2885.704	100736.5	833.9365	0.005153	1224.179	6.086619	3.7E-05	4.011781	3.324281	1045.878	17.048
20	23.26667	28.75	0.816667	101487.5	2935.207	100645.1	842.4127	0.005211	1222.259	6.141133	3.84E-05	4.011781	3.195114	1016.476	20.24471
21	22.4125	41.54167	0.883333	101361.7	2747.25	100200.7	1160.943	0.007222	1220.253	8.494487	7.75E-05	4.011781	3.128447	1001.409	21.85364
22	22.62917	55.375	0.9875	101251.7	2770.265	99699.56	1552.109	0.009697	1213.218	11.35769	0.000131	4.011781	3.024281	975.5304	24.36501
23	22.23333	61.5	0.804167	101180	2705.485	99523.45	1656.552	0.010356	1212.684	12.14828	0.00014	4.011781	3.207614	1011.882	19.84442
24	22.29583	51.08333	0.983333	101182.1	2728.221	99796.88	1385.207	0.008638	1215.801	10.15195	9.97E-05	4.011781	3.028447	978.2395	24.2846
25	21.13333	59.54167	0.9125	101596.7	2532.931	100103.1	1493.576	0.009284	1224.309	10.996	0.000115	4.011781	3.099281	999.2117	22.52749
26	21.86667	57.125	0.870833	101718.8	2641.815	100210.1	1508.627	0.009367	1222.558	11.07644	0.000115	4.011781	3.140947	1006.217	21.50049
27	22.29167	48.91667	0.758333	101329.6	2735.885	100011.4	1318.155	0.0082	1218.457	9.661996	8.79E-05	4.011781	3.253447	1026.07	18.74987
28	22.60833	48.08333	0.983333	100845.8	2773.346	99526.95	1318.885	0.008245	1211.204	9.661654	8.99E-05	4.011781	3.028447	974.4729	24.29323
29	19.54583	70.25	0.983333	100815.8	2279.608	99220.25	1595.586	0.010005	1220.025	11.81683	0.000667	4.011781	3.028447	980.7143	24.40164
30	20.0125	62.54167	0.958333	100801.7	2374.147	99362.27	1439.396	0.009015	1219.928	10.64324	0.000106	4.011781	3.053447	986.5173	23.66002
31	19.9125	52	0.7375	101230	2356.782	100014.1	1215.868	0.007564	1228.357	8.984092	4.21E-05	4.011781	3.274281	1038.899	18.23647
Average	22.79005	44.74328	1.003898	101328.8	2818.052	100024.7	1241.587	0.007727	1217.316	9.085802	9.79E-05	4.011781	3.025114	980.565	24.39417

Table A.11 Wind Power Analysis According to Two-phase flow Drift-flux Model in November

Day	Temp(°c)	Ø %	V (m/s)	Patm(pa)	Pg (pa)	P dry (pa)	Pv (pa)	ω	ρ (dry)	ρ (v)	α(D)	Vd	Vr	ρ(D)	λ
1	18.64167	48.04167	1.05	101426.7	2170.559	100396.3	1030.36	0.006384	1238.384	7.651283	5.29E-05	4.011781	2.961781	982.9703	25.98387
2	18.1625	40.875	1.0375	101555.8	2123.169	100729.9	825.8905	0.0051	1244.6	6.15001	3.39E-05	4.011781	2.974281	990.0551	25.71012
3	18.8875	42.70833	1.05	101419.2	2213.612	100485.2	933.9778	0.005784	1238.48	6.926521	4.47E-05	4.011781	2.961781	982.9138	26.00087
4	16.9875	62.875	0.8875	101540	1940.426	100323	1217.031	0.007548	1244.463	9.092803	7.56E-05	4.011781	3.124281	1020.498	21.94661
5	15.0125	82.70833	1.75	101297.9	1715.595	99887.3	1410.612	0.008786	1247.565	10.61159	0.0001	4.011781	2.261781	871.7247	43.11461
6	17.50417	65	0.9375	101653.8	2025.913	100369.5	1284.267	0.007959	1242.91	9.578206	8.16E-05	4.011781	3.074281	1009.103	23.1698
7	18.2875	49.04167	0.8125	101887.9	2138.583	100880	1007.905	0.006215	1245.917	7.498397	5E-05	4.011781	3.199281	1037.221	20.12071
8	19.29167	40.79167	0.7625	101738.3	2290.57	100836.9	901.4135	0.005562	1241.158	6.678839	4.07E-05	4.011781	3.249281	1043.897	18.8966
9	17.97917	47.75	0.583333	101755.4	2104.475	100782	973.4058	0.006009	1246.062	7.24363	4.77E-05	4.011781	3.428447	1088.666	14.45767
10	17.8375	56.20833	0.758333	101674.6	2070.969	100520.5	1154.099	0.007146	1243.398	8.587956	6.88E-05	4.011781	3.253447	1046.919	18.76735
11	17.94167	60.20833	0.629167	102162.1	2085.774	100925.7	1236.373	0.007618	1247.912	9.200738	7.58E-05	4.011781	3.382614	1079.776	15.57134
12	17.84167	56.875	1.479167	101971.7	2071.115	100819.2	1152.456	0.007111	1247.049	8.582615	6.55E-05	4.011781	2.532614	913.315	36.54091
13	21.3125	31.875	1.675	101529.6	2573.9	100749.9	779.729	0.004814	1231.518	5.745775	3.01E-05	4.011781	2.336781	870.4303	41.48382
14	20.2	52.75	1.016667	101513.3	2383.113	100269.8	1243.52	0.007718	1230.222	9.18816	8.2E-05	4.011781	2.995114	983.1708	25.12799
15	19.00417	60.91667	0.833333	101834.6	2224.6	100496.7	1337.91	0.008283	1238.104	9.921014	8.96E-05	4.011781	3.178447	1026.646	20.5969
16	18.6875	52.91667	0.608333	101756.3	2195.903	100626.6	1129.652	0.006985	1241.104	8.386387	6.42E-05	4.011781	3.403447	1078.617	15.06444
17	19.7125	43.20833	0.645833	101564.2	2350.382	100565.6	998.5756	0.00618	1236.071	7.377638	5.18E-05	4.011781	3.365947	1065.56	16.002
18	21.2875	28.70833	1.2875	101366.3	2573.986	100662.3	703.9688	0.00435	1230.557	5.186816	2.45E-05	4.011781	2.724281	932.798	31.92108
19	19.01667	48	1.45	101232.5	2232.756	100234.2	998.2967	0.0062	1234.809	7.42343	5.39E-05	4.011781	2.561781	908.8682	35.86228
20	15.36667	71.75	1.329167	101165.8	1747.863	99915.63	1250.2	0.007784	1246.364	9.394219	7.85E-05	4.011781	2.682614	938.381	32.82066
21	15.1625	53.41667	1.775	100539.6	1748.683	99649.06	890.5251	0.005568	1244.039	6.703146	4.45E-05	4.011781	2.236781	864.4426	43.91226
22	12.43333	42	1.008333	101474.2	1475.393	100867.1	607.0498	0.003744	1271.259	4.606283	1.84E-05	4.011781	3.003447	1016.799	25.02559
23	11.56667	55	0.8125	101793.3	1373.56	101047.5	745.836	0.004592	1277.388	5.677222	2.77E-05	4.011781	3.199281	1063.138	20.15263
24	13.55417	54.45833	1.033333	101957.1	1580.27	101111.5	845.6134	0.005202	1269.405	6.387564	3.55E-05	4.011781	2.978447	1010.636	25.60456
25	14.85	41.79167	1.1375	102287.9	1706.781	101598.3	689.6197	0.004222	1269.71	5.194058	2.32E-05	4.011781	2.874281	990.3238	28.21165
26	16.30833	35.83333	1.379167	102194.2	1870.963	101531.3	662.8379	0.004061	1262.459	4.963281	2.15E-05	4.011781	2.632614	940.7139	34.20218
27	15.78333	45.875	0.991667	102057.9	1814.614	101244.7	813.2543	0.004998	1261.216	6.101571	3.3E-05	4.011781	3.020114	1012.382	24.57913
28	13.40833	80.79167	1.670833	101714.2	1539.563	100471.6	1242.522	0.007693	1261.874	9.39972	7.65E-05	4.011781	2.340947	893.4963	41.22881
29	14.45417	76.79167	0.933333	101813.3	1656.701	100556	1257.36	0.007778	1258.384	9.476933	7.8E-05	4.011781	3.078447	1022.485	23.07112
30	15.22083	62.95833	0.929167	102329.6	1753.147	101243.9	1085.637	0.00667	1263.68	8.156635	5.78E-05	4.011781	3.082614	1027.438	22.99337
Average	17.05681	53.07083	1.075139	101673.6	1991.765	100659.9	1013.663	0.006269	1248.535	7.569748	5.43E-05	4.011781	2.935775	990.4462	26.6047

Table A.12 Wind Power Analysis According to Two-phase flow Drift-flux Model in December

Day	Temp(°c)	Ø %	V (m/s)	Patm(pa)	Pg (pa)	P dry (pa)	Pv (pa)	ω	ρ (dry)	ρ (v)	α(D)	Vd	Vr	ρ(D)	λ
1	15.7	60.70833	0.925	102378.8	1806.706	101301	1077.706	0.006618	1262.298	8.08465	5.68E-05	4.011781	3.086781	1027.164	22.89161
2	15.05	61.58333	0.6875	102355.8	1738.355	101314.7	1041.146	0.006392	1265.354	7.827873	5.29E-05	4.011781	3.324281	1081.238	17.02826
3	15.15833	54.16667	0.629167	102360.4	1768.739	101445.3	915.1524	0.005613	1266.58	6.87824	4.13E-05	4.011781	3.382614	1095.69	15.59654
4	15.17917	51.29167	0.5375	102098.3	1762.825	101228.1	870.2235	0.005349	1263.746	6.540483	3.74E-05	4.011781	3.474281	1115.098	13.3304
5	13.975	61.91667	0.825	101269.6	1607.683	100291	978.5419	0.006074	1257.164	7.389801	4.92E-05	4.011781	3.186781	1043.871	20.4329
6	11.69167	53.95833	1.170833	101102.1	1380.276	100354	748.0545	0.004642	1268.041	5.689509	2.98E-05	4.011781	2.840947	982.7942	29.02407
7	9.75	46.33333	1.15	102190.8	1223.376	101633.9	556.9701	0.003408	1293.07	4.266101	1.54E-05	4.011781	2.861781	1005.902	28.54824
8	10.60417	51.375	0.933333	102584.6	1302.356	101935.1	649.4392	0.003964	1293.058	4.959766	2.07E-05	4.011781	3.078447	1049.895	23.16075
9	12.42083	50.79167	0.841667	102472.9	1462.619	101745.5	727.4417	0.004448	1282.423	5.519337	2.58E-05	4.011781	3.170114	1060.923	20.87808
10	13.14167	46.79167	1.033333	102271.7	1517.461	101568.9	702.7218	0.004303	1276.868	5.322068	2.39E-05	4.011781	2.978447	1016.378	25.62927
11	13.60417	51	0.883333	102552.9	1580.072	101761.3	791.5904	0.004839	1277.306	5.981007	3.07E-05	4.011781	3.128447	1047.818	21.9015
12	14.91667	47.75	0.608333	102151.3	1744.032	101351.4	799.8408	0.00491	1266.495	6.013234	3.15E-05	4.011781	3.403447	1100.439	15.09
13	15.3	45.79167	0.608333	101654.6	2466.397	100448.8	1205.775	0.007745	1253.529	9.043311	0.000321	4.011781	3.403447	1088.784	15.13109
14	14.59167	53.375	0.783333	101687.1	1688.005	100791.1	895.9493	0.005532	1260.824	6.740148	4.16E-05	4.011781	3.228447	1055.851	19.41311
15	15.55	56.95833	0.85	101922.1	2633.217	100465.6	1456.45	0.009348	1252.605	10.88803	0.000406	4.011781	3.161781	1034.529	21.07975
16	15.1125	67.375	0.679167	102136.7	1724.76	100978.2	1158.46	0.007137	1260.767	8.709466	6.61E-05	4.011781	3.332614	1079.315	16.81181
17	16.01667	69.04167	0.645833	102094.6	1831.135	100839.4	1255.15	0.007742	1255.108	9.407358	7.74E-05	4.011781	3.365947	1082.168	15.98089
18	16.3875	58.875	0.8125	101949.6	1885.77	100859.9	1089.723	0.006721	1253.807	8.156281	5.85E-05	4.011781	3.199281	1043.871	20.1113
19	15.62917	63.625	1.1375	102117.9	1778.939	100992.7	1125.185	0.00693	1258.661	8.447981	6.22E-05	4.011781	2.874281	982.3531	28.12716
20	16.79583	60.70833	1.366667	102040	1928.725	100889.6	1150.424	0.007094	1252.376	8.601464	6.57E-05	4.011781	2.645114	936.212	33.77061
21	16.65	49.95833	0.720833	102136.7	1961.625	101165.1	971.5756	0.005976	1256.436	7.261899	4.74E-05	4.011781	3.290947	1066.048	17.85919
22	17.79583	45.54167	0.9125	101716.3	2040.927	100785.9	930.3776	0.005744	1246.738	6.930501	4.32E-05	4.011781	3.099281	1016.893	22.60269
23	16.99167	56.66667	0.883333	100844.6	1941.357	99759.81	1084.775	0.006766	1237.451	8.108885	5.99E-05	4.011781	3.128447	1015.472	21.85964
24	15	66.375	2.379167	100785	1709.666	99662.87	1122.126	0.007011	1244.857	8.440846	6.63E-05	4.011781	1.632614	784.512	58.67919
25	13.82083	56	1.183333	102041.7	1605.141	101168.6	873.0358	0.005368	1268.907	6.595295	3.72E-05	4.011781	2.828447	981.3037	29.30834
26	13.55833	56.08333	1.029167	102502.9	1574.06	101631.8	0.005333	0.005333	1275.892	6.581303	3.77E-05	4.011781	2.982614	1016.663	25.49803
27	14.49167	38.79167	0.925	102030.4	1689.219	101413.3	617.0988	0.003785	1269.1	4.653264	1.87E-05	4.011781	3.086781	1032.137	22.95844
28	16.10833	31.16667	1.191667	101759.6	1849.247	101189.6	569.9889	0.003504	1259.099	4.269951	1.62E-05	4.011781	2.820114	971.6917	29.57805
29	15.74167	37.08333	1.0625	101760	1812.373	101109.9	650.0581	0.003999	1259.741	4.879128	2.07E-05	4.011781	2.949281	996.9412	26.36063
30	13.24583	66.70833	1.095833	101595	1522.274	100581.2	1013.818	0.006271	1263.969	7.67394	5.23E-05	4.011781	2.915947	994.3197	27.11898
31	11.25417	82.33333	1.620833	101434.6	1336.854	100335.1	1099.507	0.006816	1269.708	8.380451	6.02E-05	4.011781	2.390947	906.6537	40.04337
Average	14.55591	54.84274	0.971371	101935.4	1737.877	101000	907.3648	0.005787	1263.612	7.040051	6.37E-05	4.011781	3.038864	1022.998	24.05819

APPENDIX B

Figures of Wind Power Analysis According to Two-phase flow Drift-flux Model Throughout 2017 For Each Month

1. January

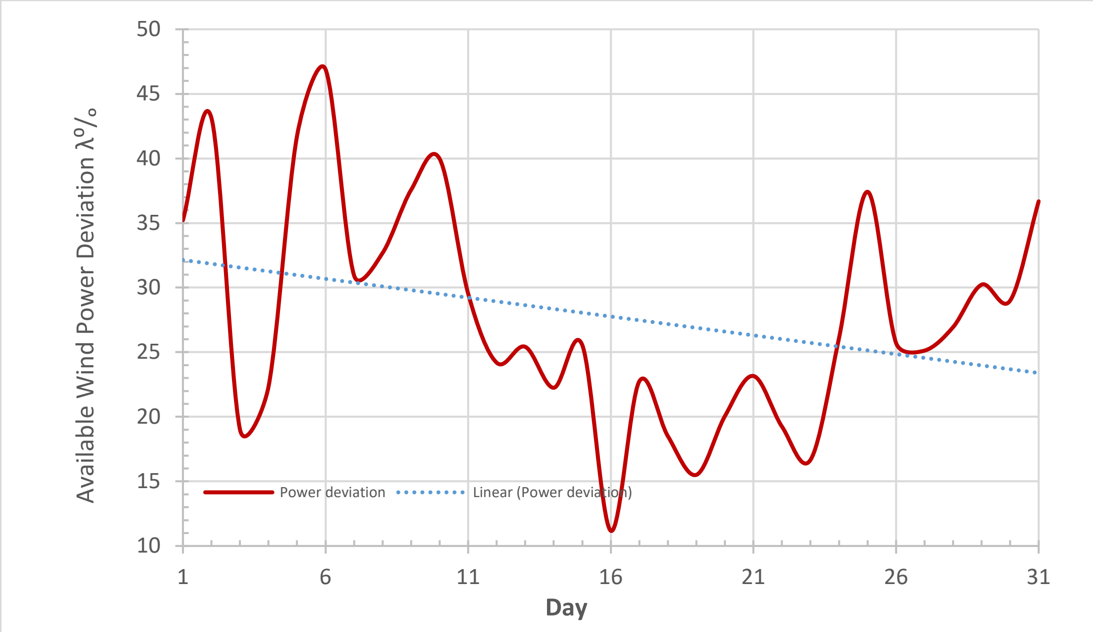

Figure B.1.1 Wind power deviation with days

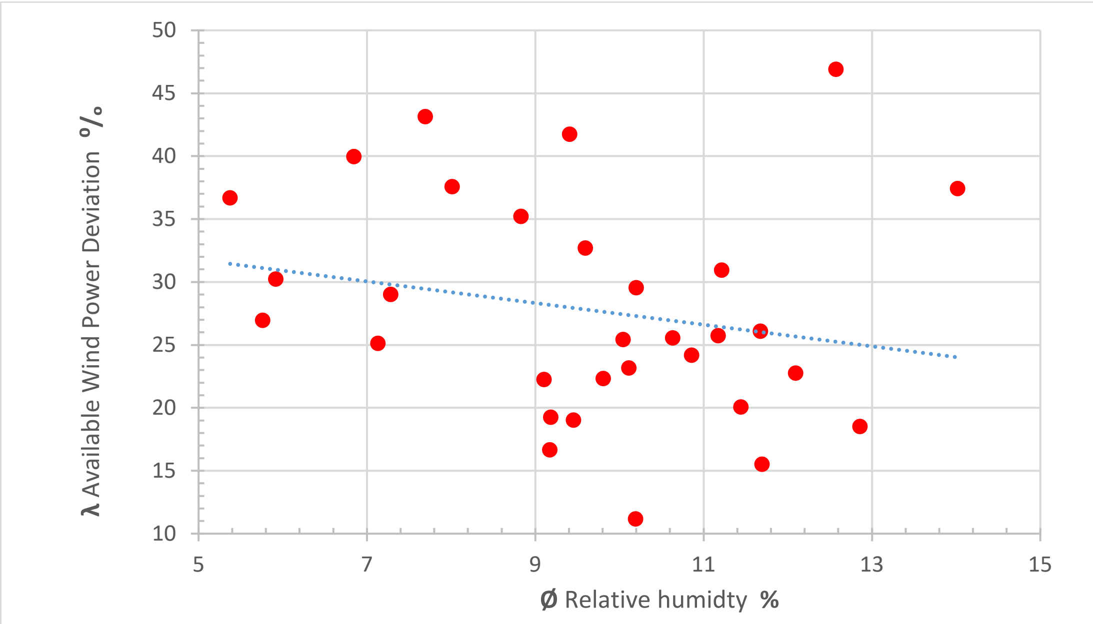

Figure B.1.2 Wind power deviation with humidity

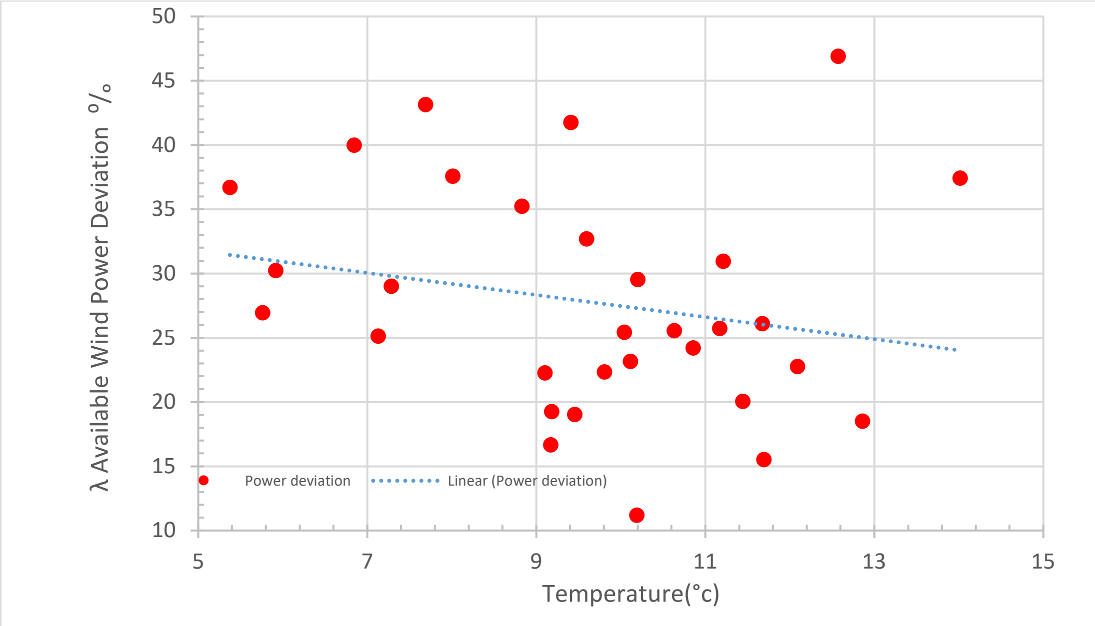

Figure B.1.3 Wind power deviation with temperature

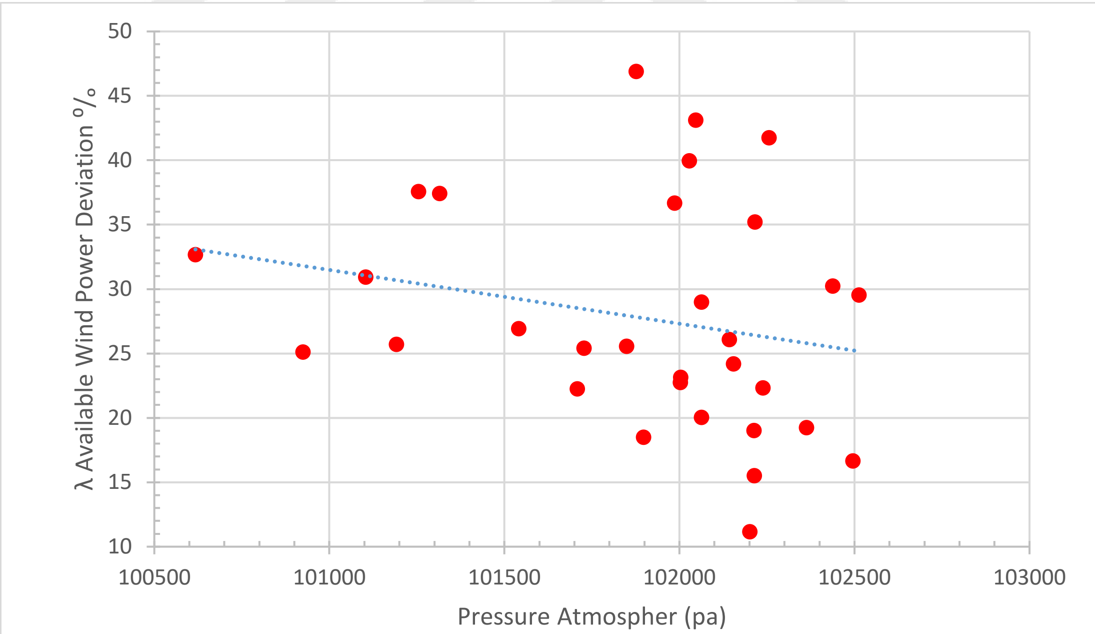

Figure B.1.4 Wind power deviation with atmospheric pressure

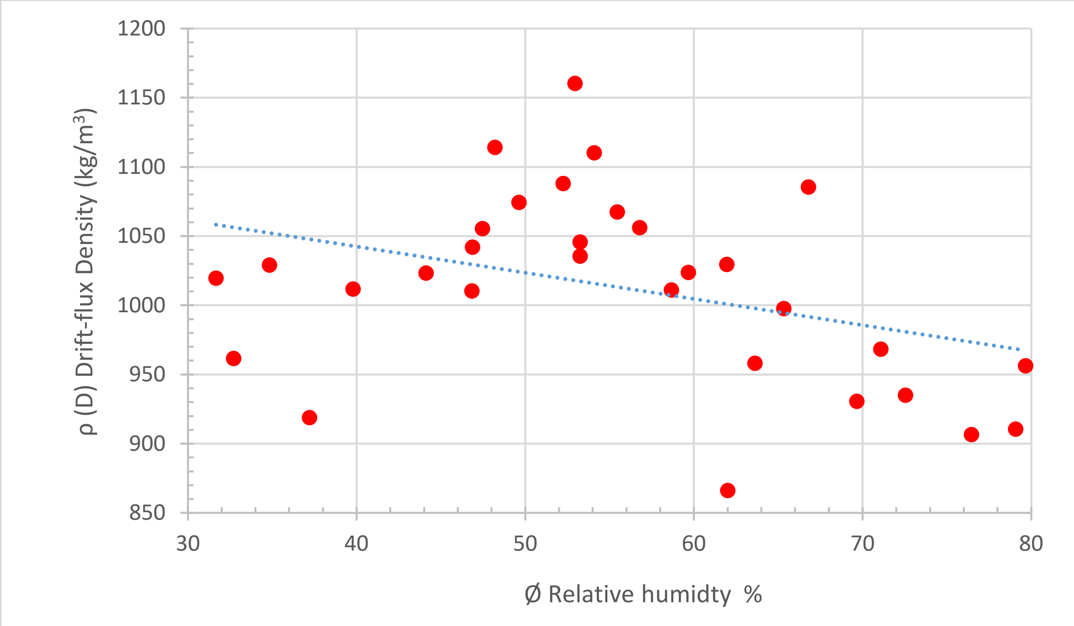

Figure B.1.5 Drift-flux density changes with the humidity

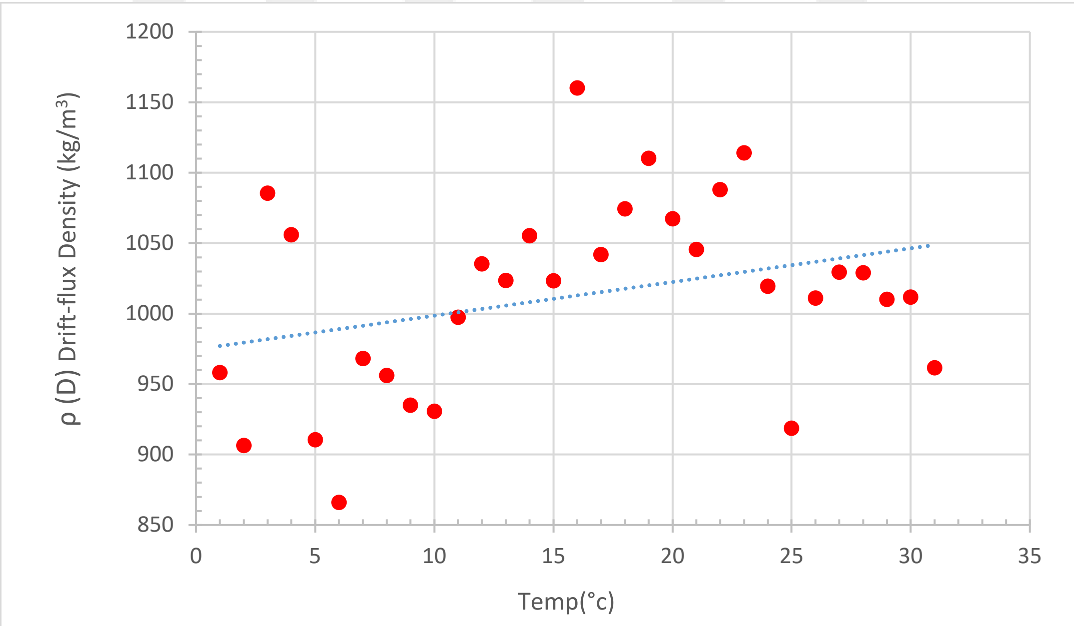

Figure B.1.6 Drift-flux density changes with the temperature

2. February

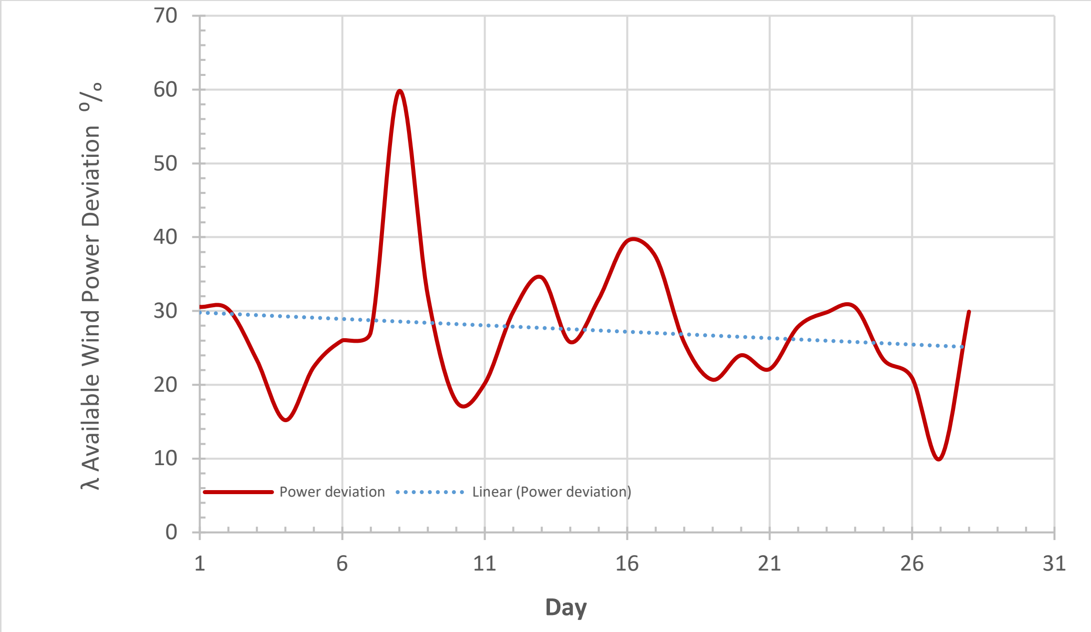

Figure B.2.1 Wind power deviation with days

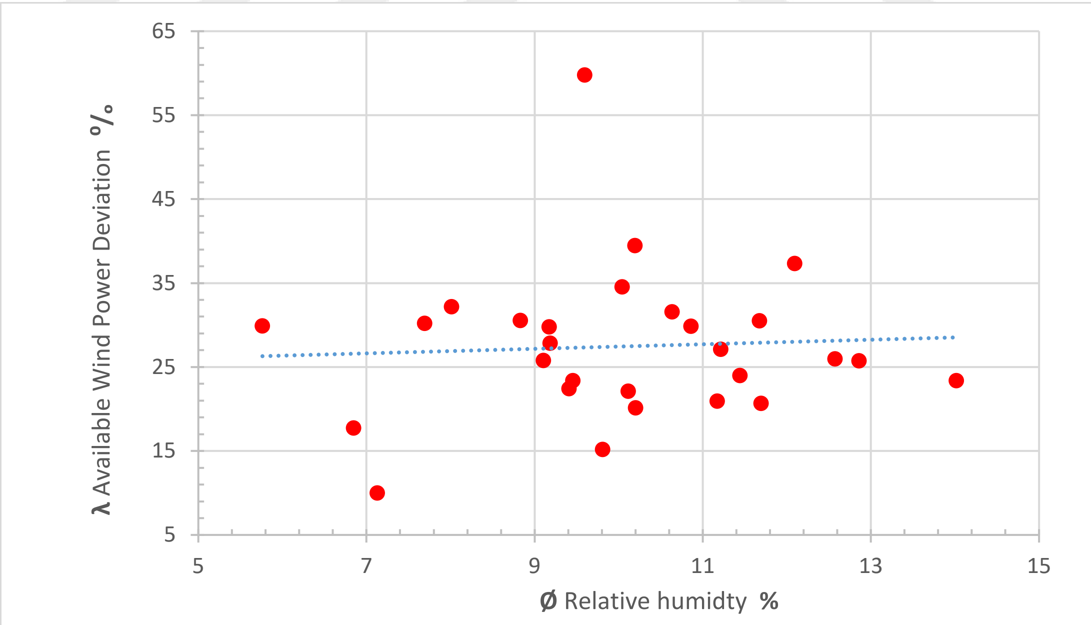

Figure B.2.2 Wind power deviation with humidity

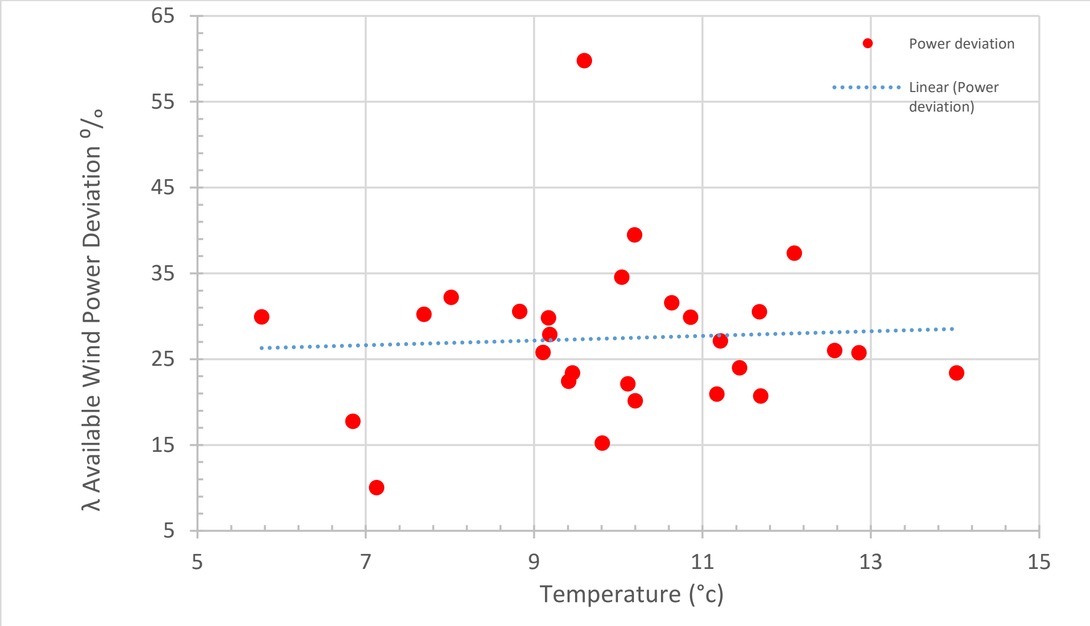

Figure B.2.3 Wind power deviation with temperature

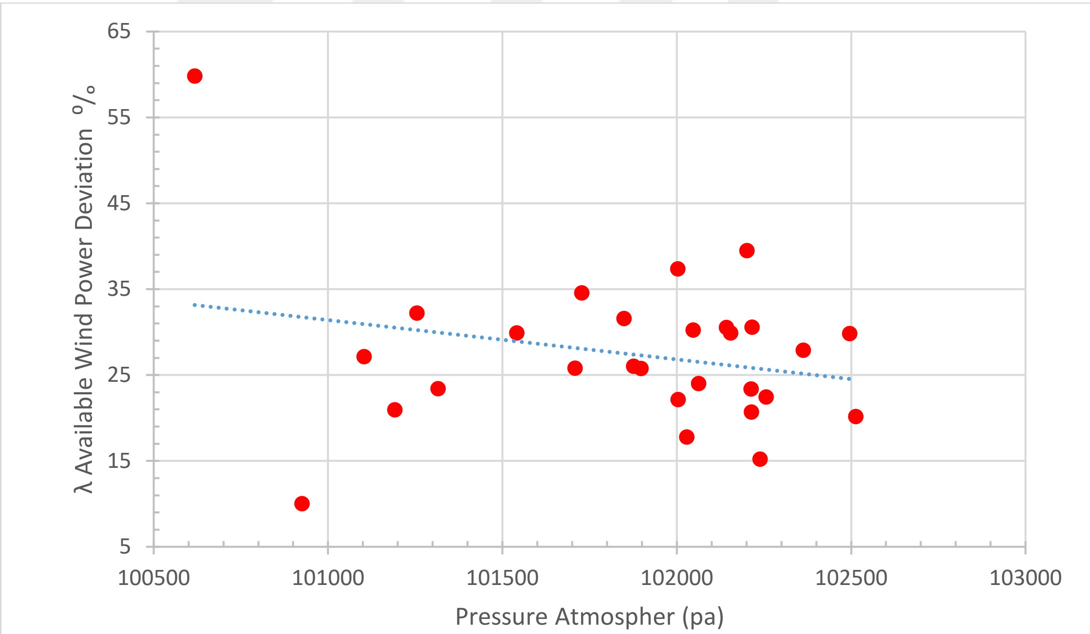

Figure B.2.4 Wind power deviation with atmospheric pressure

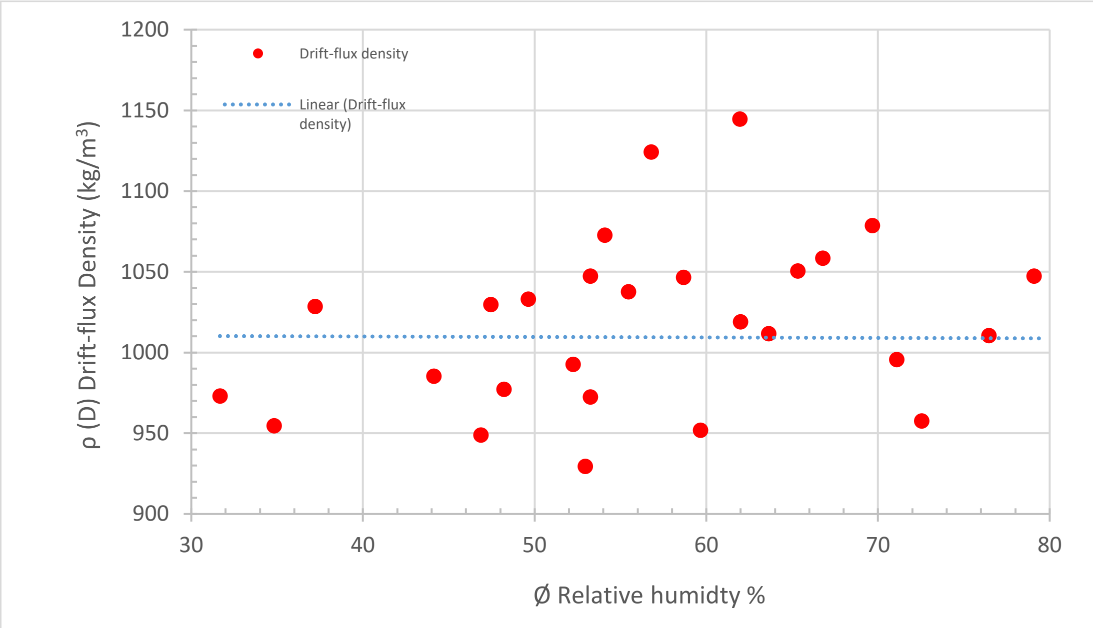

Figure B.2.5 Drift-flux density changes with the humidity

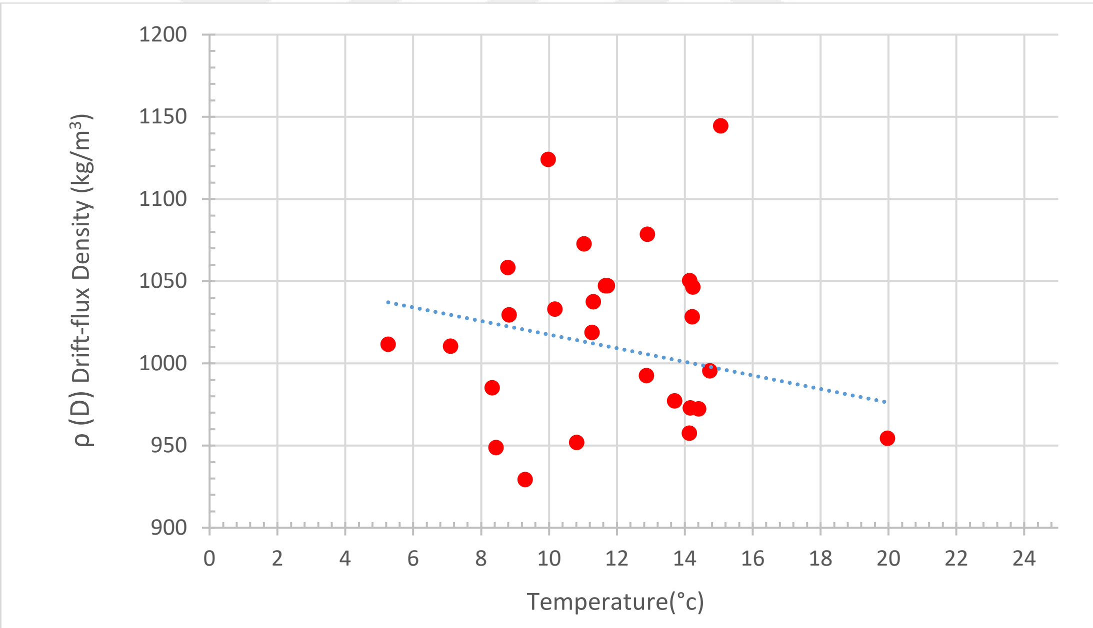

Figure B.2.6 Drift-flux density changes with the temperature

3. March

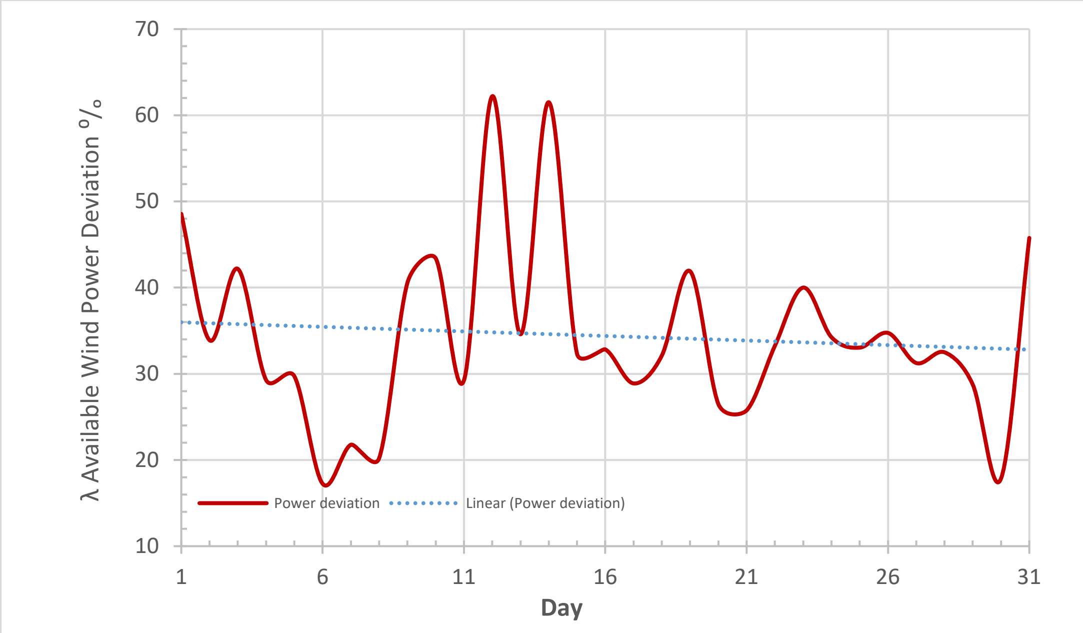

Figure B.3.1 Wind power deviation with days

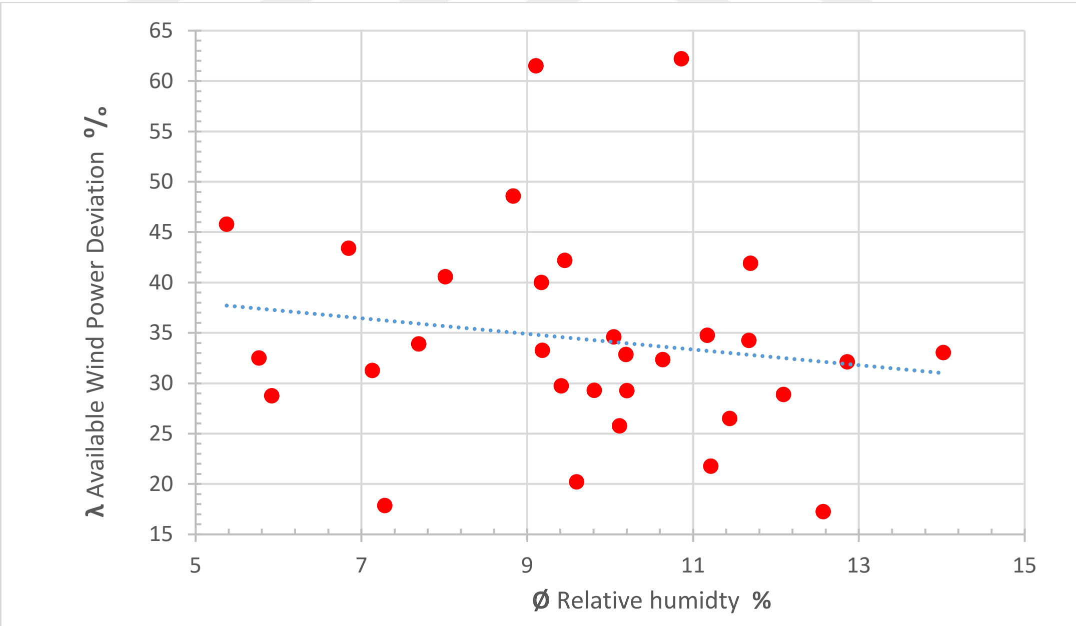

Figure B.3.2 Wind power deviation with humidity

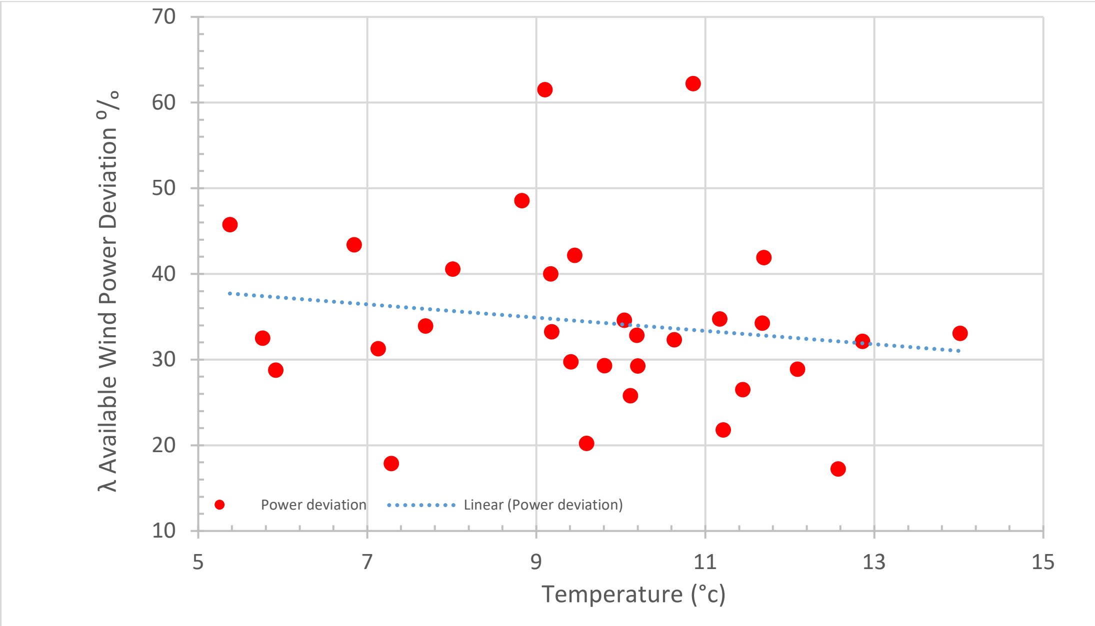

Figure B.3.3 Wind power deviation with temperature

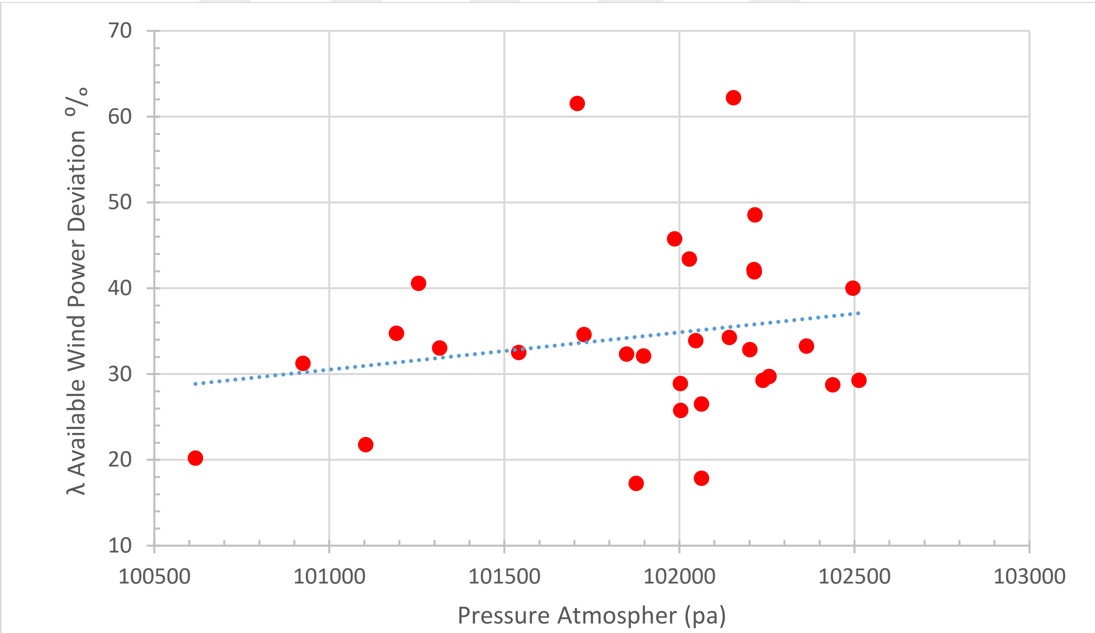

Figure B.3.4 Wind power deviation with atmospheric pressure

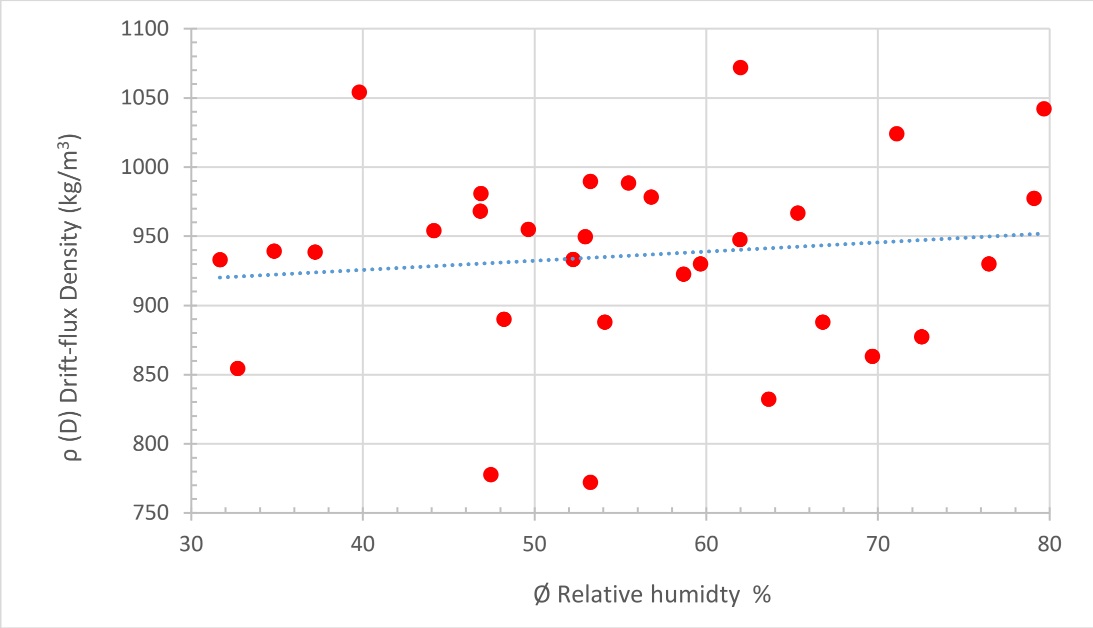

Figure B.3.5 Drift-flux density changes with the humidity

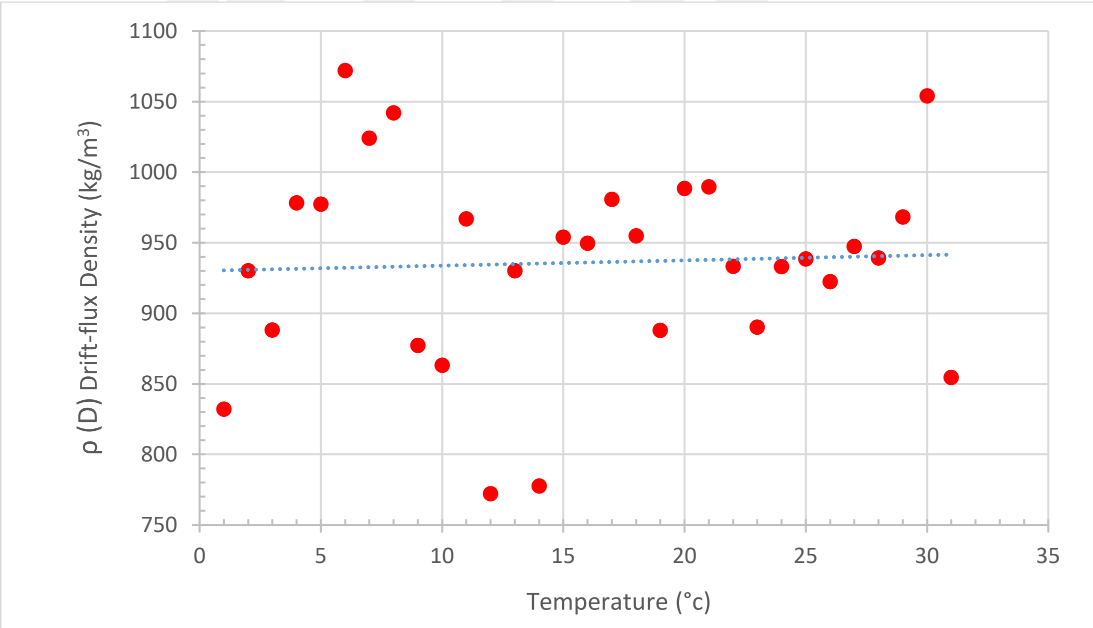

Figure B.3.6 Drift-flux density changes with the temperature

4. April

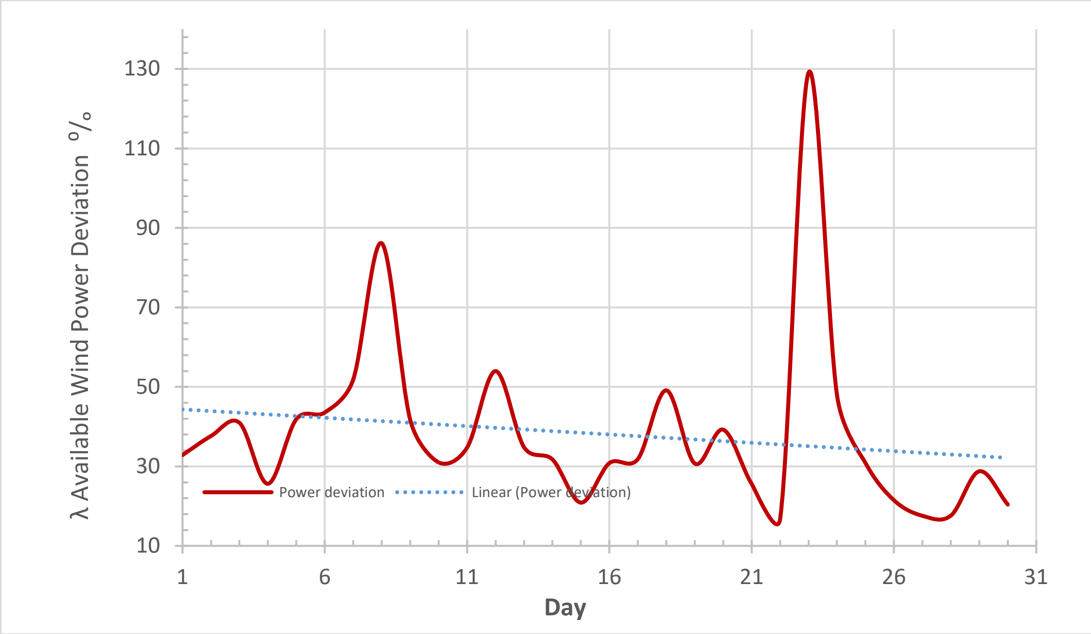

Figure B.4.1 Wind power deviation with days

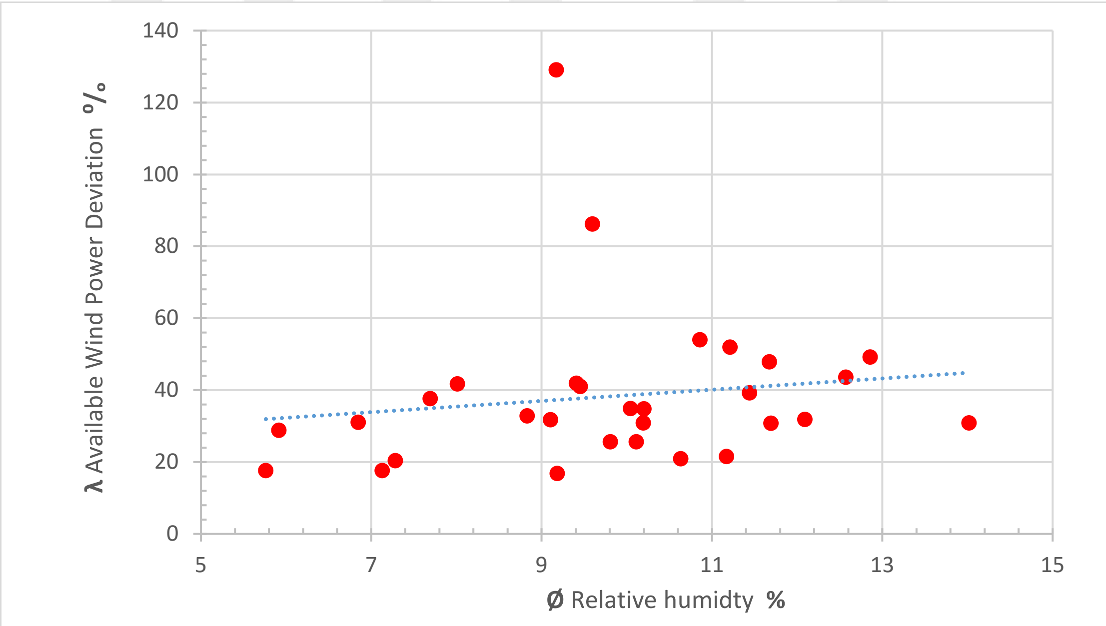

Figure B.4.2 Wind power deviation with humidity

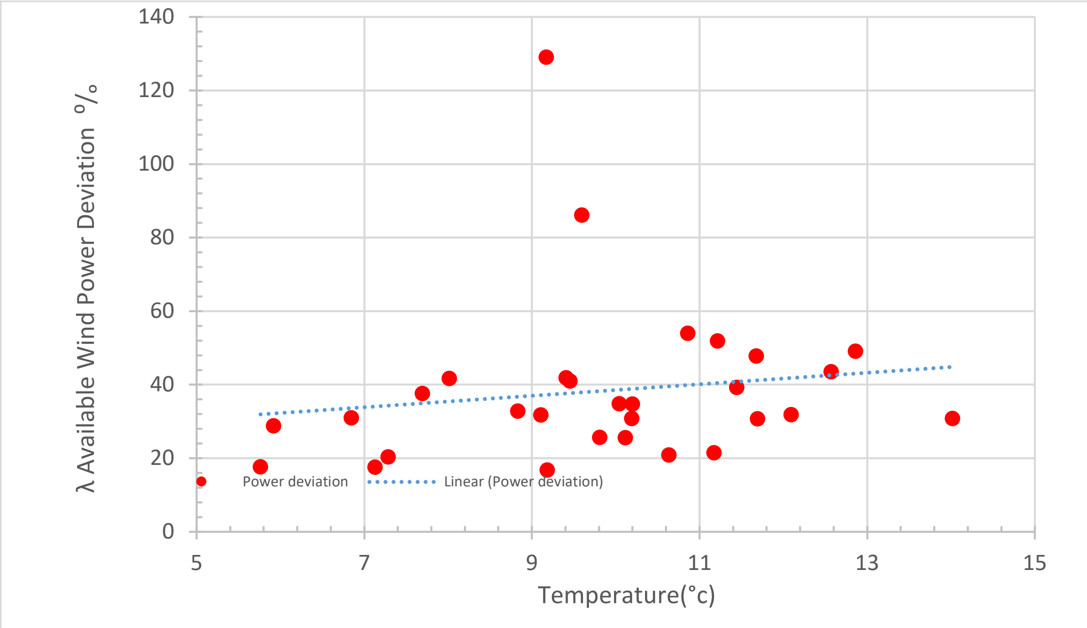

Figure B.4.3 Wind power deviation with temperature

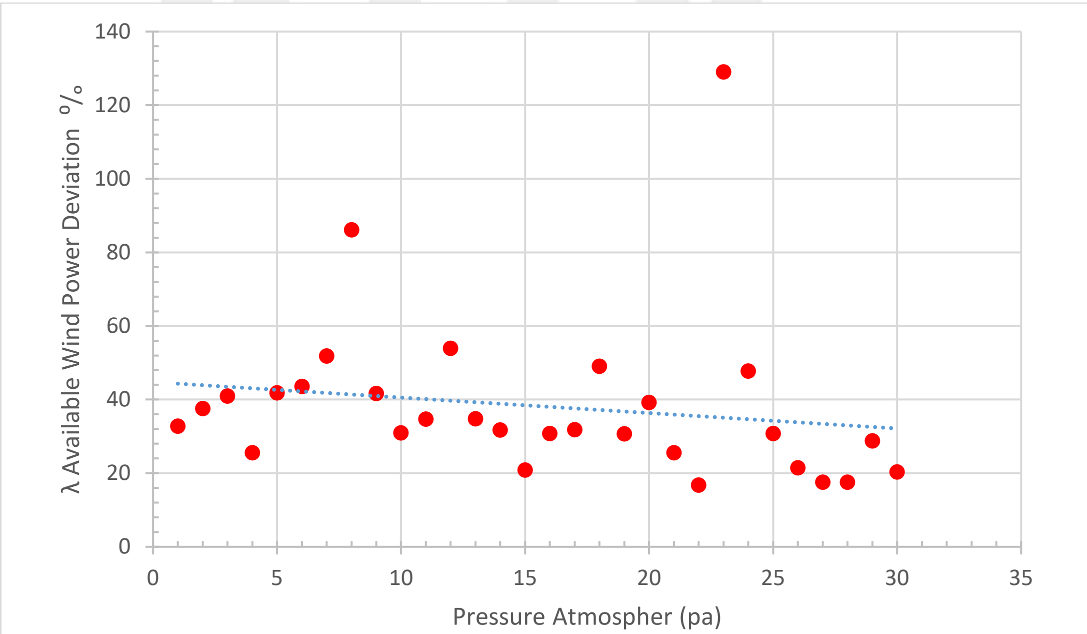

Figure B.4.4 Wind power deviation with atmospheric pressure

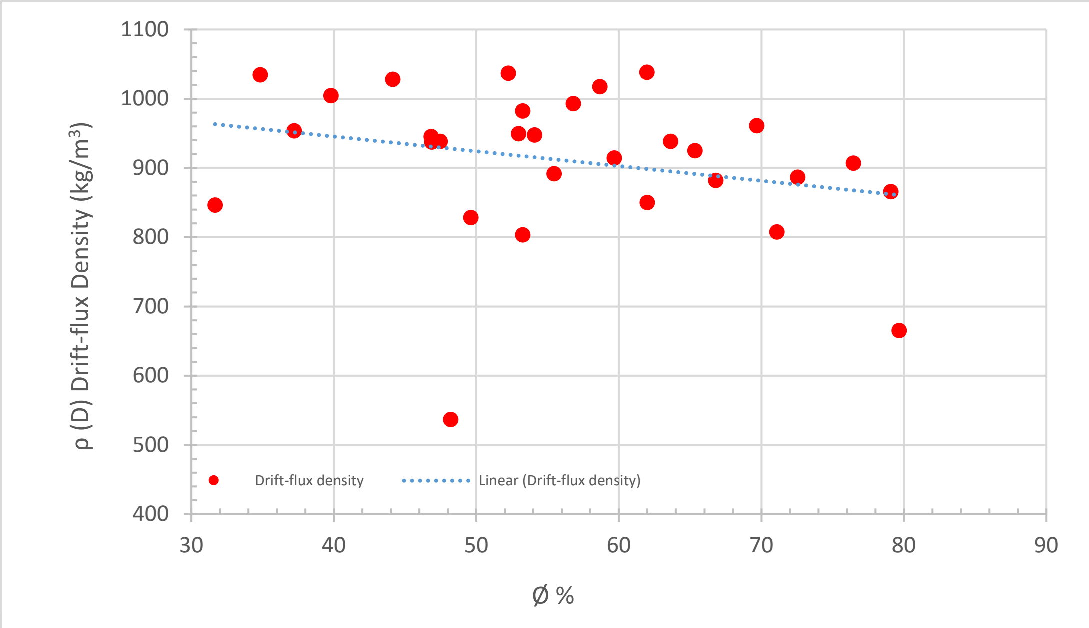

Figure B.4.5 Drift-flux density changes with the humidity

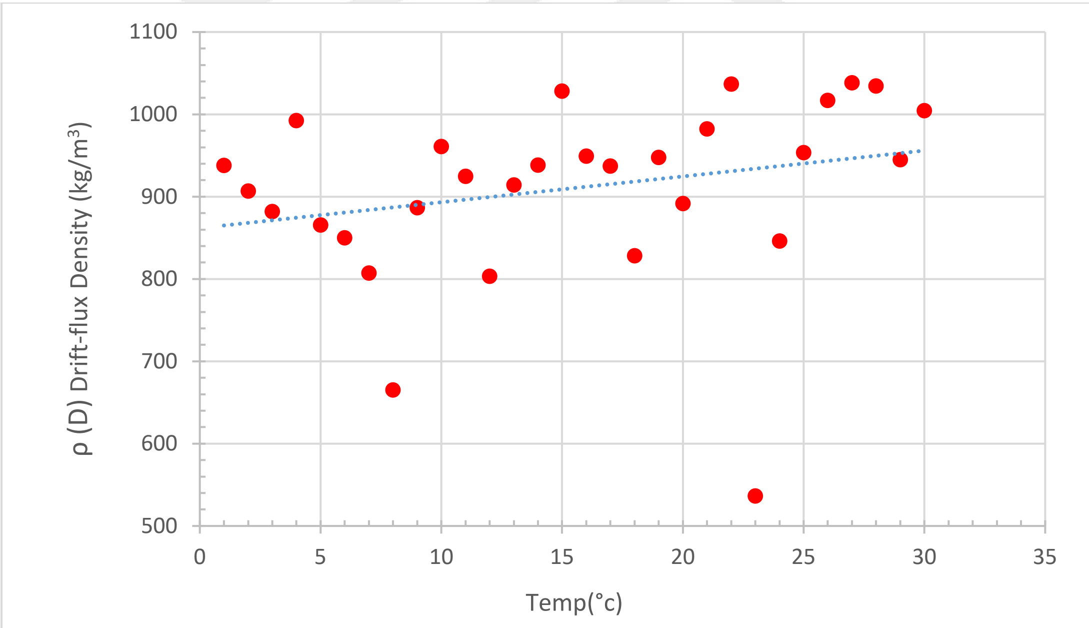

Figure B.4.6 Drift-flux density changes with the temperature

5. May

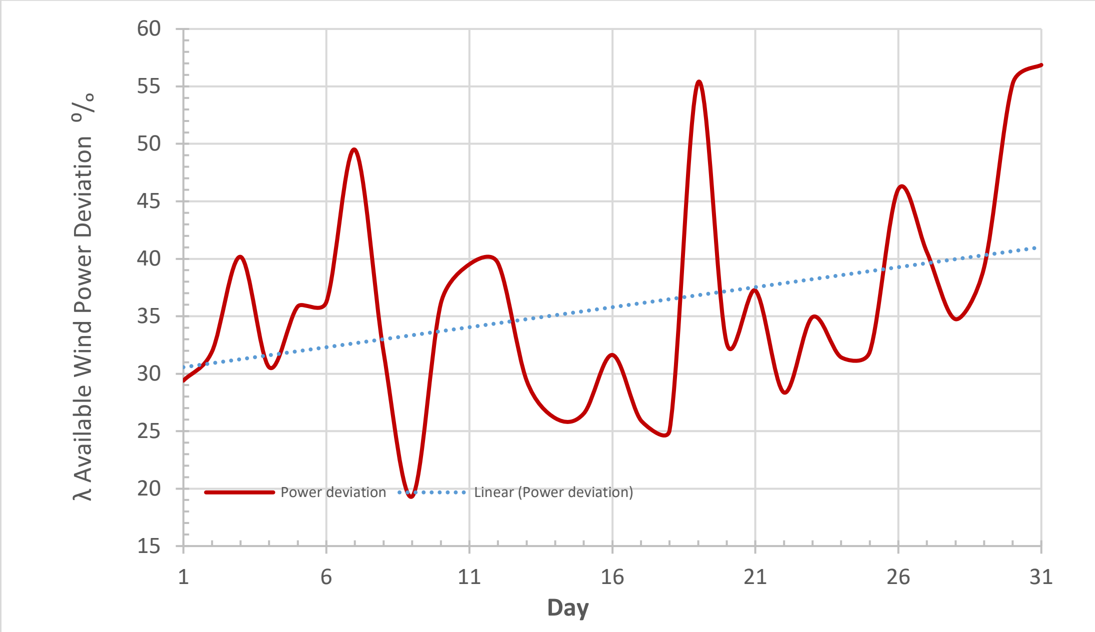

Figure B.5.1 Wind power deviation with days

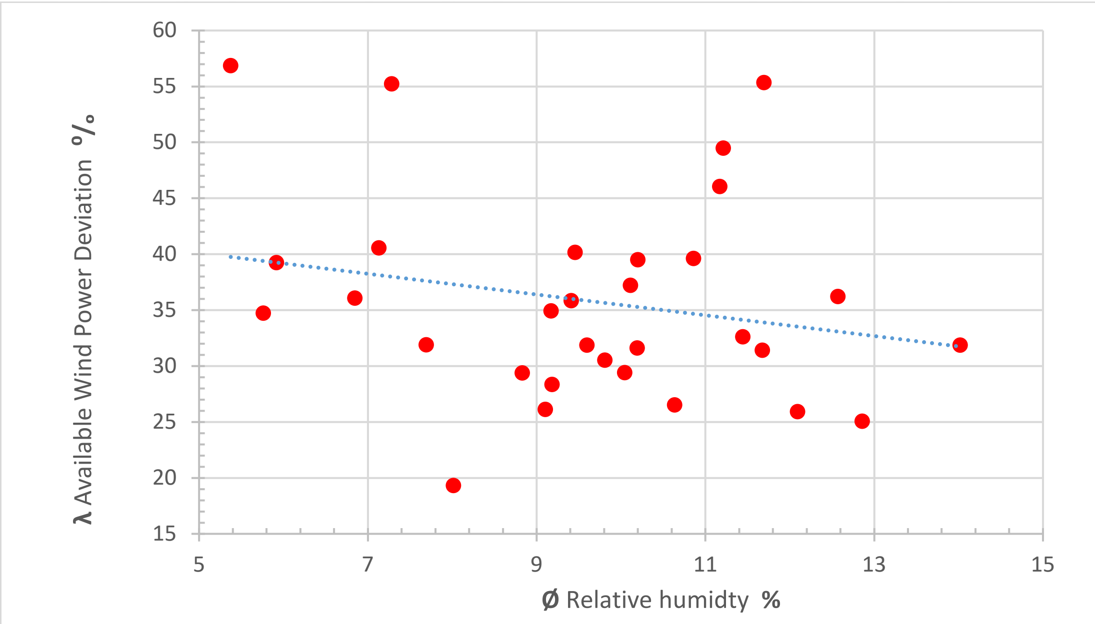

Figure B.5.2 Wind power deviation with humidity

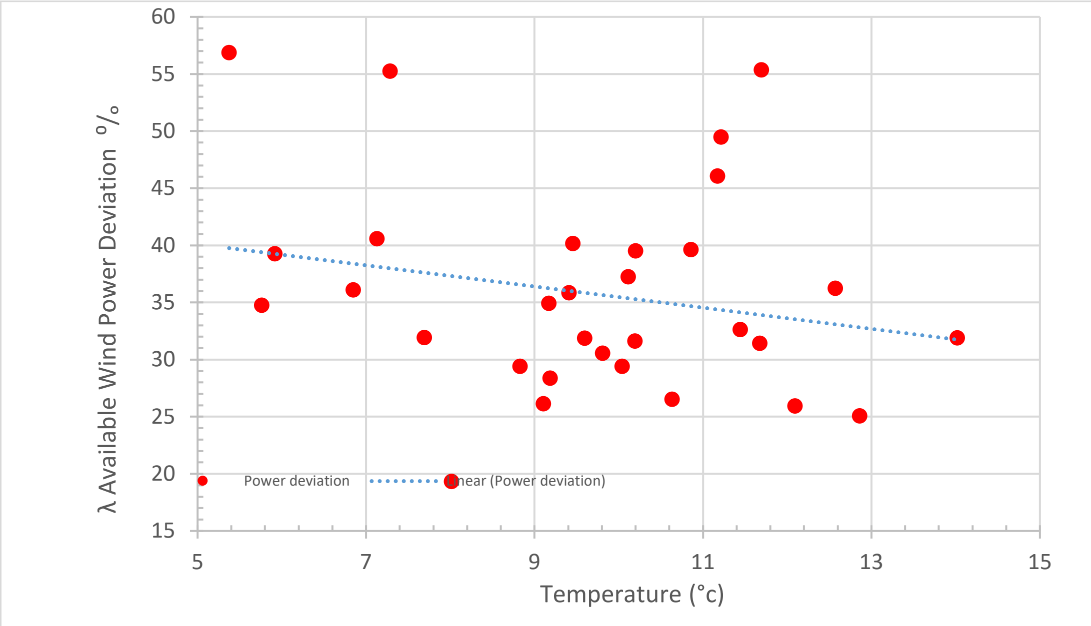

Figure B.5.3 Wind power deviation with temperature

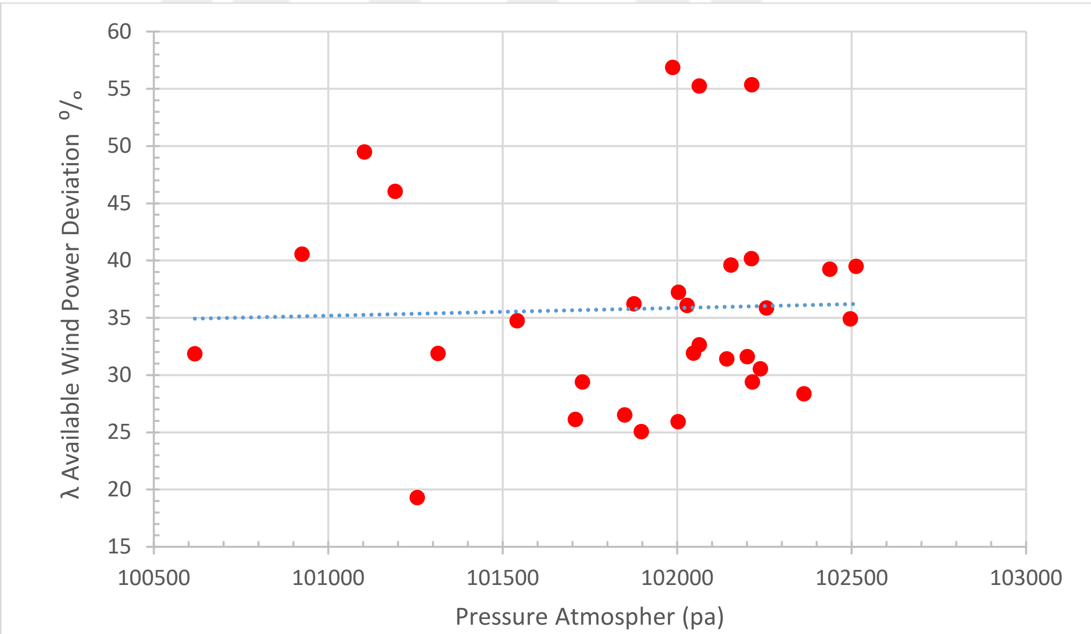

Figure B.5.4 Wind power deviation with atmospheric pressure

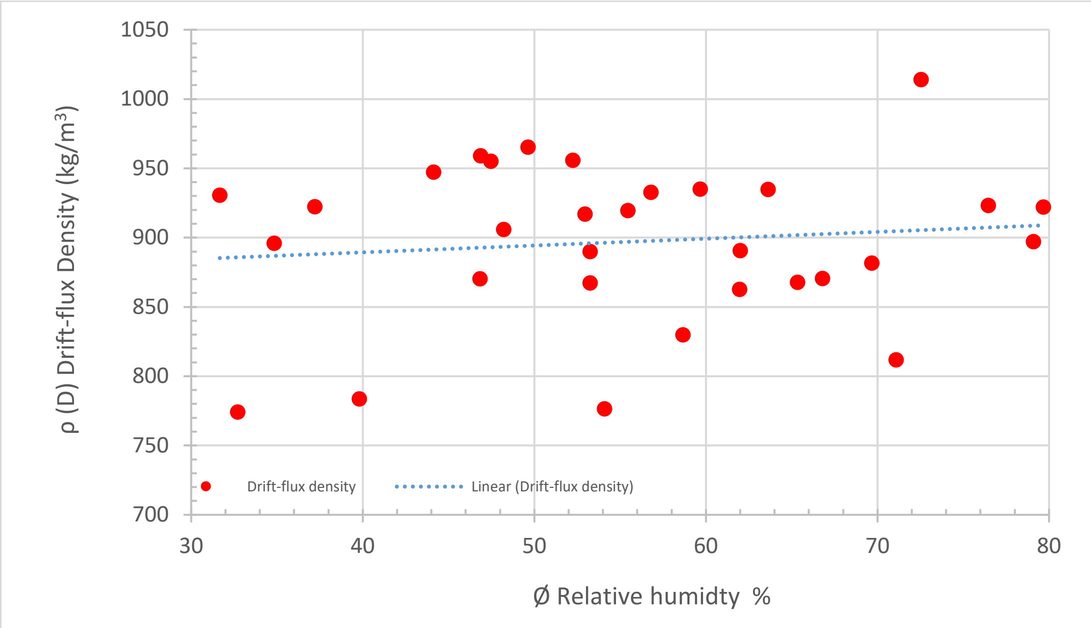

Figure B.5.5 Drift-flux density changes with the humidity

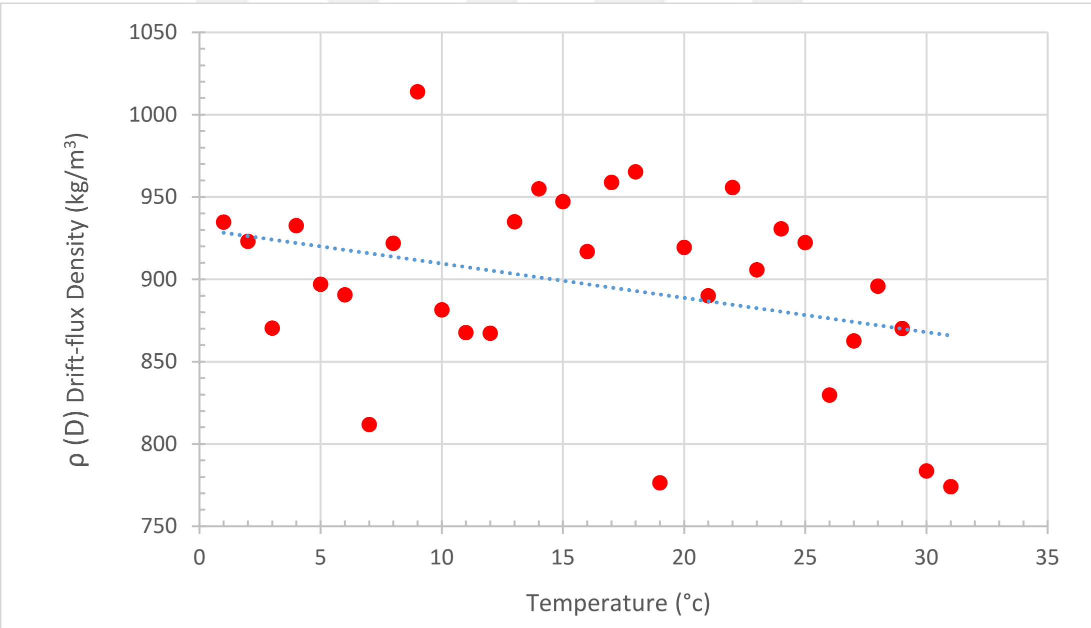

Figure B.5.6 Drift-flux density changes with the temperature

6. June

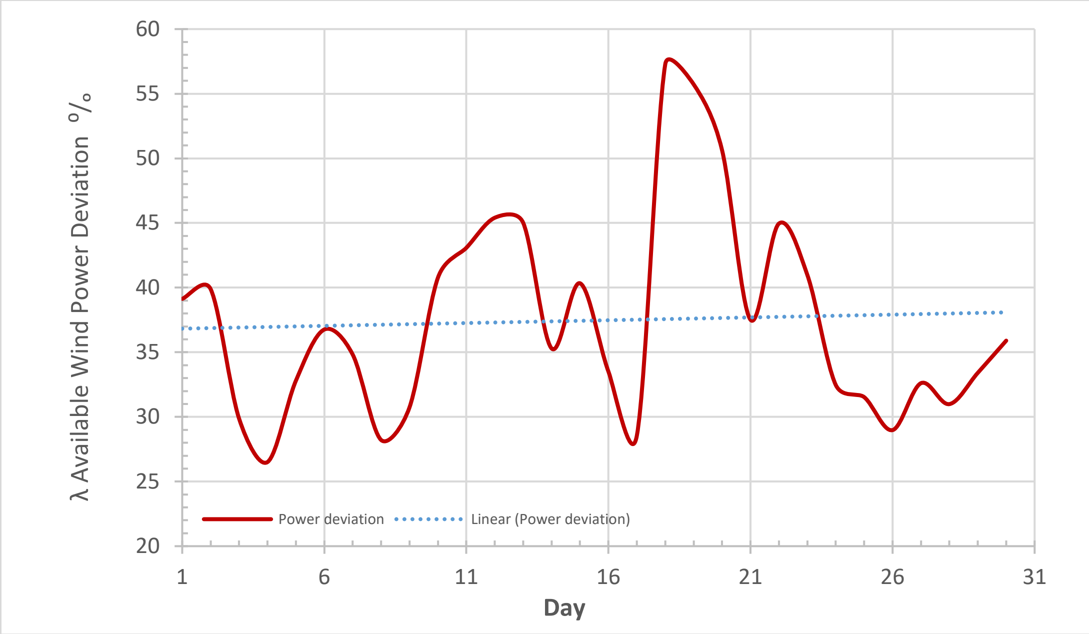

Figure B.6.1 Wind power deviation with days

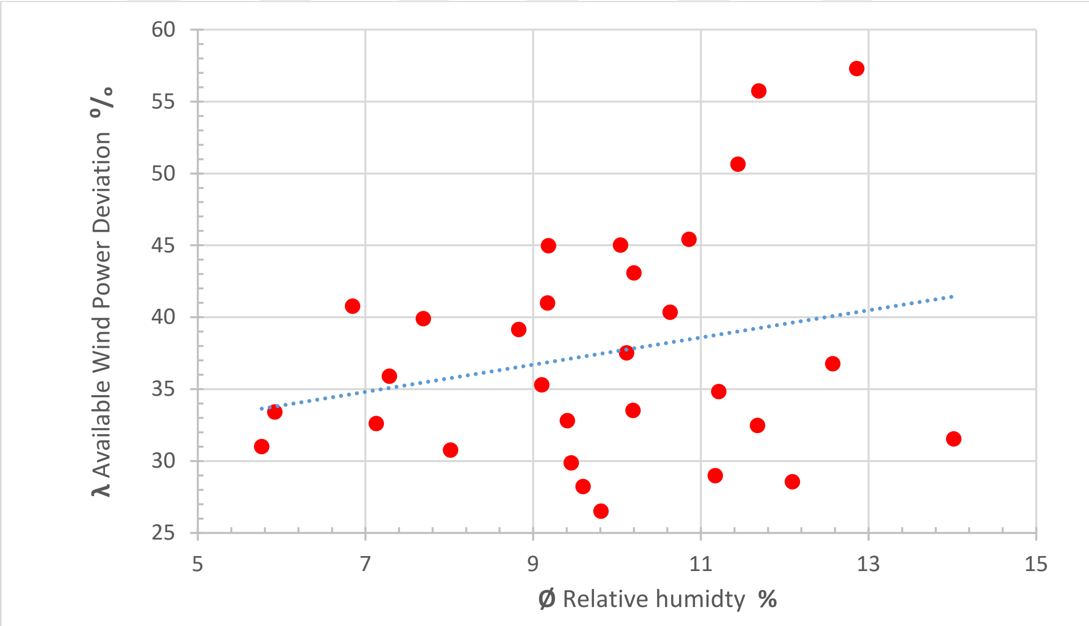

Figure B.6.2 Wind power deviation with humidity

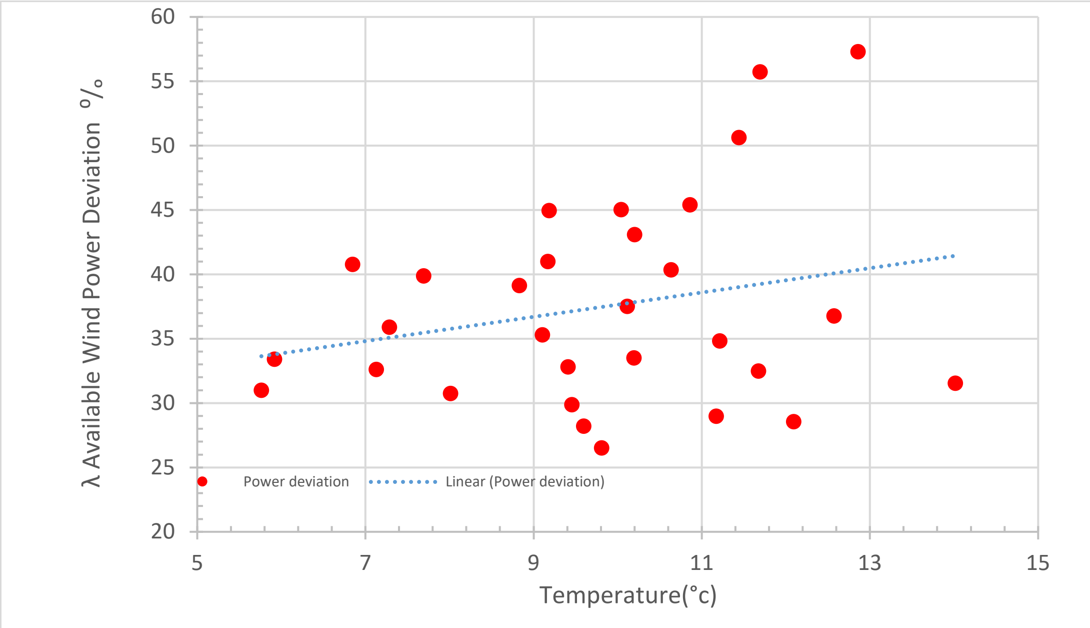

Figure B.6.3 Wind power deviation with temperature

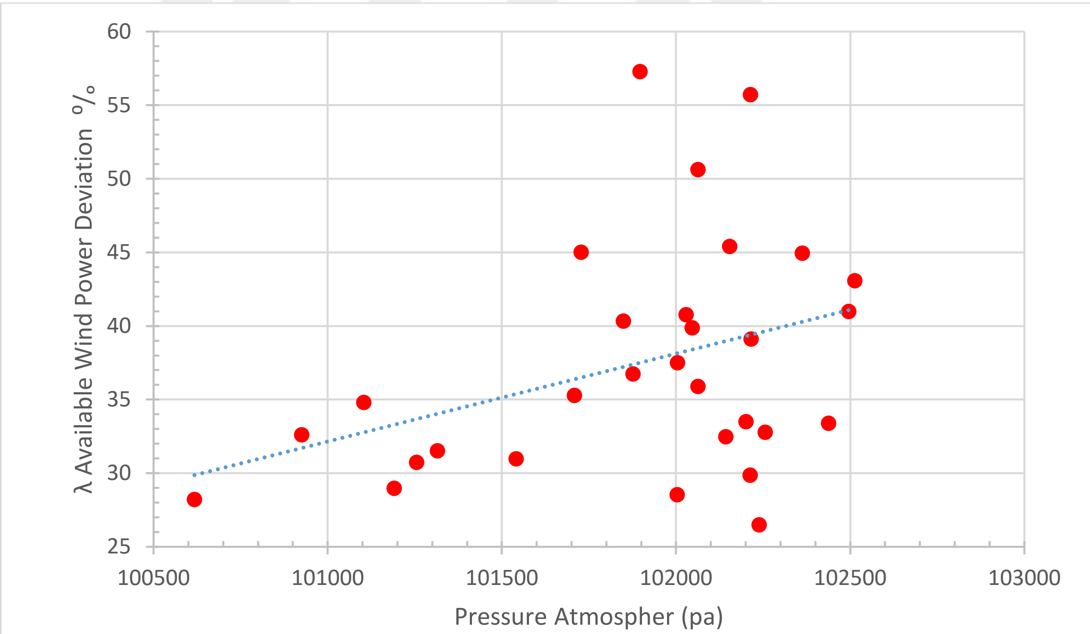

Figure B.6.4 Wind power deviation with atmospheric pressure

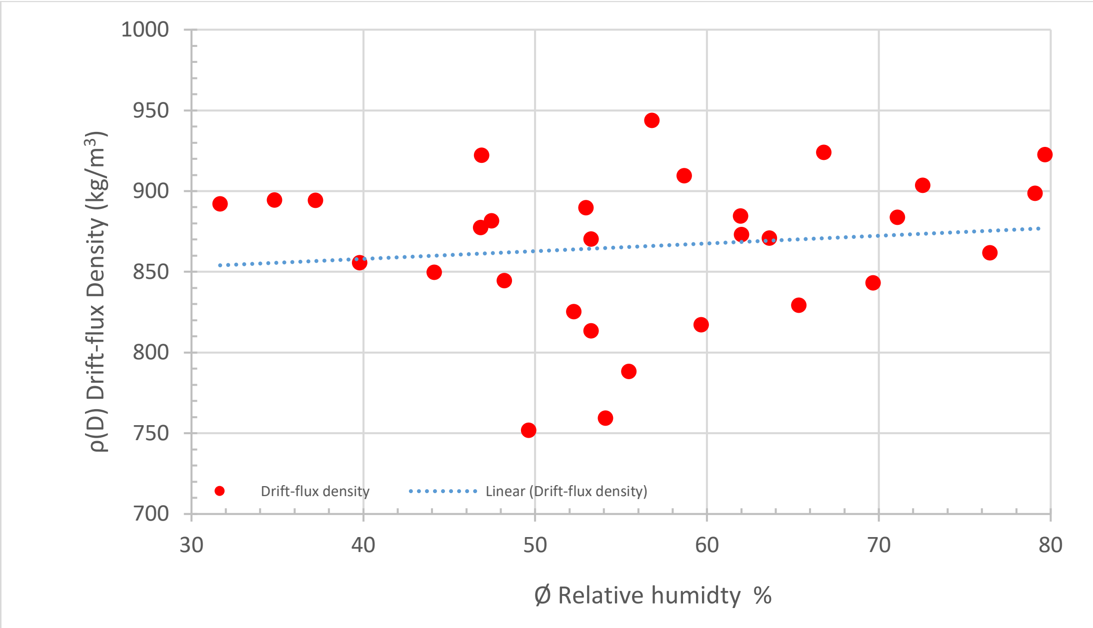

Figure B.6.5 Drift-flux density changes with the humidity

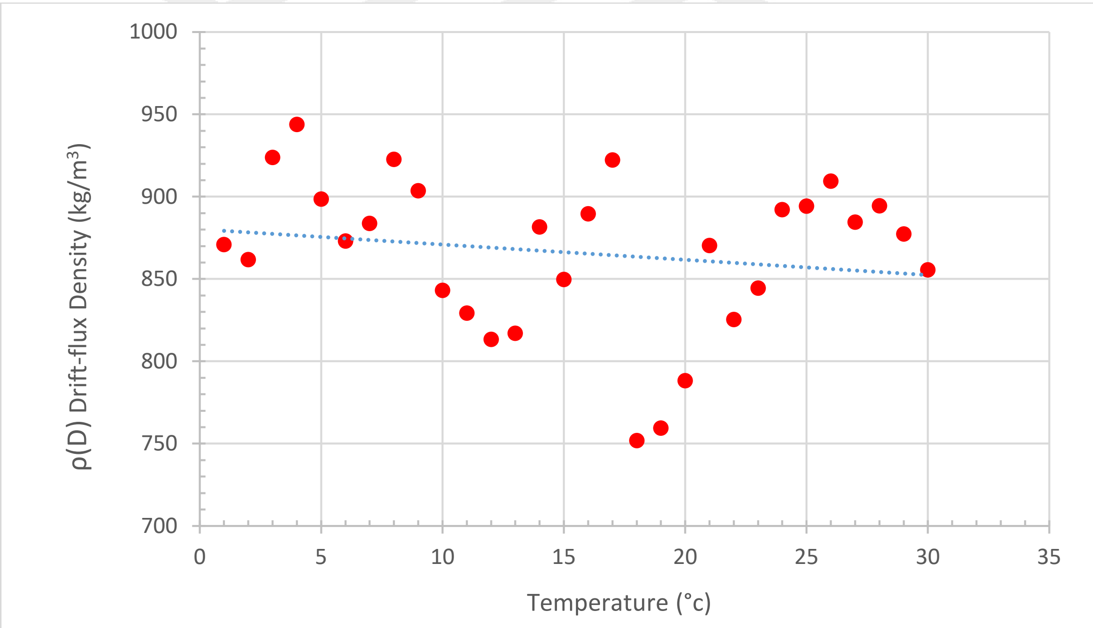

Figure B.6.6 Drift-flux density changes with the temperature

7. July

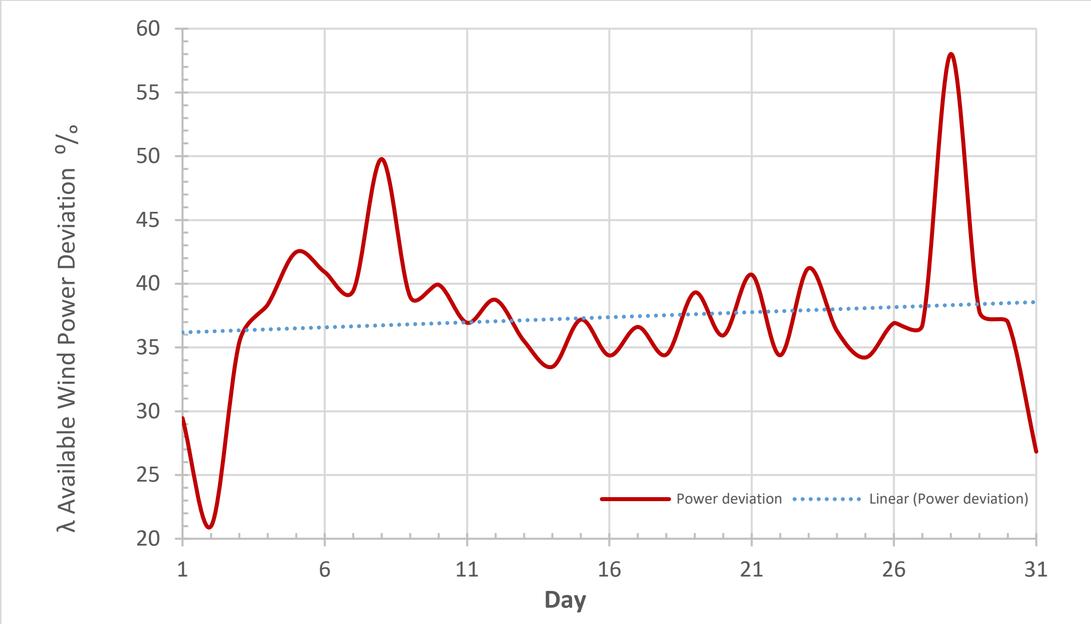

Figure B.7.1 Wind power deviation with days

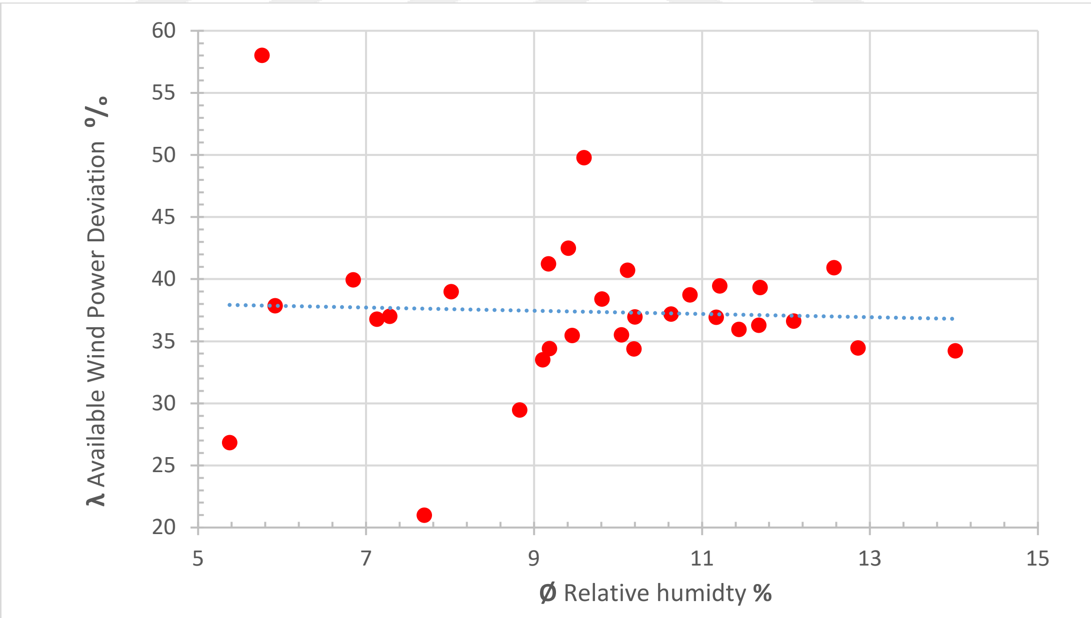

Figure B.7.2 Wind power deviation with humidity

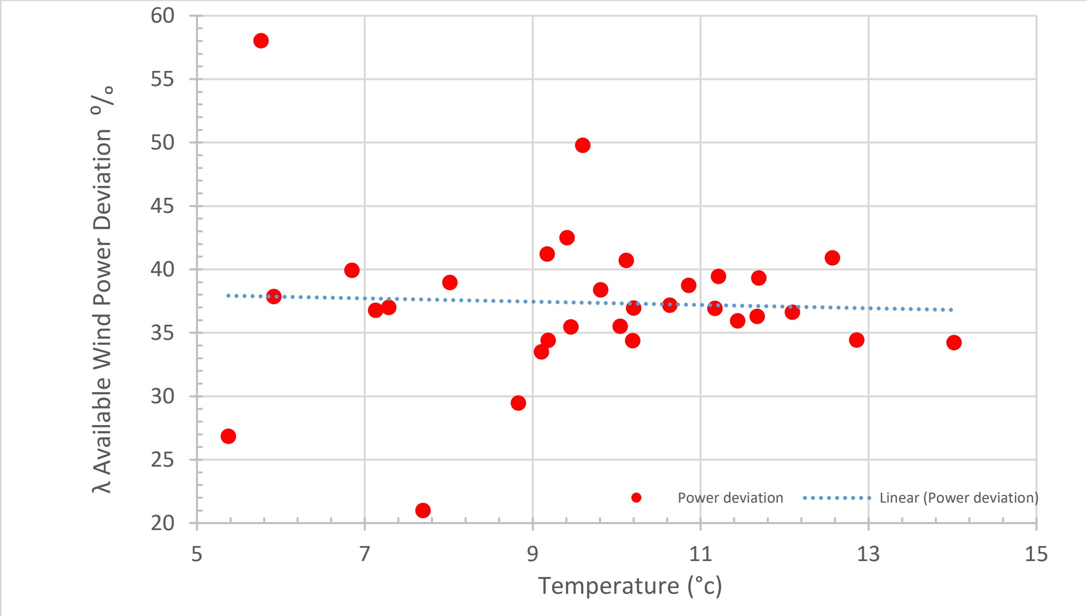

Figure B.7.3 Wind power deviation with temperature

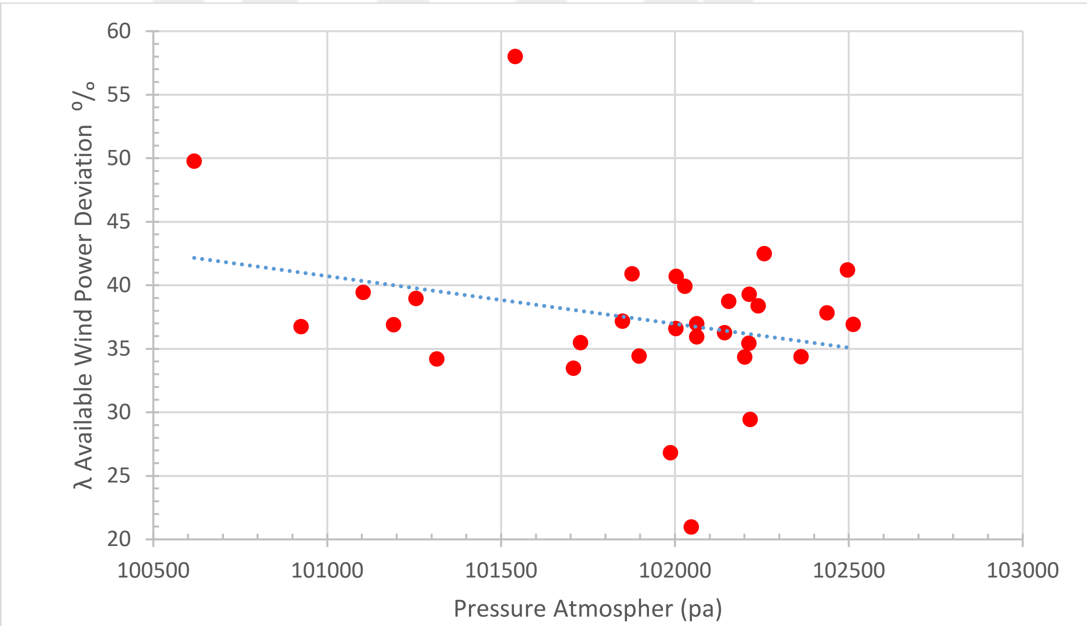

Figure B.7.4 Wind power deviation with atmospheric pressure

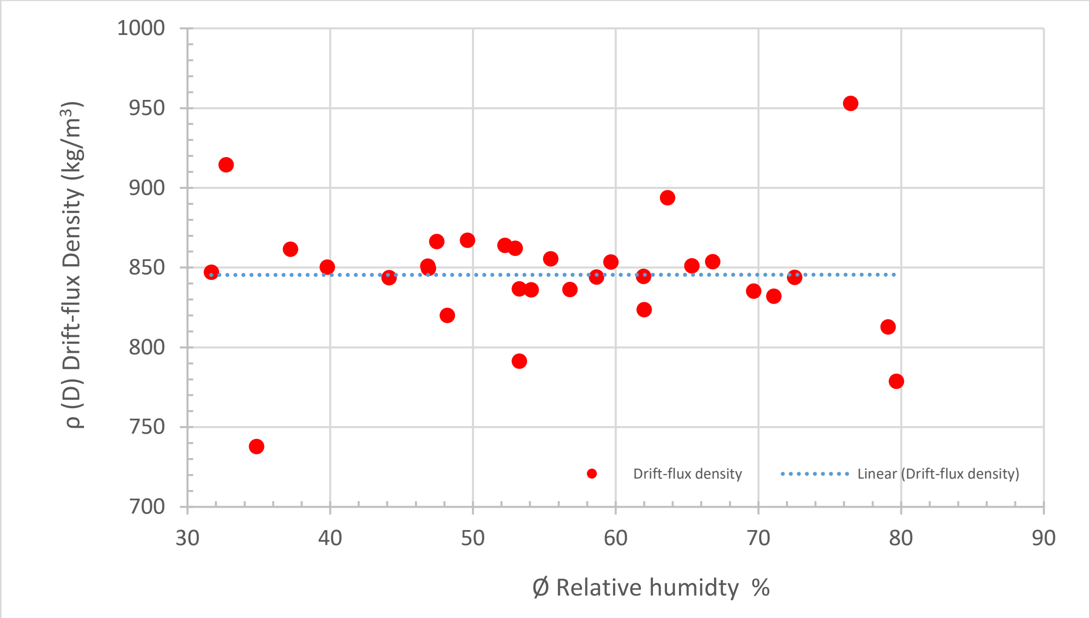

Figure B.7.5 Drift-flux density changes with the humidity

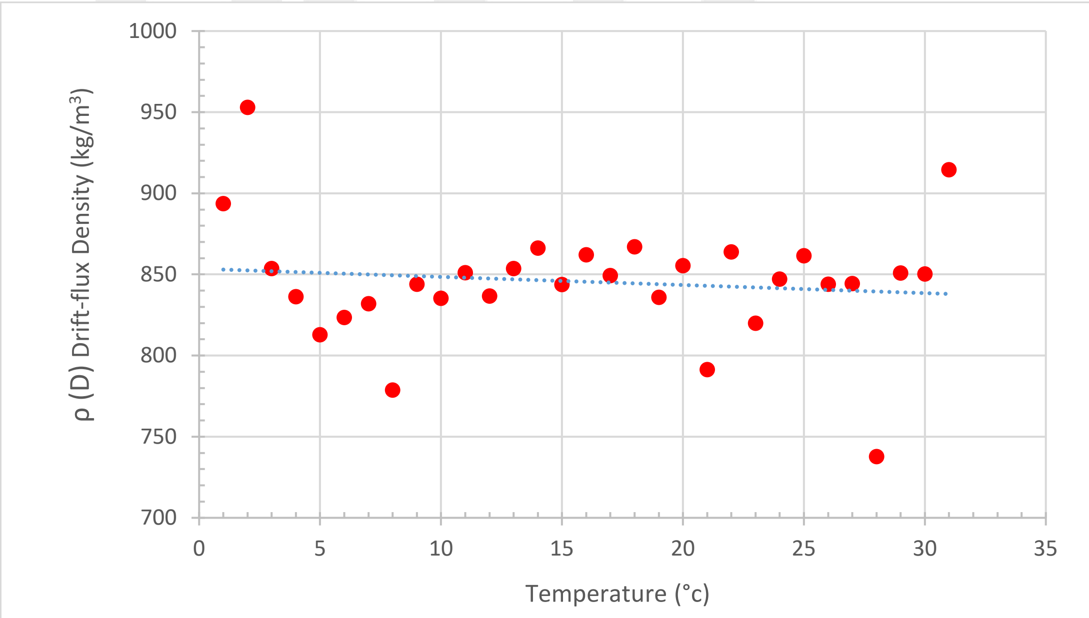

Figure B.1.6 Drift-flux density changes with the temperature

8. August

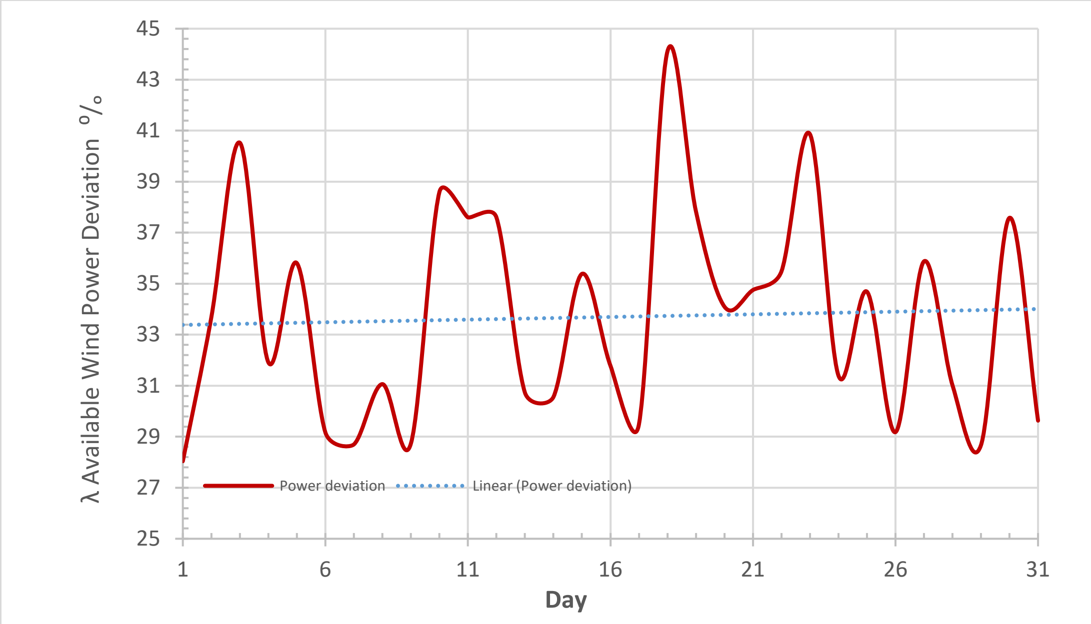

Figure B.8.1 Wind power deviation with days

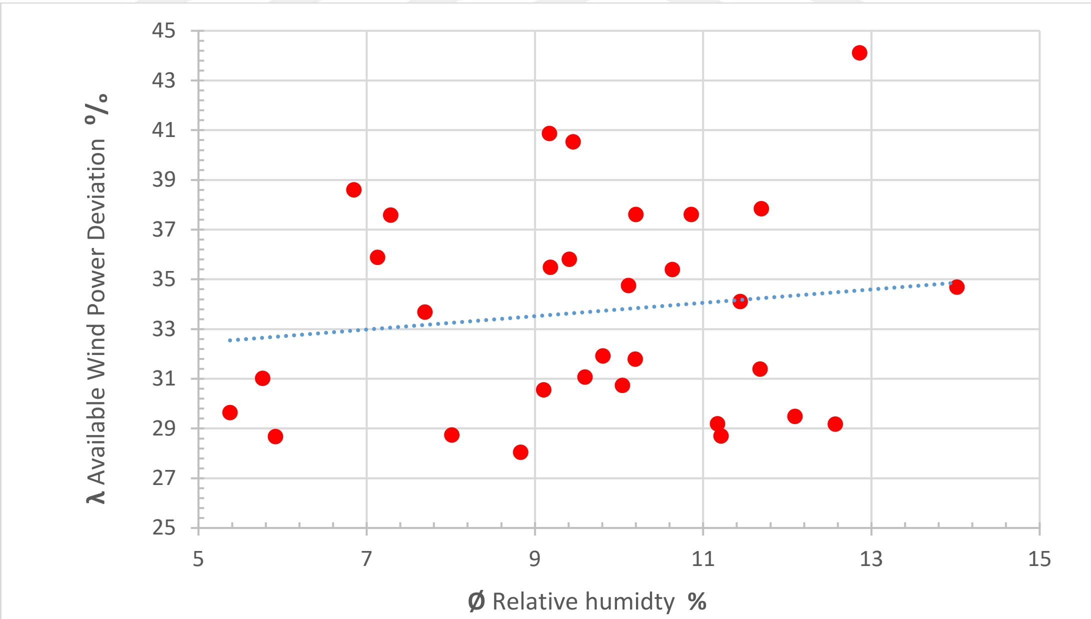

Figure B.8.2 Wind power deviation with humidity

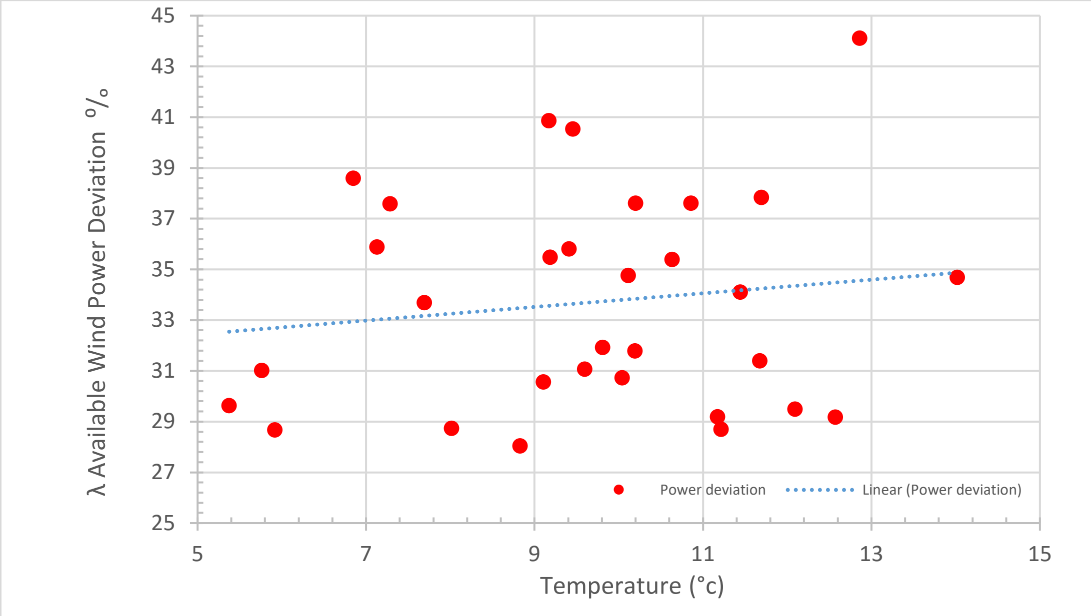

Figure B.8.3 Wind power deviation with temperature

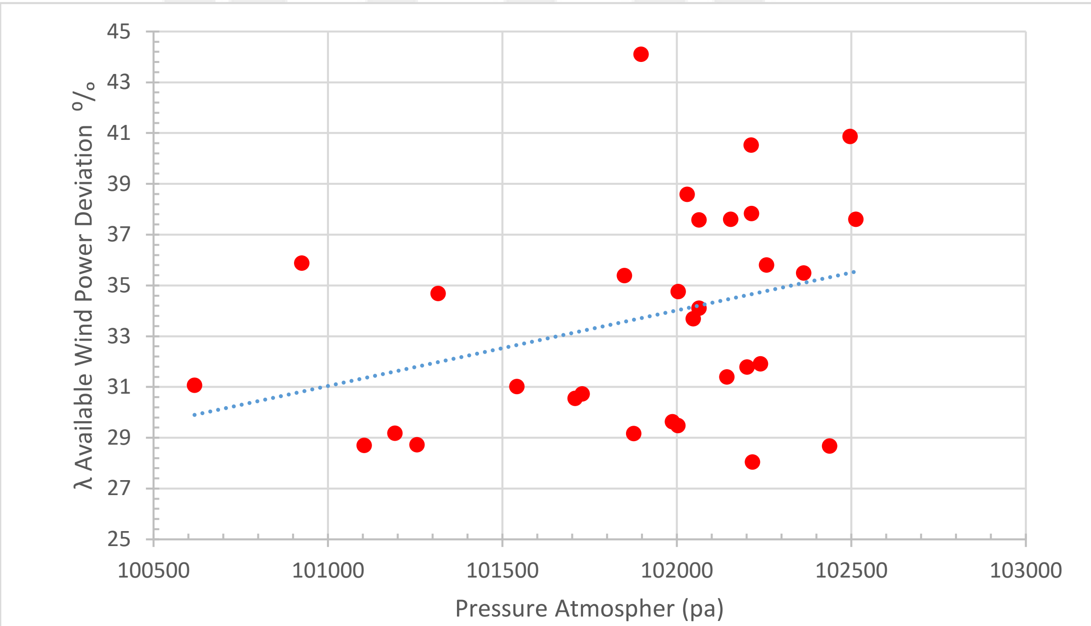

Figure B.1.4 Wind power deviation with atmospheric pressure

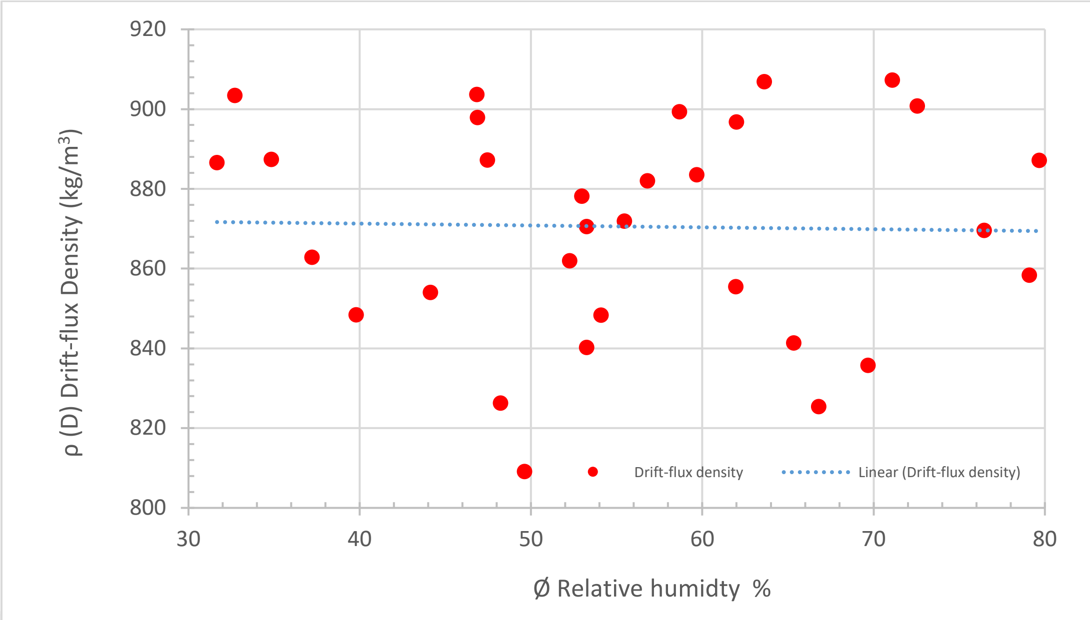

Figure B.8.5 Drift-flux density changes with the humidity

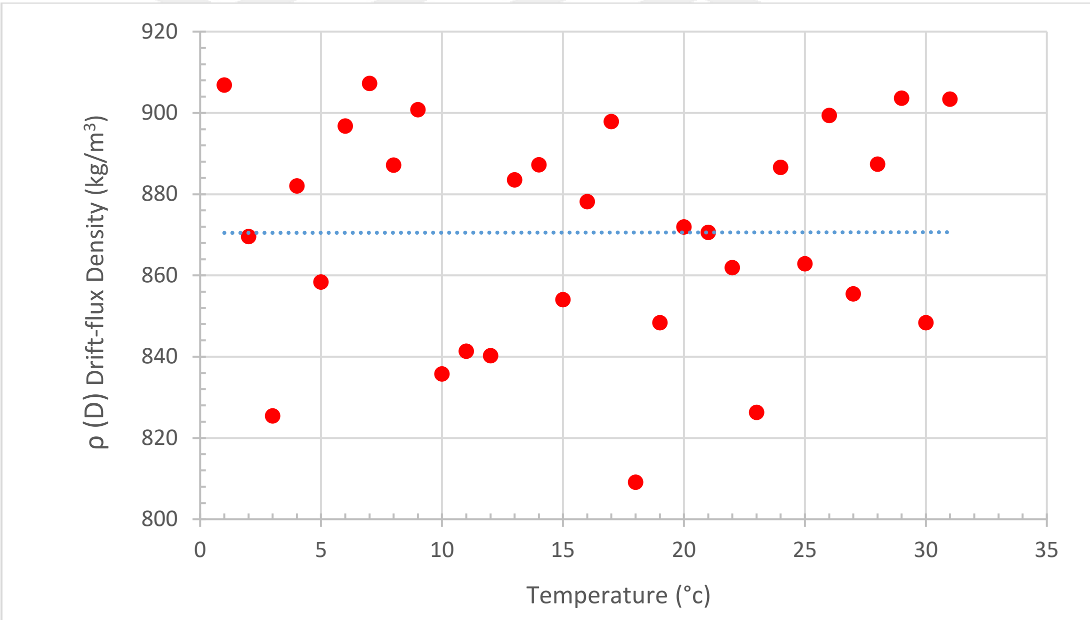

Figure B.8.6 Drift-flux density changes with the temperature

9. Septembe

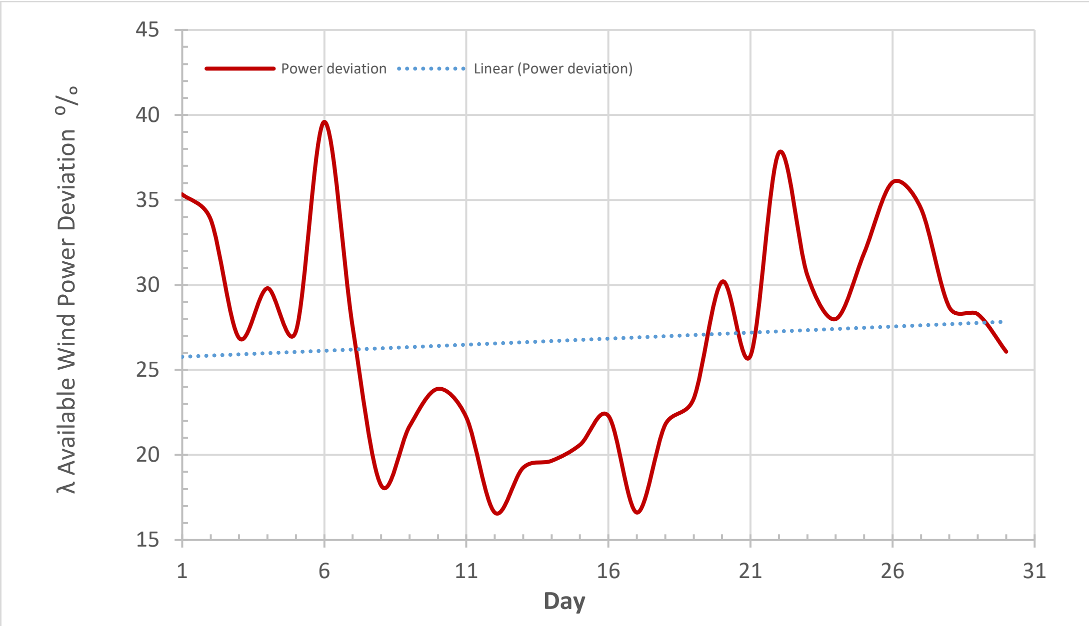

Figure B.9.1 Wind power deviation with days

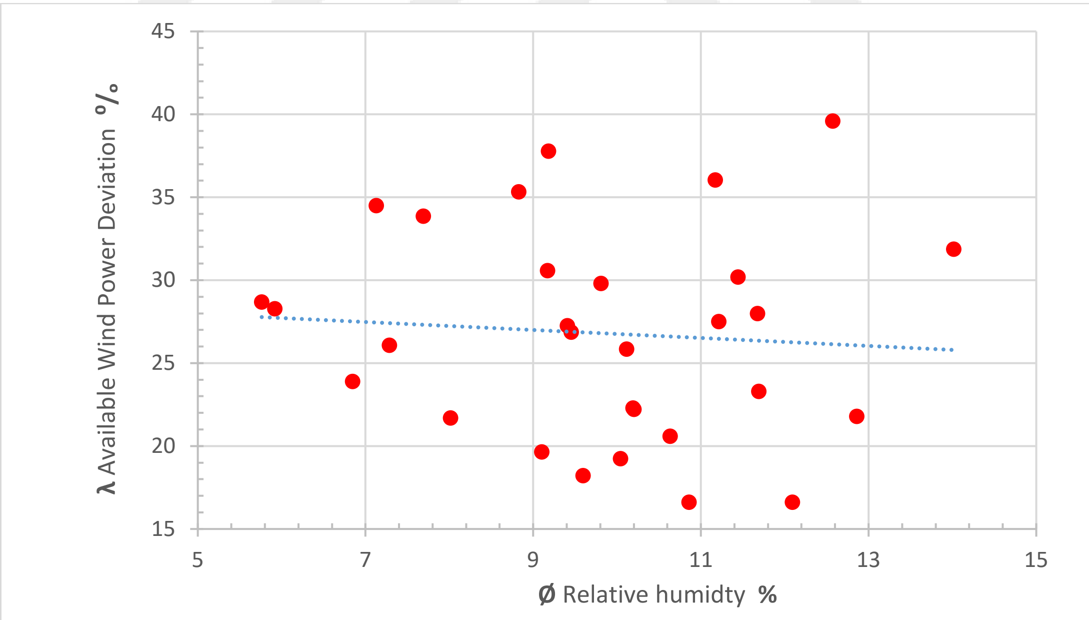

Figure B.9.2 Wind power deviation with humidity

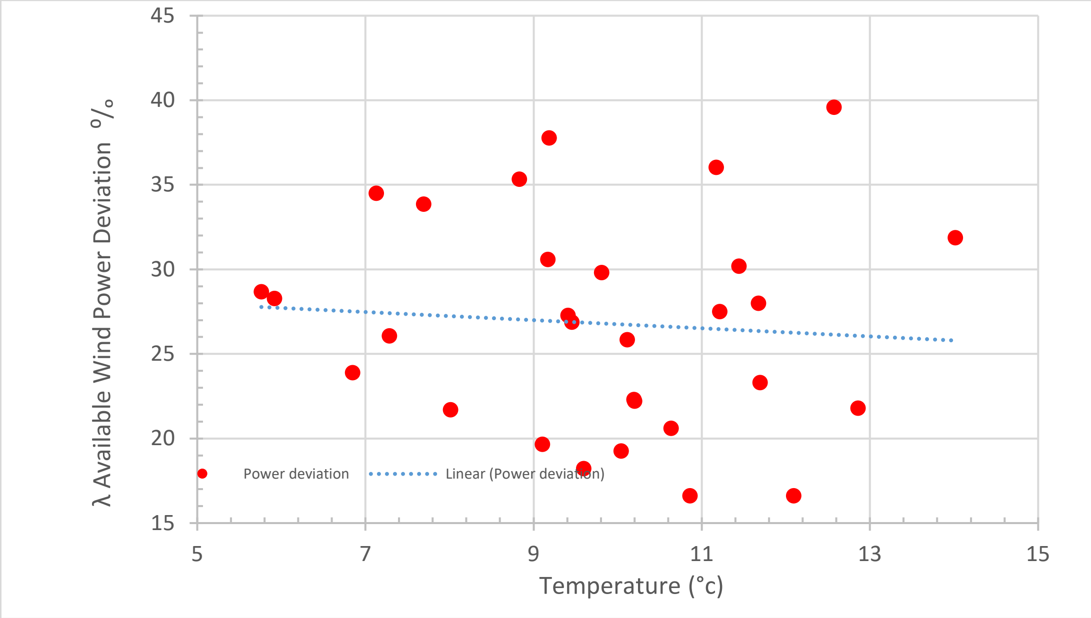

Figure B.9.3 Wind power deviation with temperature

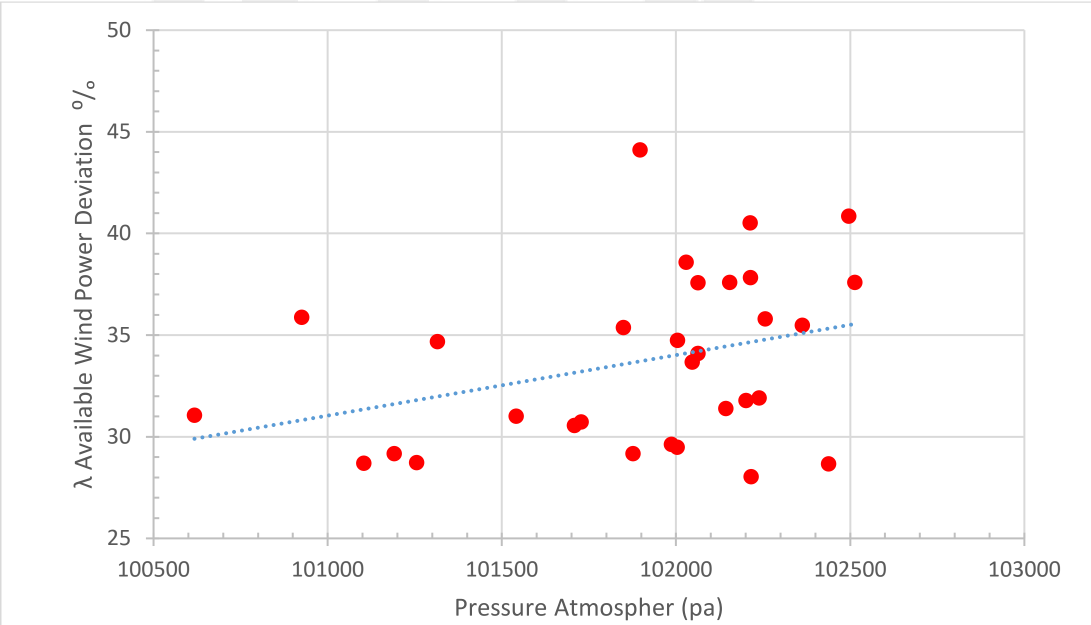

Figure B.9.4 Wind power deviation with atmospheric pressure

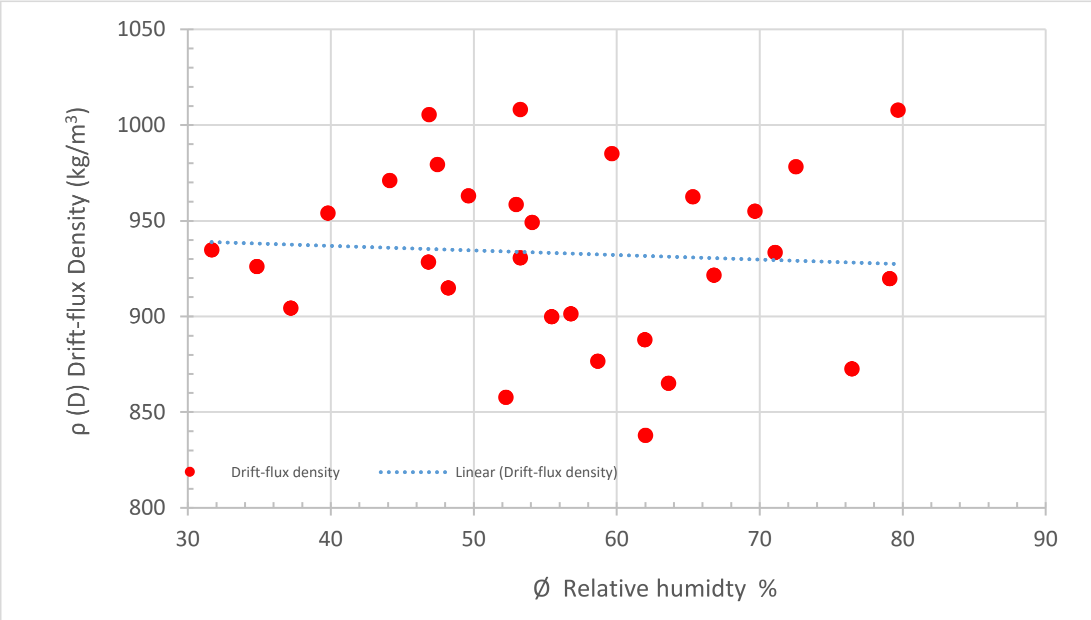

Figure B.9.5 Drift-flux density changes with the humidity

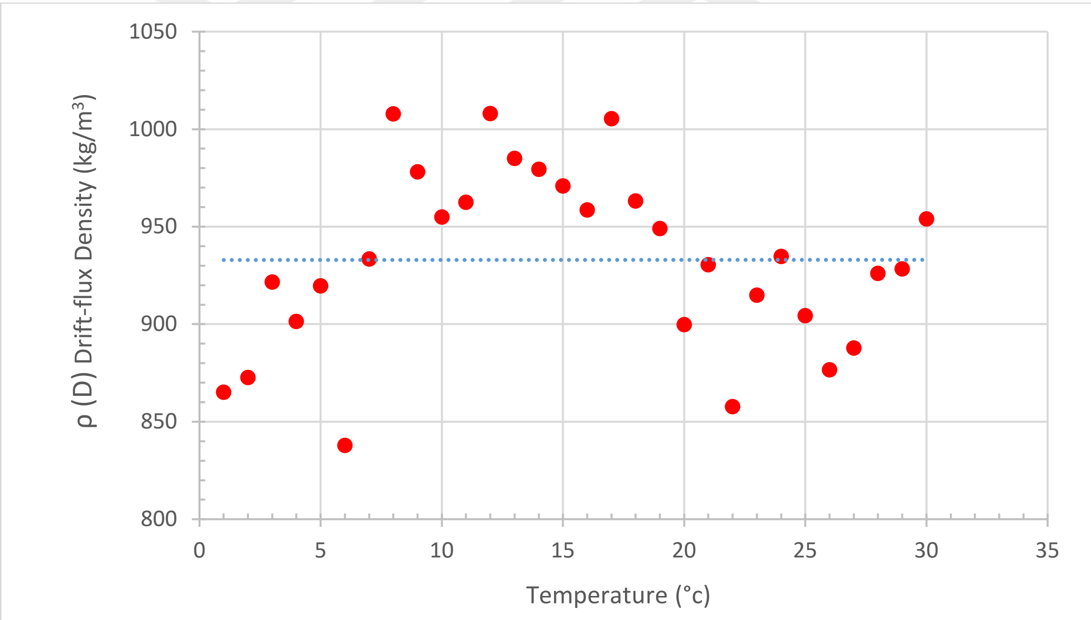

Figure B.9.6 Drift-flux density changes with the temperature

10. October

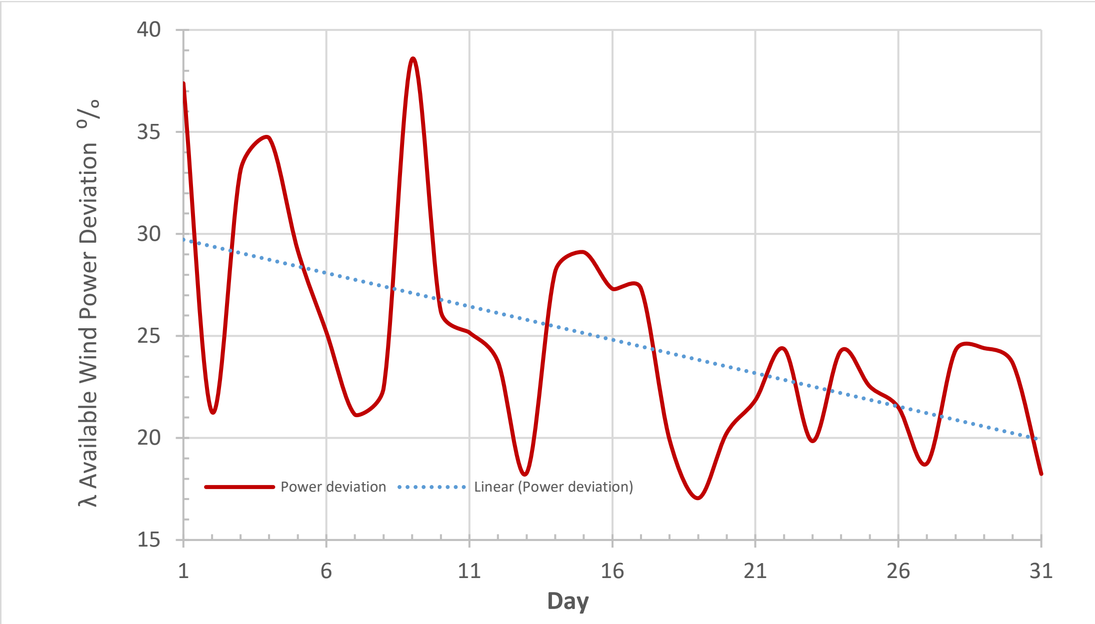

Figure B.10.1 Wind power deviation with days

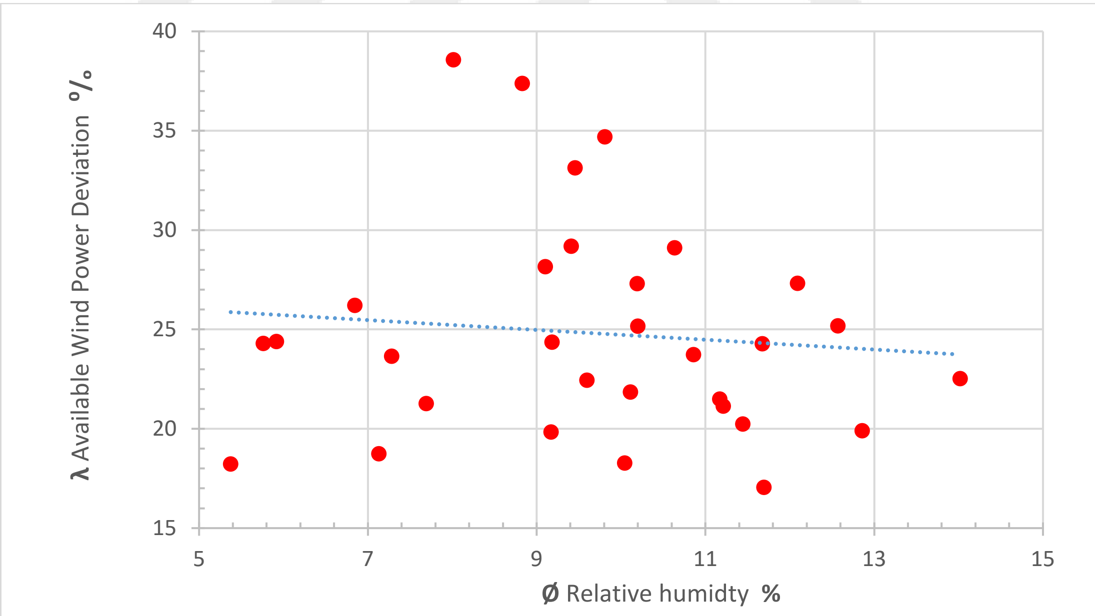

Figure B.10.2 Wind power deviation with humidity

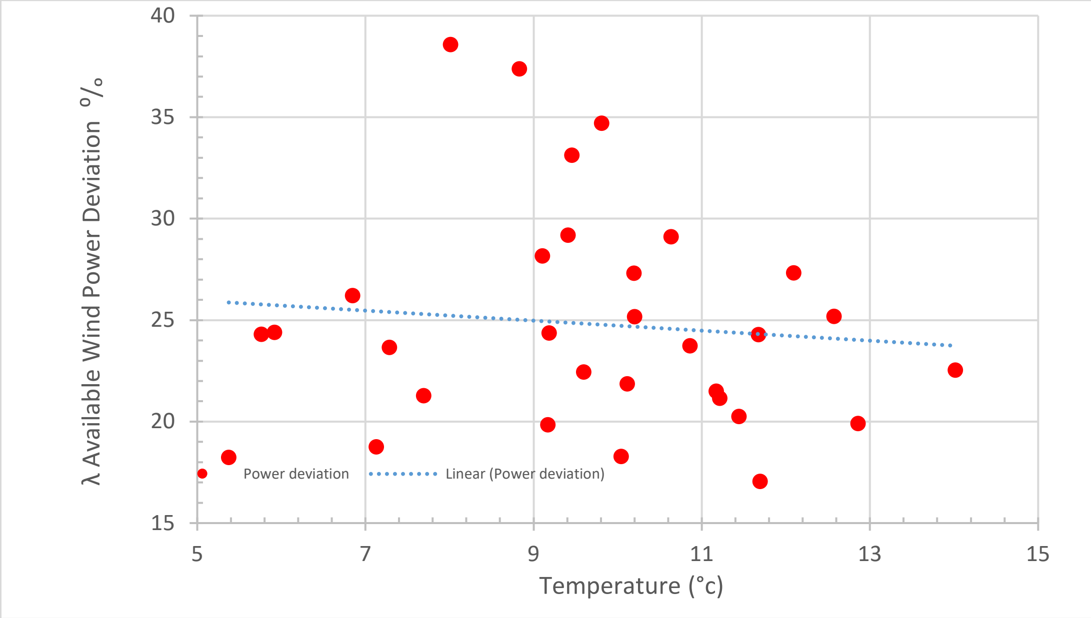

Figure B.10.3 Wind power deviation with temperature

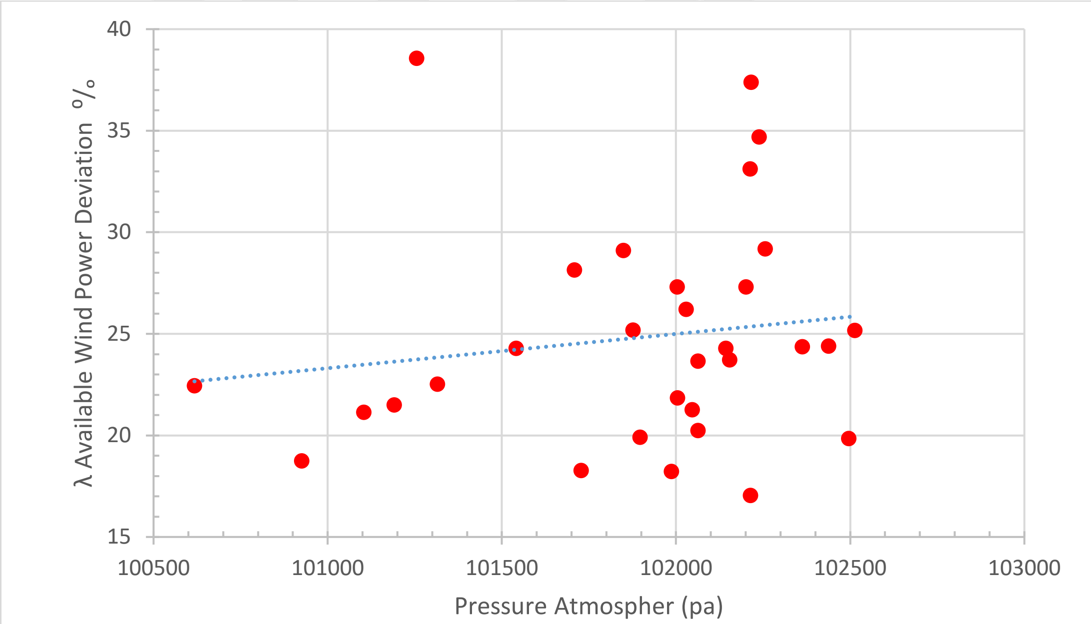

Figure B.10.4 Wind power deviation with atmospheric pressure

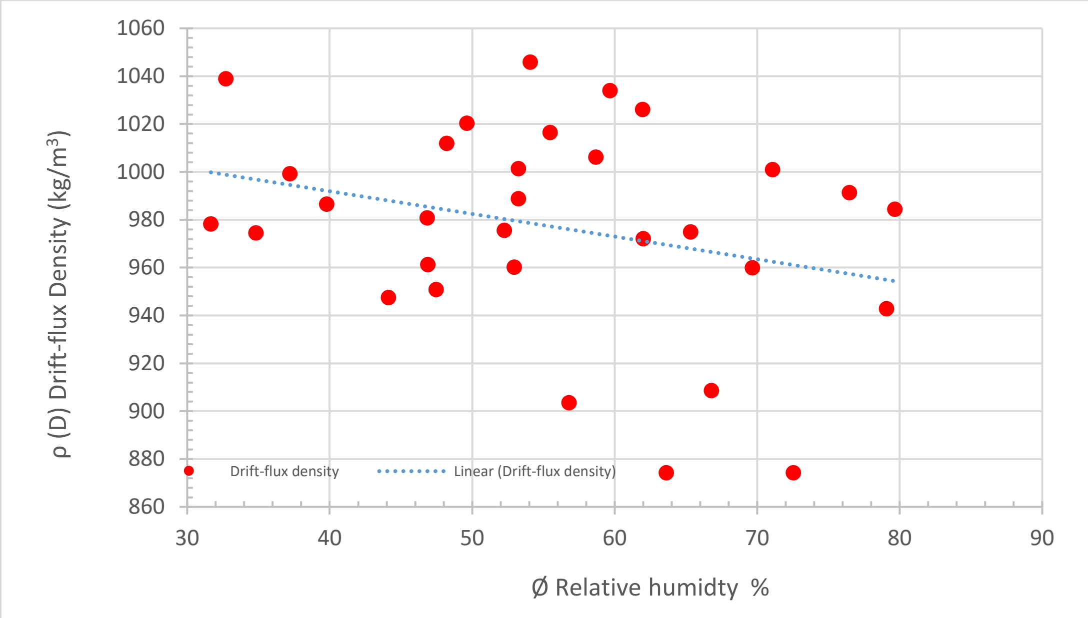

Figure B.10.5 Drift-flux density changes with the humidity

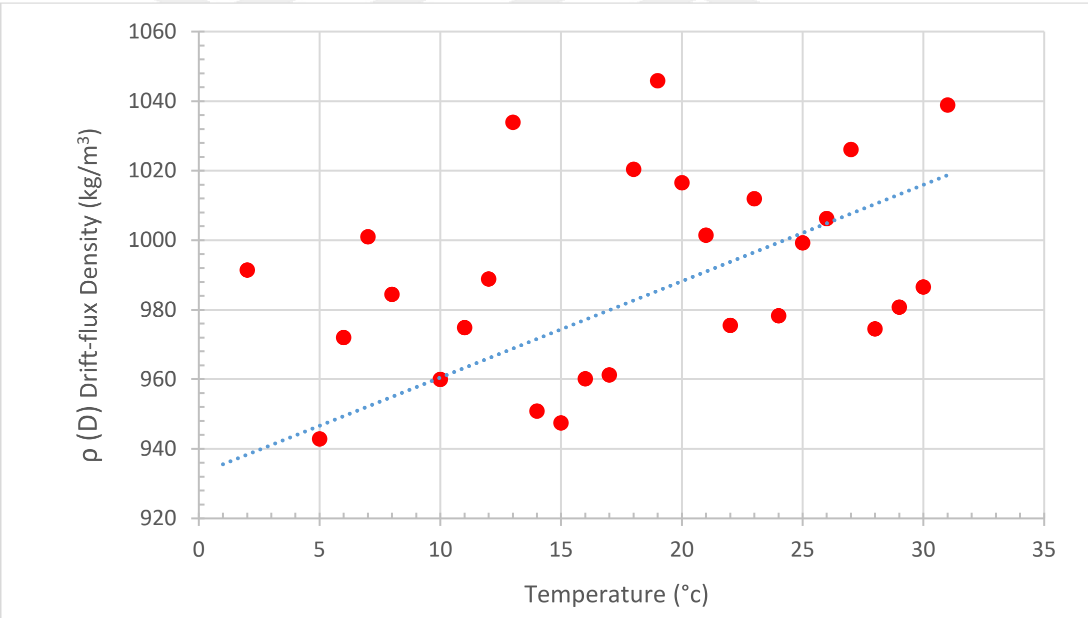

Figure B.10.6 Drift-flux density changes with the temperature

11. November

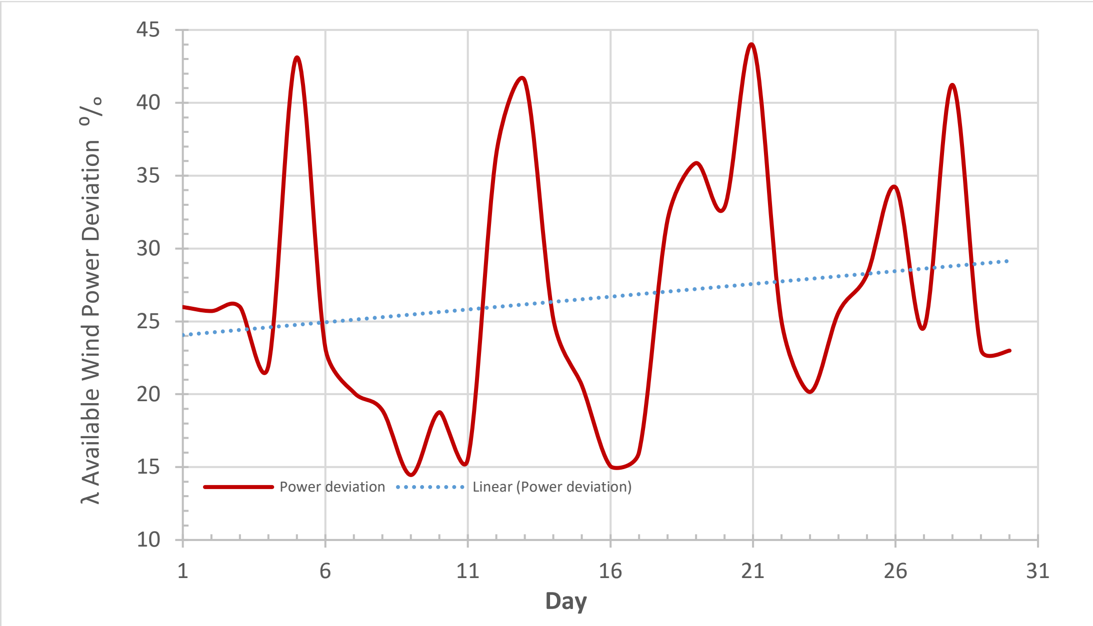

Figure B.11.2 Wind power deviation with days

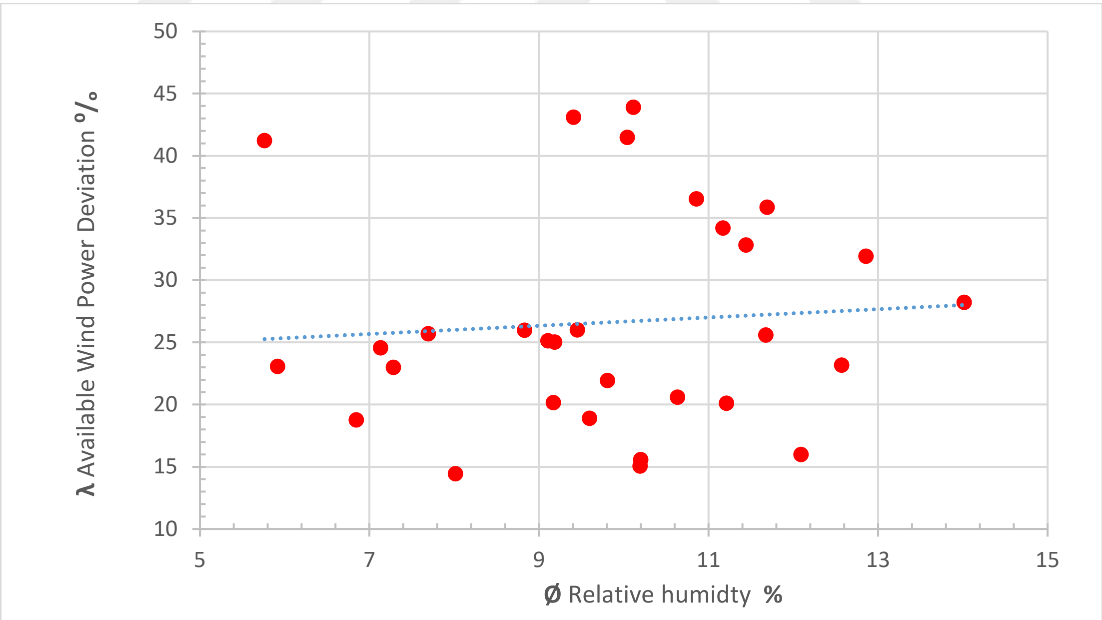

Figure B.11.2 Wind power deviation with humidity

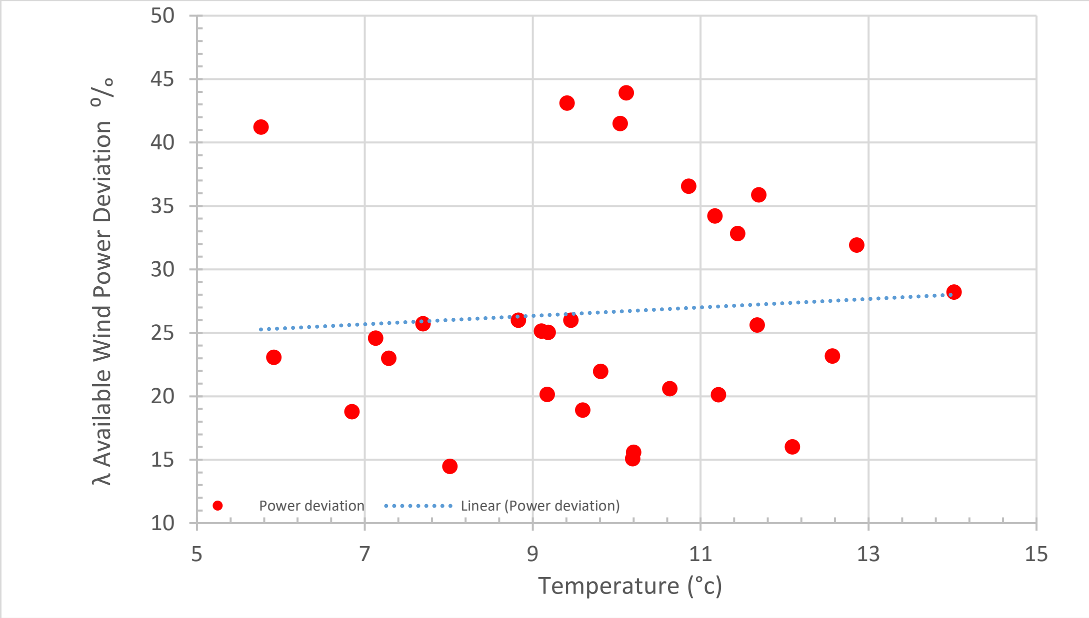

Figure B.11.3 Wind power deviation with temperature

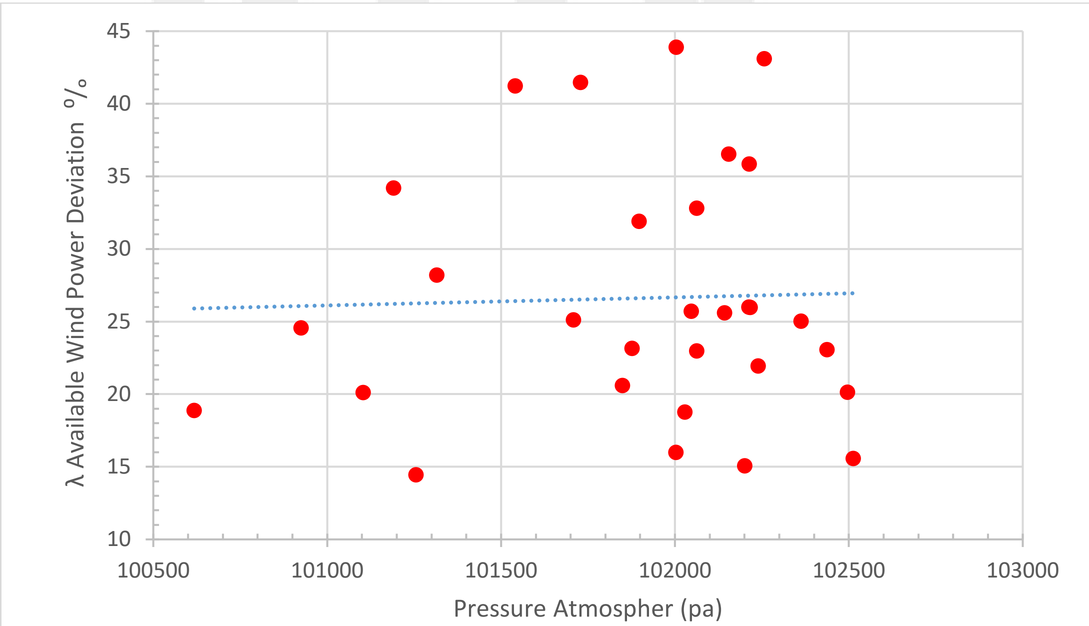

Figure B.11.4 Wind power deviation with atmospheric pressure

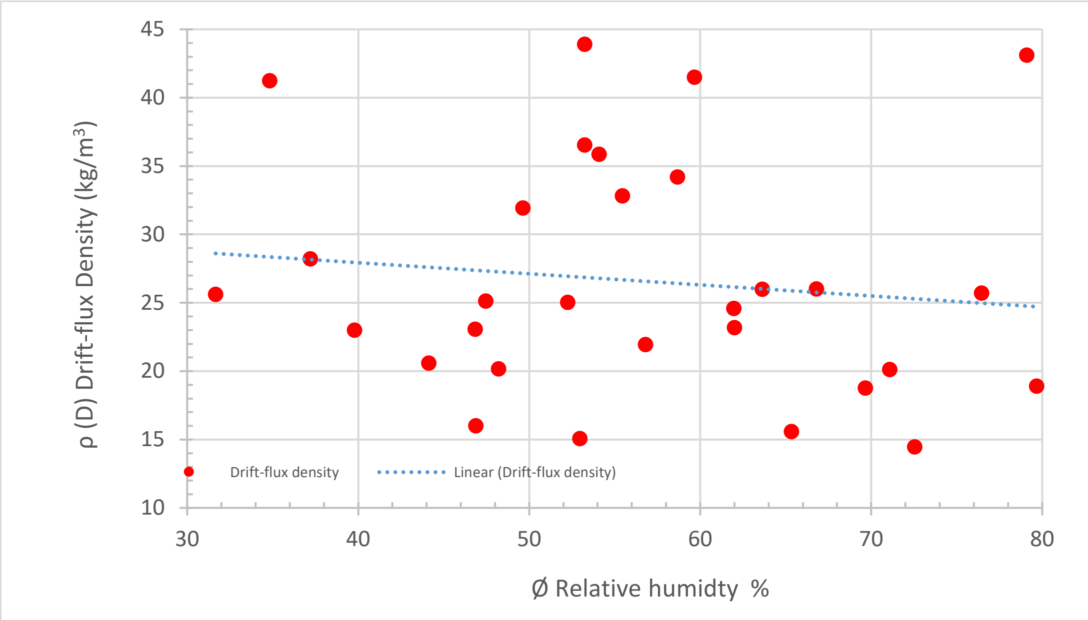

Figure B.1.5 Drift-flux density changes with the humidity

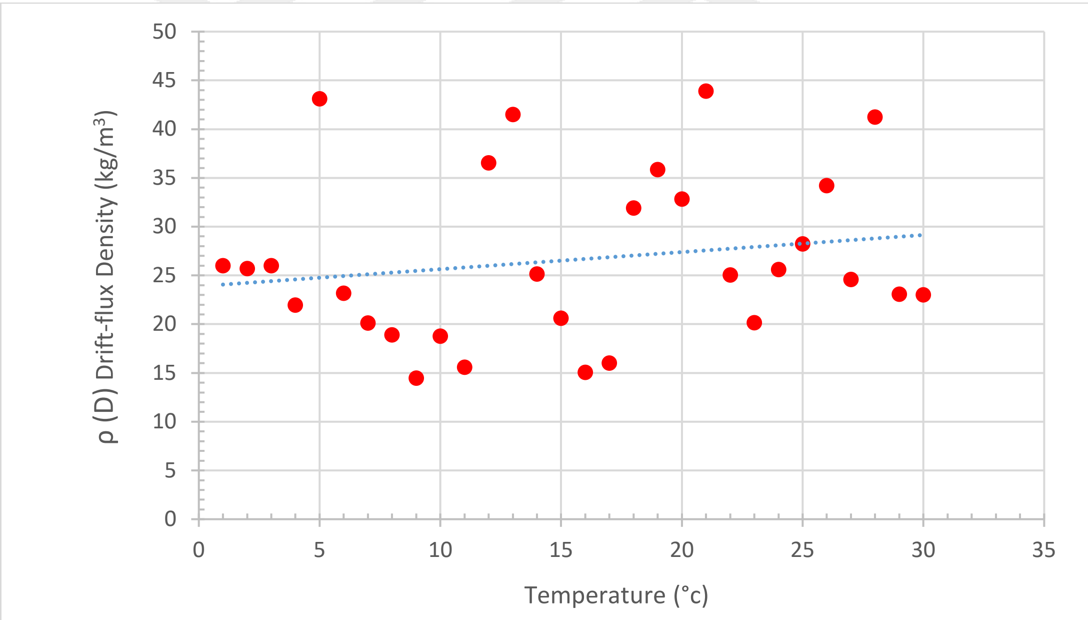

Figure B.1.6 Drift-flux density changes with the temperature

12. December

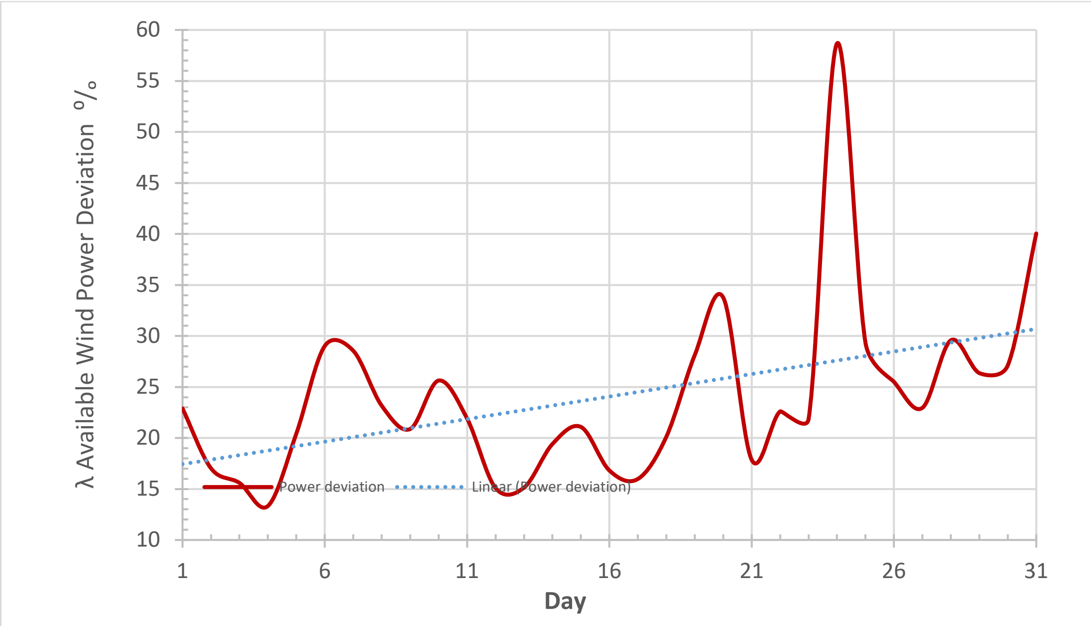

Figure B.12.1 Wind power deviation with days

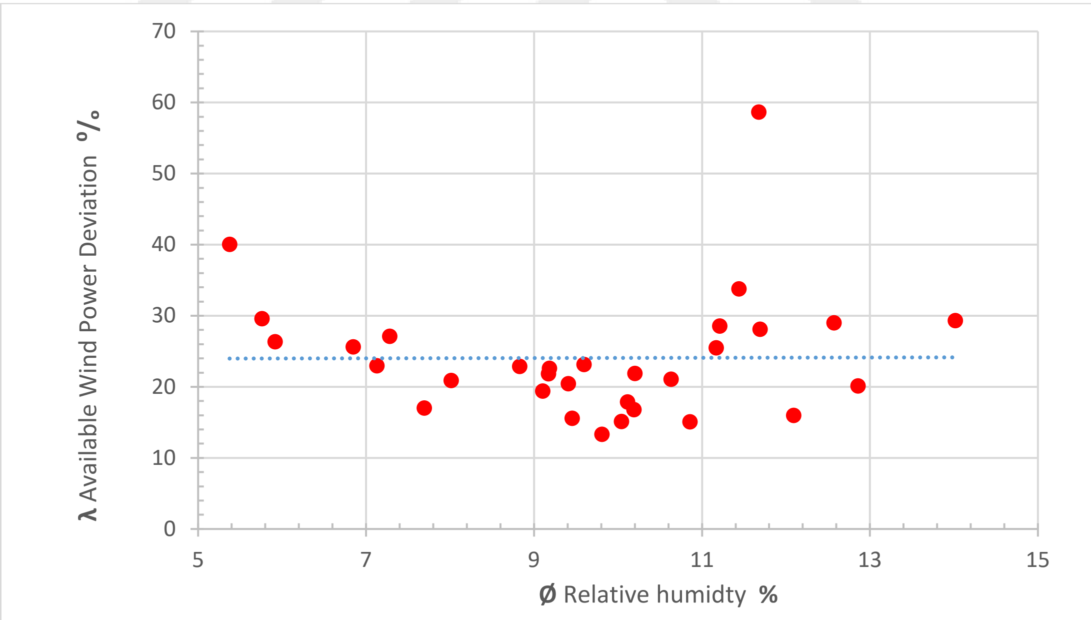

Figure B.12.2 Wind power deviation with humidity

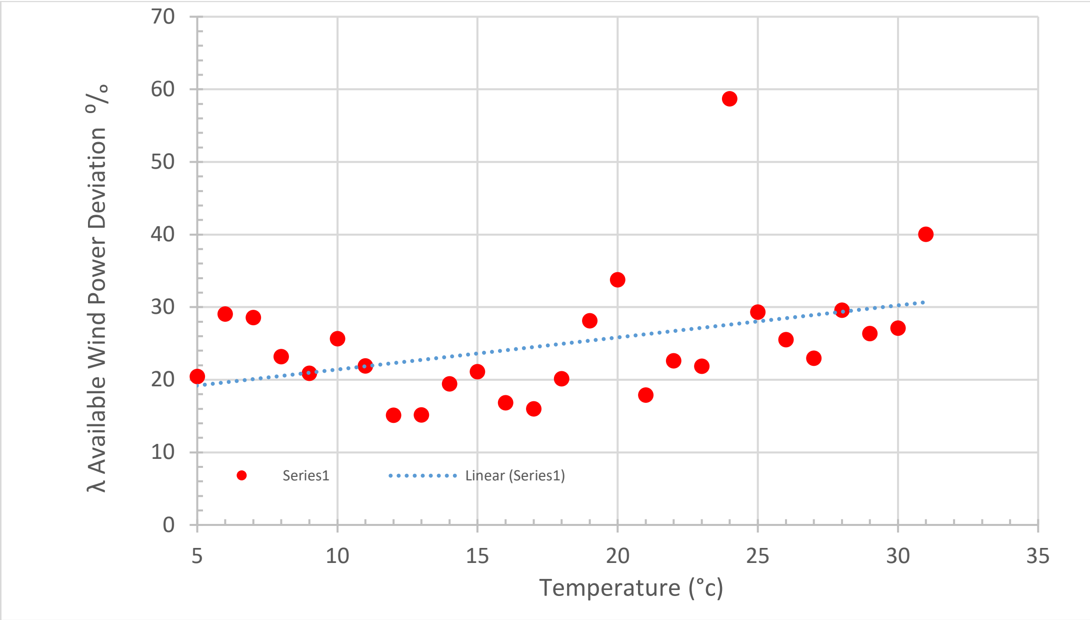

Figure B.12.3 Wind power deviation with temperature

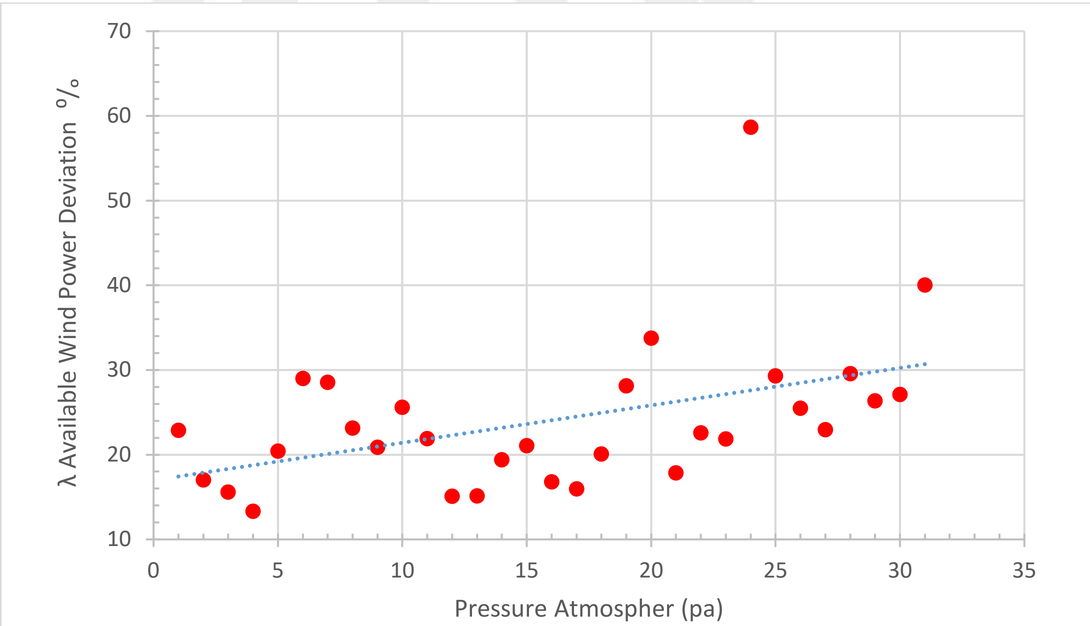

Figure B.12.4 Wind power deviation with atmospheric pressure

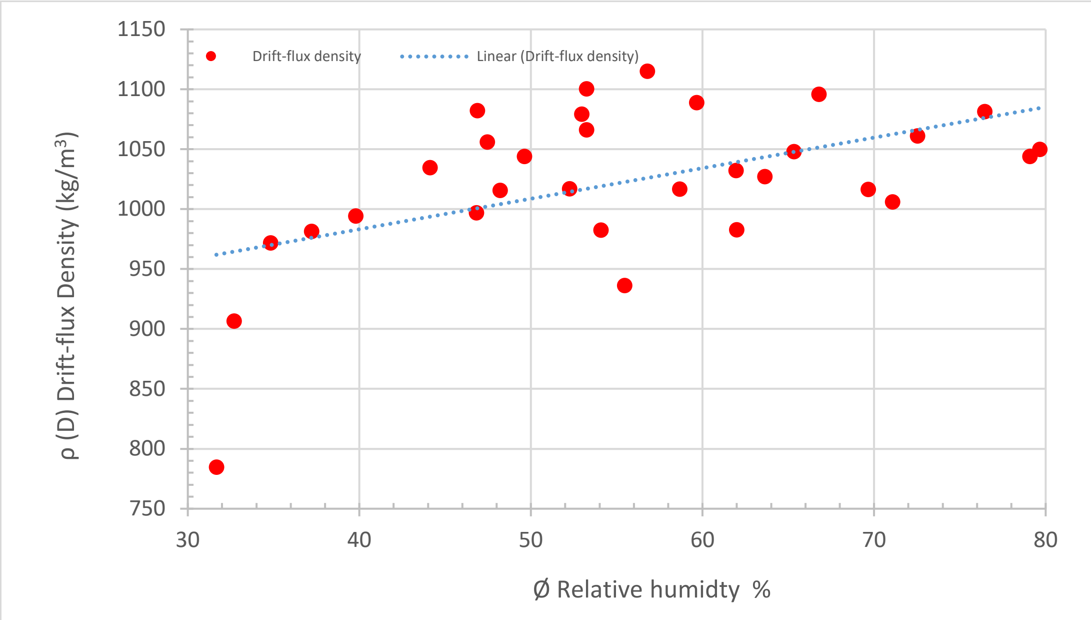

Figure B.12.5 Drift-flux density changes with the humidity

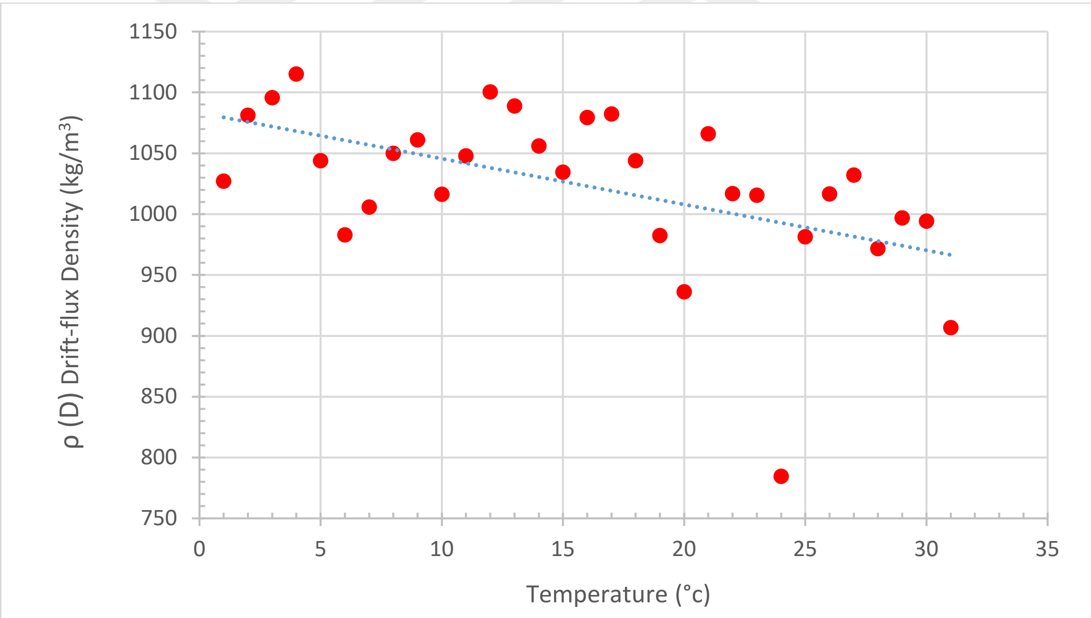

Figure B.12.6 Drift-flux density changes with the temperature

Curriculum Vitae (CV)

Personal Information

Name SURMANE: Yahya Khaleel Kareem KAREEM

Education

Degree	Extent	University/School	Year
MSc.	Mechanical	Gaziantep University	2021
BSc.	Mechanical	University of Kirkuk	2015
High school		AL-Iraq primary school	2011

Publication

Rain impact on wind density power seasonally_ Journal of Global Scientific Research (ISSN: 2523-9376) 6 (7) 2021/ 1517-1522